Fakultät für Medizin
Institut für Virologie

Molecular Mechanisms of Cytokine-induced, Non-cytolytic Control of Hepatitis B Virus Persistence

Daniela Stadler

Vollständiger Abdruck der von der Fakultät für Medizin der Technischen Universität München zur Erlangung des akademischen Grades eines

Doktors der Naturwissenschaften (Dr. rer. nat.)

genehmigten Dissertation.

Vorsitzender: Prof. Dr. Dirk H. Busch

Prüfende der Dissertation:

1. Prof. Dr. Ulrike Protzer
2. Prof. Dr. Bernhard Küster
3. Prof. Dr. Oliver T. Keppler

Die Dissertation wurde am 17.05.2017 bei der Technischen Universität München eingereicht und durch die Fakultät für Medizin am 06.12.2017 angenommen.

Table of contents

Abbreviations

3D-PCR	differential DNA denaturation-PCR
A	adenine
A3A	APOBEC3A
A3B	APOBEC3B
A3G	APOBEC3G
AdV	adenovirus, adenoviral vector
AID	activation-induced cytidine deaminase
ALT	alanine aminotransferase
AP site	apurinic/apyrimidinic site
APC	antigen presenting cell
APEX	apurinic/apyrimidinic site endonuclease
APOBEC3	apolipoprotein B editing complex 3
APS	ammonium persulfate
BS1	LTβR agonist (bispecific antibody)
C	cytosine
cccDNA	covalently closed circular DNA
ChIP	chromatin immunoprecipitation; Chromatin-Immunopräzipitation
cIAP	cellular inhibitor of apoptosis
CMV	cytomegalovirus
c-myc	myelocytomatosis gene
DAB	3,3'-diaminobenzidine
DHBV	duck hepatitis B virus
DIG	digoxigenin
DMSO	dimethyl sulfoxide
DNase	deoxyribonuclease
dpi	days post-infection
DR1	direct repeat 1
DR2	direct repeat 2
DZIF	Deutsches Zentrum für Infektionsforschung
ELISA	Enzyme-linked immunosorbent assay
FADD	Fas-associated death domain
FasL	Fas ligand
FBS	fetal bovine serum
FCS	fetal calf serum
FRET	fluorescence resonance energy transfer
G	guanine
GAF	IFN-γ activation factor
GAPDH	glyceraldehyde-3-phosphate dehydrogenase gene
GAS	gamma-activated sequence
GFP	green fluorescent protein
HBc	HBV core protein

HBeAg	hepatitis B e antigen
HBs	HBV surface protein
HBsAg	hepatitis B surface antigen
HBV	hepatitis B virus; Hepatitis-B-Virus
HBx	HBV X protein
HCV	hepatitis C virus
HDV	hepatitis D virus
HEM45	HeLa Estrogen Modulated, band 45
HIV-1	human immunodeficiency virus type 1
IFNAR1	IFN-α receptor 1
IFNAR2	IFN-α receptor 2
IFNGR	IFN-γ receptor
IFNLR1	interferon-lambda receptor 1
IFN-α	interferon-alpha
IFN-β	interferon-beta
IFN-γ	interferon-gamma
IL-10R2	interleukin-10 receptor 2
IPTG	isopropyl-β-D-thiogalactopyranosid
IRF9	interferon-regulatory factor 9
ISG	interferon-stimulated gene
ISG20	interferon-stimulated gene product of 20 kDa
ISGF3	interferon-stimulated gene factor 3
ISRE	interferon-stimulated response element
IU	infectious units
IκB	inhibitor of κB
JAK1	Janus kinase 1
L protein, LHBs	large HBV surface protein
LB	Luria-Bertani
LDH	lactate dehydrogenase
LTα	lymphotoxin-alpha
LTβ	lymphotoxin-beta
LTβR	lymphotoxin β receptor; Lymphotoxin-β-Rezeptor
M protein, MHBs	middle HBV surface protein
MHC I	major histocompatibility complex I
MNase	micrococcal nuclease
MOI	multiplicity of infection
mRNA	messenger RNA
MxA	myxoma resistance protein 1
nd	not detectable
NIK	NF-κB-inducing kinase
ns	not significant
NTCP	sodium taurocholate cotransporting polypeptide

P protein	polymerase protein of HBV (reverse transcriptase, RNaseH, primer)
p53	tumour suppressor p53 gene
PBS	phosphate buffered saline
PBS-T	phosphate buffered saline with Tween 20
PCR	polymerase chain reaction
PD-1	programmed death-1
PEG	polyethylene glycol
PELO	protein pelota homolog gene
pgRNA	pregenomic RNA
PHH	primary human hepatocytes
PLA	proximity ligation assay
PNPT1	human polynucleotide phosphorylase (hPNPase) gene
POLK	DNA polymerase κ
PRNP	prion protein gene
PTM	post-translational modification
PVDF	polyvinylidene fluoride
qPCR	quantitative PCR
qRT-PCR	quantitative reverse transcription PCR
RAD9A	RAD9 checkpoint clamp component A gene
rcDNA	relaxed-circular DNA
RIN	RNA integrity number
RNA pol II	RNA polymerase II
RNase	ribonuclease
S protein, SHBs	small HBV surface protein
S-CAR	chimeric antigen receptor recognizing HBsAg
SDS	sodium dodecyl sulphate
SDS-PAGE	sodium dodecyl sulphate-polyacrylamide gel electrophoresis
shRNA	short hairpin RNA
siRNA	small interfering RNA
Src	cellular/sarcoma tyrosine kinase gene
SSC	saline-sodium citrate (buffer)
STAT1	signal transducers and activators of transcription 1
STAT2	signal transducers and activators of transcription 2
T	thymine
TBP	TATA-box binding protein gene
TBS-T	Tris-buffered saline with Tween 20
TCR	T-cell receptor
TDP	tyrosyl-DNA-phosphodiesterase
TEMED	tetramethylethylenediamine
Tet	tetracycline
TNFR1	TNF receptor 1
TNFR2	TNF receptor 2

TNF-α	tumour necrosis factor-alpha; Tumornekrosefaktor-alpha
TR	tetracycline repressor
TRADD	TNFR1-associated death domain
TYK2	tyrosine kinase 2
U	unit
UNG	uracil DNA glycosylase
WT	wild type
X-gal	5-bromo-4-chloro-3-indolyl-β-D-galactopyranoside
XRN1	5’ to 3’ exoribonuclease 1 gene
XTT	2,3-Bis-(2-Methoxy-4-Nitro-5-Sulfophenyl)-2H-Tetrazolium-5-Carboxanilide

Abstract

Despite an effective vaccine, an estimated 257 million humans worldwide are suffering from chronic hepatitis B resulting in more than 800,000 deaths yearly. Current treatments for chronic hepatitis B can control the replication of the hepatitis B virus (HBV) but cannot eradicate it completely due to the persistence of the covalently closed circular DNA (cccDNA) form of HBV. The cccDNA is therefore a major therapeutic target. Thus, the aim of this thesis was to elucidate the mechanisms of non-cytolytic cccDNA purging through cytokines in more detail.

In the first part, transwell co-culture and cytokine neutralization experiments demonstrated that activated T-cells secrete the cytokines interferon-gamma (IFN-γ) and tumour necrosis factor-alpha (TNF-α), which mediated the reduction of cccDNA in HBV-infected hepatoma cells without cytolysis. These cytokines induced the expression of APOBEC3A (A3A) and APOBEC3B (A3B), that deaminated nuclear HBV DNA. A3A and A3B were essential for cytokine-triggered cccDNA loss as shown by knockdown experiments.

In the second part, the specificity of cccDNA reduction was studied. Only cccDNA but not an episomal HBV DNA construct (pEpi-H1.3) was affected by cytokine-induced deamination and decay through T-cell cytokines, interferon-alpha (IFN-α) or lymphotoxin β receptor (LTβR) activation. Since all these treatments trigger the expression of A3A or A3B, these deaminases were overexpressed in HBV-replicating hepatoma cells leading to hypermutations on cccDNA. Furthermore, A3A and HBV core protein were shown to associate with cccDNA by chromatin immunoprecipitation (ChIP) experiments, supporting the hypothesis of HBV-core-assisted targeting of nuclear APOBEC3 proteins to cccDNA.

Since A3A expression in human hepatoma cells led to deamination but was not sufficient for cccDNA reduction itself, the third part of this thesis aimed at identifying the nuclease involved in cccDNA purging. Gene expression profiling under IFN-α treatment revealed three upregulated candidate nucleases with nuclear localization. ISG20 (interferon-stimulated gene product of 20 kDa), the strongest interferon-induced nuclease, was stained immunohistochemically in liver tissue samples from patients with acute but not chronic hepatitis B. Knockdown of ISG20 rescued the interferon-induced cccDNA loss. Overexpression of ISG20 together with A3A was sufficient to reduce cccDNA without further treatment.

Overall, the results of this thesis lead to the conclusion that T-cell cytokines IFN-γ and TNF-α as well as IFN-α and LTβR activation lead to the non-cytolytic purging of cccDNA, the HBV persistence form, from the nucleus of infected hepatocytes involving APOBEC3 family deaminases and the interferon-induced nuclease ISG20. Concerted expression of the deaminase A3A and the nuclease ISG20 suffices to reduce cccDNA, providing a relevant basis for advancing therapies of chronic hepatitis B.

Zusammenfassung

Trotz einer wirksamen Impfung leiden weltweit geschätzte 257 Millionen Menschen an chronischer Hepatitis B, dies führt jährlich zu mehr als 800.000 Todesfällen. Derzeitige Therapien können die Replikation des Hepatitis-B-Virus (HBV) zwar hemmen, führen aber nicht zu einer vollständigen Eliminierung des Virus aufgrund der Persistenz der nukleären cccDNA (*covalently closed circular* DNA) des HBV. Die cccDNA ist folglich ein wichtiges therapeutisches Zielmolekül. Daher war es das Ziel dieser Arbeit, die Mechanismen der nicht-zytolytischen Reduktion der cccDNA durch Zytokine detaillierter aufzuklären.

Im ersten Teil der Arbeit zeigten Zytokin-Neutralisierungsversuche im Transwell, dass aktivierte T-Zellen die Zytokine Interferon-gamma (IFN-γ) und Tumornekrosefaktor-alpha (TNF-α) sekretieren, welche den Verlust der cccDNA in HBV-infizierten Hepatomzellen ohne Zytolyse vermitteln. Diese Zytokine induzierten die Expression von APOBEC3A (A3A) und APOBEC3B (A3B), die nukleäre HBV-DNA desaminierten, und dabei essenziell für die Reduktion der cccDNA waren, wie Knockdown-Experimente belegten.

Im zweiten Teil wurde die Spezifität der cccDNA-Reduktion durch verschiedene Behandlungen untersucht: IFN-γ, TNF-α, Interferon-alpha (IFN-α) und Aktivierung des Lymphotoxin-β-Rezeptors (LTβR). Die induzierte Desaminierung und Mengenreduktion betraf nur cccDNA, nicht aber episomale HBV-DNA (pEpi-H1.3). Da alle diese Behandlungen die Expression von A3A und A3B auslösen, wurden diese Desaminasen überexprimiert, was zu Hypermutationen auf der cccDNA führte. Außerdem zeigte Chromatin-Immunopräzipitation (ChIP), dass A3A und das HBV-Coreprotein mit der cccDNA assoziieren, was die Hypothese stützt, dass das HBV-Coreprotein die nukleären APOBEC3-Proteine zur cccDNA bringt.

Da die Expression von A3A zwar Desaminierung verursachte, jedoch allein nicht ausreichend für den Verlust der cccDNA war, strebte der dritte Teil der Arbeit die Identifizierung der involvierten Nuklease an. Eine Genexpressionsanalyse unter Behandlung mit IFN-α ergab drei hochregulierte Kandidatennukleasen mit nukleärer Lokalisierung. ISG20 (*interferon-stimulated gene product of 20 kDa*), die am stärksten induzierte Nuklease, konnte in Lebergewebeproben von Patienten mit akuter, nicht aber chronischer, Hepatitis B angefärbt werden. ISG20-Knockdown verhinderte die Abnahme der cccDNA unter Interferonbehandlung. Überexpression von ISG20 zusammen mit A3A reichte aus, um die cccDNA ohne weitere Behandlung zu reduzieren.

Insgesamt führen die Ergebnisse dieser Arbeit zur Schlussfolgerung, dass die T-Zellzytokine IFN-γ und TNF-α sowie IFN-α und die Aktivierung des LTβR zum nicht-zytolytischen Verlust der cccDNA, der Persistenzform des HBV, führen, wobei APOBEC3-Desaminasen und die Interferon-induzierte Nuklease ISG20 eine entscheidende Rolle spielen. Die gemeinsame Expression der Desaminase A3A und der Nuklease ISG20 reicht aus, um die cccDNA zu reduzieren. Diese Ergebnisse bilden eine solide Basis für die Weiterentwicklung der Therapien gegen chronische Hepatitis B.

1 Introduction

Despite an effective prophylactic vaccine, an estimated 257 million humans worldwide are suffering from chronic hepatitis B with the risk of developing liver cirrhosis or hepatocellular carcinoma, which cause more than 800,000 deaths per year (Naghavi et al. 2015, WHO 2017). A major problem in treatment of chronic hepatitis B is the viral persistence in infected liver cells. Therefore, this thesis deals with mechanisms of the control of viral persistence, induced by cytokines and without cytolysis.

1.1 Hepatitis B virus (HBV)

Since the present study focuses on molecular, cytokine-triggered mechanisms against HBV, the following chapters introduce the molecular biology of HBV, characteristics of HBV infection and therapy options.

1.1.1 Classification of HBV

Human HBV is the prototype member of the *hepadnaviridae* (Schaefer 2007), a family of small, enveloped DNA viruses. Members share tropism for liver tissue and a narrow host specificity (Modrow et al. 2010). Based on their ability to infect mammals or birds, *hepadnaviridae* are divided into the genera *orthohepadnaviridae* and *avihepadnaviridae* (Schaefer 2007). An example for *orthohepadnaviridae* is, beside human HBV, woodchuck hepatitis virus (Schaefer 2007, Summers et al. 1978), while duck HBV (DHBV) is representative for *avihepadnaviridae* (Mason et al. 1980, Schaefer 2007). Since these DNA viruses replicate via an RNA intermediate, they are designated as para-retroviruses (Hu and Liu 2017).

HBV is subdivided phylogenetically into nine genotypes, A – I, based on a sequence divergence of more than 7.5 % across the whole genome between the groups. HBV genotypes have a diverse geographical distribution. For instance, genotype A appears in Africa, Europe and the Americas, genotypes B and C in Asia and genotypes F and H are prevalent in Southern and Central America. Genotype D is found worldwide, genotype G in parts of America and Europe, whereas genotype E is distributed in Western and Central Africa and genotype I in Asia (Kramvis 2014). A putative 10th genotype (“J”) was isolated from a single individual (Tatematsu et al. 2009). Further, HBV can be classified based on the epitopes of the surface protein into 9 different serological subtypes, which can be summarized in the four major serotypes *ayw*, *ayr*, *adw* and *adr* (Kramvis 2014).

1.1.2 Structure of HBV particles

Hepatitis B virions - also named “Dane particles” after their first visualisation - are enveloped particles of 42 nm in diameter (Dane et al. 1970). Figure 1 depicts their composition: The envelope consists of small (S), middle (M) and large (L) HBV surface proteins (HBs) in a lipid bilayer and engulfs a nucleocapsid (Nassal 2015). The icosahedral nucleocapsid is formed by 180 (T=3) or 240 (T=4) HBV core protein (HBc) subunits, which form dimers (Crowther et al. 1994). Inside, the partially double-stranded, relaxed-circular (rcDNA) genome of HBV is situated. The 5’ end of the minus strand of rcDNA is covalently bound to the viral polymerase protein (P protein) (Gerlich and Robinson 1980, Nassal 2015). Beside these infectious HBV particles, DNA-free subviral particles exist: 22 nm spheres and filaments, which consist of envelope proteins but lack nucleocapsid and rcDNA inside, as well as enveloped nucleocapsids without an rcDNA genome (Hu and Liu 2017).

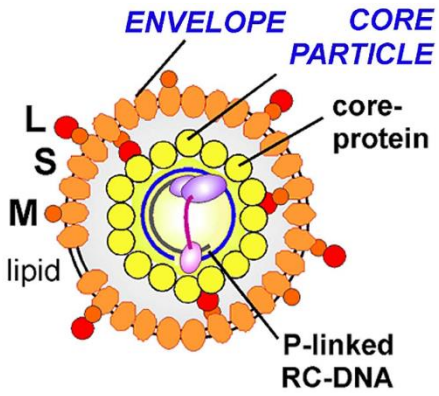

Figure 1: Structure of HBV. The envelope consists of small (S), middle (M) and large (L) surface proteins, embedded in a lipid layer. It encloses the nucleocapsid (core particle), which is composed of HBV core proteins, and the relaxed-circular DNA (rcDNA) genome of HBV, which is covalently linked to the viral polymerase (P) protein (Nassal 2015).

1.1.3 HBV genome organisation

The HBV rcDNA genome is only 3.2 kb long and therefore tightly organized with overlapping open reading frames and each nucleotide having coding function. Figure 2 shows the arrangement of the open reading frames (Nassal 2015) encoding seven viral proteins: All three HBV surface proteins have the same carboxy-terminal domain (S), the additional parts of the M and L protein are N-terminal extensions named preS2 and preS1, respectively. HBV core protein (C) serves as subunit of the viral nucleocapsid as described above. The HBV core sequence with an additional N-terminal peptide (precore, preC) is proteolytically processed and secreted as hepatitis B e antigen (HBeAg) (Seeger and Mason 2015) and seems to have immunoregulatory functions (Chen et al. 2005). The P protein or polymerase protein functions as reverse transcriptase, RNaseH and primer during synthesis of the rcDNA genome (Seeger and Mason 2015). The non-structural HBV X protein (HBx; X) is needed for initiation and maintenance of viral transcription (Lucifora, Arzberger et al. 2011).

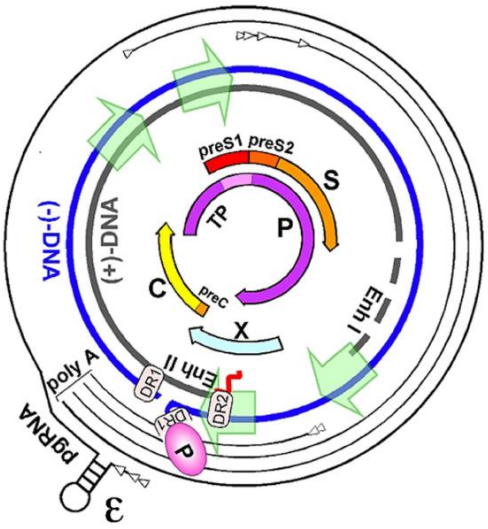

Figure 2: HBV genome organisation. Outer lines depict viral transcripts with transcription starts shown as white arrowheads, ε stands for the encapsidation signal on pregenomic RNA (pgRNA). Green arrows denote promotors, Enh I / Enh II transcriptional enhancers, DR1 / DR2 direct repeats, TP the terminal protein domain of P protein. HBV DNA is shown as rcDNA but transcriptional template is the covalently closed circular DNA (see replication cycle below). Further details are given in the text (Nassal 2015).

1.1.4 Replication cycle of HBV

The replication cycle of HBV is presented schematically in figure 3: To enter susceptible cells, viral LHBs attach to glycosaminoglycan side chains of cellular surface heparan sulphate proteoglycans (Schulze et al. 2007). Further, the myristoylated preS1 domain of LHBs interacts with sodium taurocholate cotransporting polypeptide (NTCP), which was identified as a functional receptor of HBV (Yan, Zhong et al. 2012). This multiple transmembrane transporter is expressed on primary hepatocytes and makes otherwise resistant hepatoma cell lines susceptible for HBV infection. For instance, human HepG2 cells support HBV infection after NTCP expression (Yan, Zhong et al. 2012). HBV entry into hepatocytes involves clathrin-dependent endocytosis (Huang et al. 2012). After uncoating and release of the genome-containing nucleocapsids into the host cell cytoplasm, nucleocapsids are translocated to the nuclear membrane. In the nuclear basket, the nucleocapsid shell disassembles and rcDNA is released into the nucleus (Schmitz, Schwarz et al. 2010). Nuclear rcDNA is completed to form the fully double-stranded, covalently closed circular DNA (cccDNA), which stays episomally in the nuclei of infected cells. cccDNA is the template for transcription by host RNA polymerase II of all viral RNAs, including subgenomic mRNAs for expression of HBs and HBx as well as the pregenomic RNA (pgRNA) and precore RNA. Precore RNA is translated, proteolytically processed and secreted as HBeAg whereas pgRNA is transmitted into P protein and HBV core protein. Additionally, pgRNA is reverse-transcribed by the viral P protein into rcDNA within the nucleocapsid (Nassal 2015, Seeger and Mason 2015). Mature rcDNA-containing nucleocapsids are either transported back to the nucleus and increase cccDNA copy number or are enveloped and secreted, depending on the concentration of available envelope proteins at the endoplasmic reticulum (Modrow et al. 2010, Nassal 2015). Enveloped virions (Watanabe et al. 2007) and subviral filaments (Jiang et al. 2016) exit the cell via multivesicular bodies while subviral spheres are secreted via the endoplasmic reticulum and Golgi complex (Patient et al. 2007).

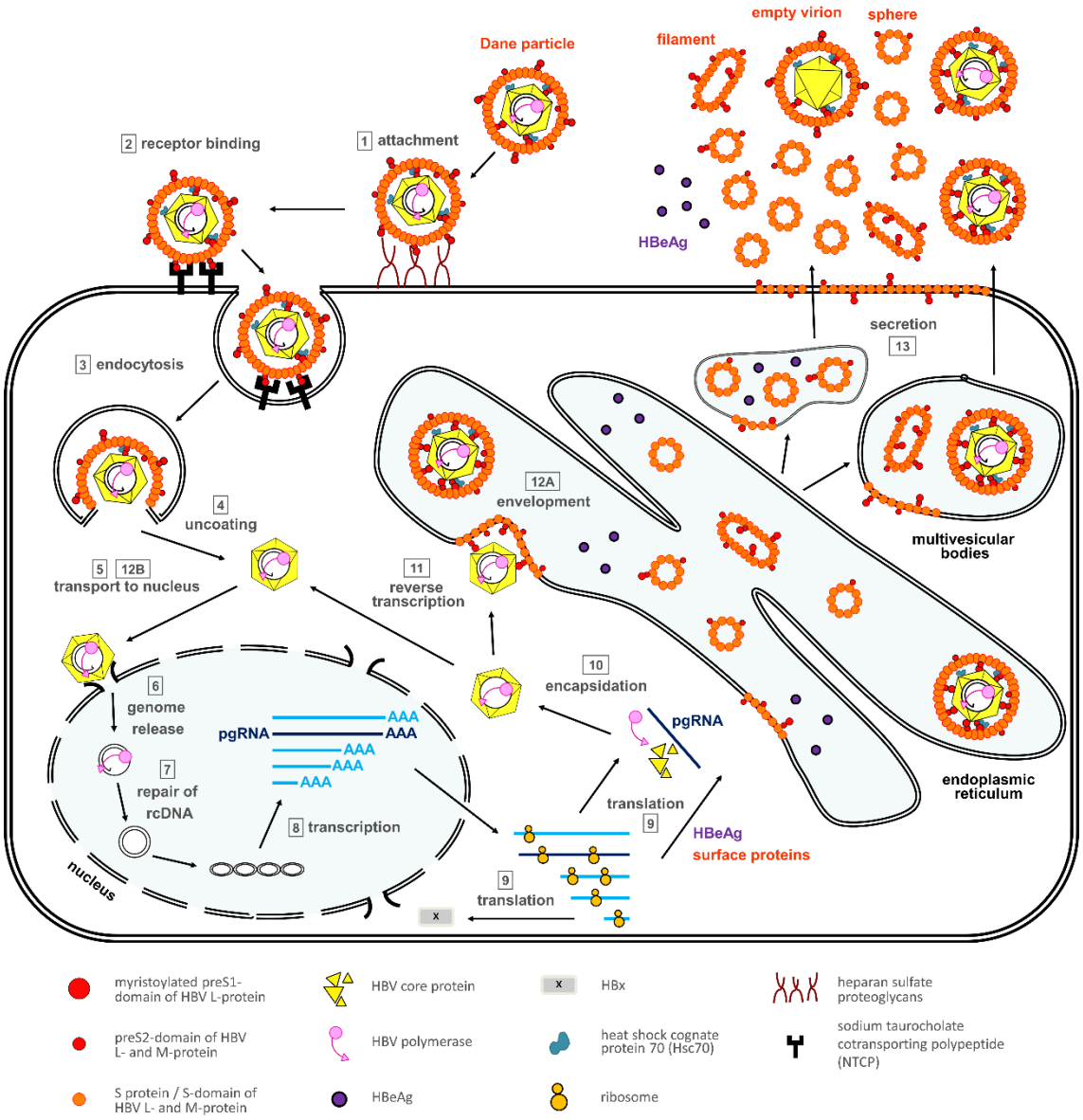

Figure 3: Replication cycle of HBV. HBV attaches to heparan sulphate proteogylcans on the cell surface and interacts specifically with NTCP during entry. After uncoating, nucleocapsids are brought to the nucleus and rcDNA (relaxed-circular DNA) genomes are released into the nucleus. There, rcDNA is completed to form cccDNA (covalently closed circular DNA), the viral persistence form. cccDNA serves as transcription template for all viral RNAs. pgRNA (pregenomic RNA) is encapsidated together with HBV polymerase (P protein) and reverse transcribed. Newly formed rcDNA-containing capsids are either transported back to the nucleus or enveloped at the endoplasmic reticulum and released via multivesicular bodies (Ko et al. 2017).

The process of reverse transcription is depicted in figure 4: P protein binds to the ε stem-loop structure of pgRNA and mediates co-packaging of pgRNA and P protein into newly forming nucleocapsids, whereby the carboxy-terminal domain of HBV core protein is needed. A tyrosine residue in the terminal protein domain of P protein provides the 3’ OH

group for priming reverse transcription of minus-strand DNA, resulting in covalent binding (Nassal 2015, Zlotnick et al. 2015). After synthesis of some nucleotides of the minus-strand DNA, P protein and covalently bound DNA are translocated to the 3' end of pgRNA to hybridize with the complementary sequence of direct repeat 1 (DR1). Extension yields whole minus-strand DNA, while P protein degrades pgRNA through its RNaseH activity except for a 5' residue. When proper rcDNA is formed, this RNA oligomer is translocated to the complementary direct repeat 2 (DR2) at the 5' end of the minus-strand DNA, where it primes plus-strand DNA synthesis; the RNA primer stays bound to the 5' end of the plus strand in the end. However, if primer translocation and circularization fail, double-stranded linear DNA may be formed. A final template switch circularizes minus-strand DNA within the nucleocapsid and provokes that plus-strand DNA synthesis spans the gap caused by the covalently bound P protein at the minus strand. The plus strand remains incomplete forming the partially double-stranded rcDNA (Modrow et al. 2010, Nassal 2015, Zlotnick et al. 2015).

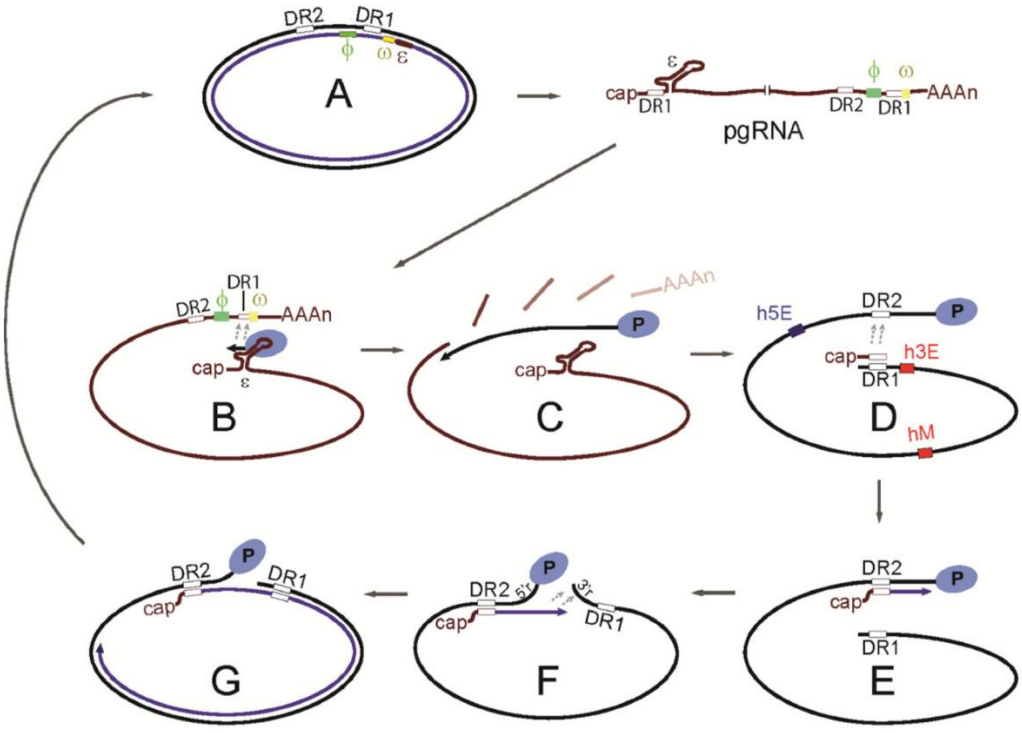

Figure 4: Reverse transcription. (A) Transcription of pgRNA from cccDNA. **(B)** Binding of P protein to pgRNA, start of transcription of minus-strand DNA and minus-strand template switch. **(C)** Minus-strand DNA elongation, RNase H digestion of pgRNA. **(D)** RNA primer translocation. **(E)** Start of plus-strand DNA synthesis. **(F)** Circularization by template switch. **(G)** Plus-strand DNA elongation. More details are given in the main text (Zlotnick et al. 2015).

1.1.5 Formation and persistence of HBV cccDNA

The cccDNA is the persistence form of HBV and, thus, a major therapeutic target in chronic hepatitis B. It is formed from rcDNA in the nucleus of infected cells. The rcDNA differs from cccDNA by having a covalently linked P protein, an RNA primer at the 5' end of the plus-strand DNA, terminal redundancies at the minus-strand DNA, an incomplete plus strand and it is nicked. Because of the distinct molecular properties of rcDNA and cccDNA, several enzymatic steps are supposedly involved in the conversion but only few details of this process are known so far (Nassal 2015). Königer *et al.* provided evidence for the involvement of tyrosyl-DNA-phosphodiesterase (TDP) 2 in generation of cccDNA. Viral P protein is linked to rcDNA by a tyrosyl-DNA phosphodiester bond and resembles thereby cellular topoisomerase-DNA adducts, which are repaired by cellular TDP1 or TDP2 enzymes. Human TDP2 can release P protein from HBV rcDNA *in vitro* (Königer et al. 2014). Furthermore, Qi *et al.* demonstrated that inhibition of host DNA polymerase κ (POLK) impairs cccDNA generation, an effect which can be rescued partially by ectopic expression of POLK. Results indicated that POLK is involved in cccDNA formation during HBV infection by repairing the gap of rcDNA (Qi et al. 2016). However, further steps in cccDNA generation remain elusive.

After formation of cccDNA, it persists as episome in the nucleus of the infected cell and gets organized into a viral minichromosome, i.e. it acquires a chromatin-like structure by nucleosomal packaging (Levrero et al. 2009, Nassal 2015), as shown in figure 5. The HBV minichromosome consists of histones H3 and H2B and to lower levels of histones H4, H2A and H1 (Bock et al. 2001). Additionally, HBV core protein binds to cccDNA (Bock et al. 2001, Guo, Li et al. 2011, Pollicino et al. 2006), which results in a reduction of the nucleosomal spacing (Bock et al. 2001). Histone posttranslational modifications favouring active transcription are enriched on cccDNA and repressive histone marks are underrepresented (Tropberger et al. 2015), but histone modifications are changeable. Modification of histone methylation patterns influences transcription from cccDNA (Rivière et al. 2015) as well as acetylation of cccDNA-bound H3 and H4 histones modulates HBV replication (Pollicino et al. 2006). Also, the viral HBx was shown to enable transcription from cccDNA by preventing deacetylation of cccDNA-attached histones (Belloni et al. 2009, Lucifora, Arzberger et al. 2011) and to avoid transcriptional repression of cccDNA by modification of histone methylation (Rivière et al. 2015). Moreover, interferon-alpha (IFN-α) treatment leads to hypoacetylation of cccDNA-bound histones and, thus, inhibition of transcription from cccDNA (Belloni et al. 2012, Tropberger et al. 2015). Furthermore, cccDNA itself can be methylated and hypermethylation correlates with decreased transcription and HBV replication (Guo, Li et al. 2011, Guo et al. 2009). The epigenetic features of cccDNA, which determine its permissiveness for transcription, are summarized in figure 6.

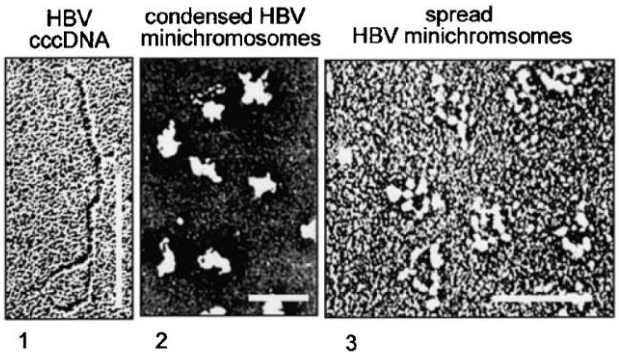

Figure 5: Electron microscopy of HBV cccDNA forms. (1) *In vitro* reconstituted HBV nucleoprotein complexes, **(2)** HBV nucleoprotein complexes under physiological ionic conditions and **(3)** in low salt buffer showing "beads-on-a-string" appearance. Scale bar: 0.2 µm (Bock et al. 2001).

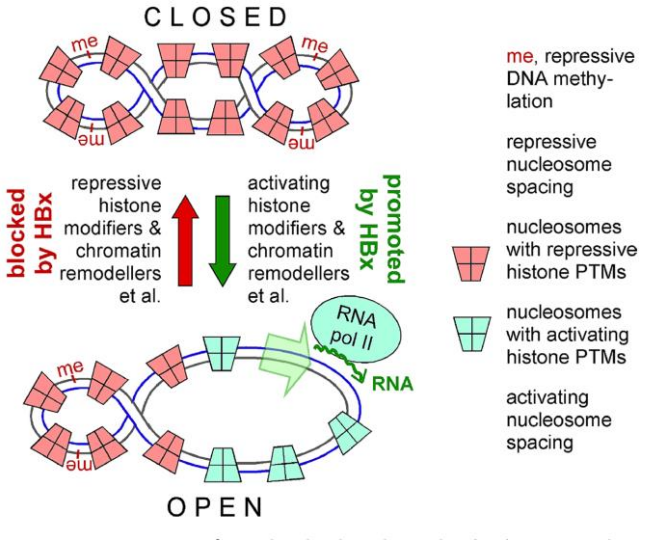

Figure 6: Epigenetic features of cccDNA. cccDNA is associated with nucleosomes consisting of histones H2A, H2B, H3, H4 and H1. Histone post-translational modifications (PTM) and DNA methylation (me) regulate the epigenetic permissiveness of cccDNA. The HBx modulates the epigenetic status of cccDNA and, thus, transcription by RNA polymerase II (RNA pol II) (Nassal 2015).

Few cccDNA copies per nucleus of infected cell are reported. In livers of chronically infected ducks, a mean of 10 cccDNA copies/cells were detected, whereby copy numbers distributed between one and 17 cccDNA copies/cell (Zhang et al. 2003). In human, HBV-infected HepG2-NTCP cells, cccDNA copy number was estimated to 2.4 copies/cell (Tropberger et al. 2015). Half-life of cccDNA in DHBV-infected ducks was determined at 35 to 57 days (Addison et al. 2002), in HBV-infected human HepG2-NTCP cells at approx. 30 days (Ko et al. 2017). Cell division of *in vivo* proliferating HBV-infected hepatocytes can lead to cccDNA loss (Lutgehetmann, Volz et al. 2010), but in cell culture systems cccDNA endures several rounds of cell division (Ko et al. 2017). Whether reimport of rcDNA-containing nucleocapsids from the cytoplasm refills the cccDNA pool, depends on the model system. In DHBV infection, cccDNA can recycle efficiently (Köck et al. 2010) but dHepaRG cells, differentiated human hepatoma cells, favour long-term persistence of HBV without cccDNA amplification (Hantz et al. 2009). Due to the stability of the cccDNA pool in dHepaRG cells, this cell culture system was preferentially used in this thesis.

1.1.6 HBV infection and therapy

Transmission of HBV occurs via blood or blood products, sexual contacts and from mother to child during birth (Modrow et al. 2010). Infection with HBV is often asymptomatic in adults, only one third shows symptoms of an acute, icteric hepatitis and 0.5 – 1 % of infected adults develop a fulminant hepatitis with liver failure. 5 – 10 % of HBV-infected adults develop chronic hepatitis (RKI 2015). In contrast, children up to six months of age develop chronic hepatitis B in 90 % of infection cases. Besides young age, the risk of developing chronic hepatitis B increases to 30 – 90 % under immune suppression (RKI 2015, Schweitzer et al. 2015).

HBV is a non-cytopathic virus, i.e. liver damage and viral control are mediated by the immune system. Hepatitis B surface antigen (HBsAg), that mainly consists of spherical subviral particles, appears two to ten weeks after HBV infection. In acute hepatitis B, alanine aminotransferase (ALT) concentrations as indicator of liver inflammation raise one to two weeks after the appearance of HBsAg, simultaneously to appearance of symptoms and anti-HBV-core antibodies. Anti-HBsAg antibodies raise several weeks later, approximately at the time point when HBsAg is cleared from serum in people who recover. In this case, ALT levels normalize and viral marker and symptoms disappear. If HBsAg persists for more than six months, HBV infection is considered as chronic. Following a high replicative phase without obvious liver disease, HBV DNA levels decrease and ALT levels increase in the “immune clearance” phase of chronic HBV infection. The immune response, however, fails to clear the virus. When HBeAg seroconversion takes place, HBV DNA levels are lowered and when ALT concentrations normalize, transition into the inactive phase takes place. In 20 – 30 % of patients, reactivation will occur with increase of HBV DNA and/or ALT levels after HBeAg seroconversion. These patients have an increased risk to develop liver cirrhosis and hepatocellular carcinoma (Trépo et al. 2014).

Currently, seven antivirals are approved for therapy of chronic hepatitis B: conventional or PEGylated IFN-α and the nucleoside or nucleotide analogues entecavir, lamivudine, tenofovir, adefovir and telbivudine. IFN-α has antiviral as well as immunomodulatory effects. A big disadvantage of IFN-α, however, are the side-effects, such as influenza-like symptoms, fatigue, bone marrow suppression, depression and unmasking of autoimmune diseases (Trépo et al. 2014). Treatment with PEGylated IFN-α is rather inefficient with response rates below 10 % defined by HBsAg seroconversion (Janssen et al. 2005).
Nucleos(t)ide analogues inhibit viral reverse transcription of pgRNA into rcDNA and affect therefore HBV replication late in the viral replication cycle. They are not directly targeting the persistence form cccDNA, which makes viral relapse common after treatment stop (Revill et al. 2016, Trépo et al. 2014). Nucleos(t)ide analogue treatment suppresses HBV but cannot eradicate the virus completely. Therefore, further research is needed to cure chronic HBV infection. The current opinion in the field is, that a

“functional cure” might suffice, which is characterized by HBsAg loss and HBsAg seroconversion, undetectable serum HBV DNA amounts and transcriptionally inactive cccDNA, enabling to stop treatment (Revill et al. 2016).

1.2 Antiviral T-cell immunity

A proper adaptive immune response early in HBV infection is essential for an efficient control of the virus infection. Thus, the following chapters focus on the antiviral role of T cells in HBV infection, their cytotoxic and non-cytolytic functions.

1.2.1 T-cell responses in acute and chronic hepatitis B

The initial phase after HBV infection, when HBV DNA is not yet or only weakly detected, is followed by an exponential increase of HBV replication. In acute HBV infection, HBV-specific CD4 and CD8 T-cell responses are detected (Bertoletti and Ferrari 2012). CD4 helper and CD8 cytotoxic T cells react to epitopes of HBV core protein, P protein and envelope proteins (Said and Abdelwahab 2015). T-cell responses in acute and self-limiting HBV infection are typically multispecific, strong and polyfunctional (Bertoletti and Ferrari 2012, Said and Abdelwahab 2015). Additionally, T-cells secrete cytokines and contribute to the antiviral effect against HBV without liver cell destruction (Guidotti et al. 1999). When acute HBV infection is controlled, T cells mature into memory cells, marked by increased expression of CD127 and decreased expression of programmed death (PD)-1 on HBV-specific CD8 T cells (Boettler, Panther et al. 2006).

In chronic hepatitis B, HBV persistence is linked to impaired functions of HBV-specific CD4 and CD8 T cells. High viremia correlates with suppressed HBV-specific T-cell responses and T cells in the liver are less functional than in the periphery (Bertoletti and Ferrari 2012). High viral antigen loads and tolerogenic features of hepatocytes might contribute to a weak, oligoclonal and exhausted T-cell response in chronic hepatitis B (Bertoletti and Ferrari 2012, Protzer et al. 2012). Exhaustion (i.e. functional inactivation) is driven by increased negative co-regulation, mediated by e.g. PD-1 expression, which can inhibit antiviral immunity in the liver (Iwai et al. 2003). Further, virus-specific cytotoxic T cells are depleted during chronic HBV infection, in part by enhanced susceptibility to apoptosis (Lopes et al. 2008).

1.2.2 Cytotoxic T-cell response

As part of the adaptive immune system, cytotoxic T cells (also: cytotoxic T lymphocytes, cytolytic T cells, CD8 T cells) can recognize and eliminate cells presenting foreign antigen, e.g. virus-infected cells. Cytotoxic T cells are primed in lymphoid organs by professional antigen presenting cells (APCs) or dendritic cells. Activation of naïve T cells

by APCs requires contact with an antigen via their specific T-cell receptor (TCR), CD8 or CD4 co-receptor binding, co-stimulation by interaction of T-cell CD28 with its ligand B7 on the APC and cytokine stimulation for T-cell proliferation and differentiation. T cells with CD8 receptors interact with MHC I (major histocompatibility complex I) molecules. When a cell is infected with a virus, its MHC I molecule can get loaded with viral antigen processed into a peptide of approximately nine amino acids allowing recognition of the peptide/MHC I complex by the TCR. After clonal expansion, cytotoxic T cells migrate from lymph nodes to the infected tissue, where they recognize foreign antigen and elicit their effector functions without the need for co-stimulation (Murphy and Weaver 2016).

CD8 T cells have two major pathways to perform their cytotoxic effector functions: They can release granzyme B and perforin. Perforin enables entry of granzyme B into the cytoplasm of the target cells and granzyme B induces apoptosis. Additionally, the membrane-bound Fas ligand (FasL) binds to the death receptor Fas (CD95), which triggers activation of a caspase cascade resulting in apoptosis (Thome and Tschopp 2001).

1.2.3 Non-cytolytic T-cell functions

Beside target cell killing, CD8 T cells secrete cytokines and elicit non-cytolytic antiviral functions. Evidence for it comes from studies with HBV transgenic mice. HBV-specific cytotoxic T cells suppress HBV gene expression through the cytokines interferon-gamma (IFN-γ) and tumour necrosis factor-alpha (TNF-α) in a non-cytolytic manner, which is stronger than the cytolytic effect (Guidotti et al. 1994). Also, HBV-specific cytotoxic T cells from perforin-deficient mice were still able to inhibit HBV replication without inducing liver disease (Guidotti et al. 1996). In acute HBV infection in chimpanzees, HBV DNA in the liver was diminished before liver disease and CD8 T cell infiltration reached their maxima, indicating that non-cytolytic mechanisms contribute to the purging of HBV cccDNA from infected cells (Guidotti et al. 1999). Similarly, Wieland, Spangenberg *et al.* showed in HBV-infected chimpanzees that cccDNA is reduced initially in a non-cytolytic manner. In this phase, cccDNA declined in parallel to appearance of IFN-γ producing CD8 T cells in the liver, while HBV-core-positive hepatocytes persisted longer (figure 7) (Wieland, Spangenberg et al. 2004). *In vitro* experiments further evidenced that HBV-specific CD8 T cells can control HBV replication without cytolysis via IFN-γ and TNF-α and that these non-cytolytic mechanisms contribute importantly to the antiviral function of CD8 T cells (Phillips et al. 2010).

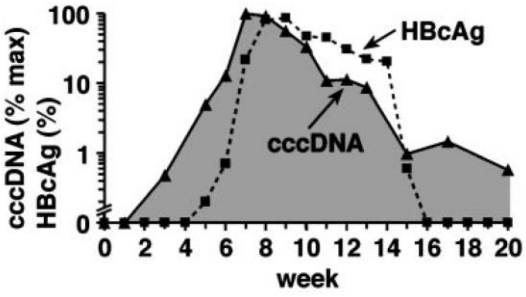

Figure 7: Decline of cccDNA in acutely HBV-infected chimpanzee. While cccDNA decreases after week 8, HBV core protein (HBcAg) starts to diminish after week 9, indicating that the loss of cccDNA is not reflecting target cell lysis but non-cytolytic effects (Wieland, Spangenberg et al. 2004).

1.3 Antiviral effects of cytokines

As inflammatory mediators, cytokines are involved in antiviral defence. There are more than 60 different cytokines (Murphy and Weaver 2016), of which the four important ones for this thesis are described in the following chapters in more detail.

1.3.1 Interferon-alpha (IFN-α)

Interferons are small, secreted proteins and have been discovered as substances that interfere with influenza virus infection. The largest class of interferons are type I interferons, which compromise IFN-α and interferon-beta (IFN-β) among others. Nearly all cells can produce IFN-α but during infection it is mainly produced by plasmacytoid dendritic cells. Type I interferons bind to a heterodimeric receptor consisting of an IFN-α receptor 1 (IFNAR1) and IFNAR2 subunit. Intracellular signalling is mediated by phosphorylation of Janus kinase 1 (JAK1) and tyrosine kinase 2 (TYK2) leading to phosphorylation and heterodimerisation of signal transducers and activators of transcription 1 (STAT1) and STAT2 proteins. After association with interferon-regulatory factor 9 (IRF9), the whole complex translocates to the nucleus to activate transcription of interferon-stimulated genes (*ISGs*) (figure 8) (Schneider et al. 2014). ISGs with antiviral activity against HBV are, for instance, myxoma resistance protein 1 (MxA), which inhibits HBV replication at posttranscriptional level (Gordien et al. 2001), apolipoprotein B editing complex 3 (APOBEC3) deaminases (Janahi and McGarvey 2013) and interferon-stimulated gene product of 20 kDa (ISG20) (Leong, Funami et al. 2016, Liu et al. 2017, Ma et al. 2016).The latter two are described in the chapters below in more detail.

Type I interferons can modulate innate and adaptive immune responses, e.g. by stimulating effector functions of natural killer cells, cytotoxic T cells and macrophages, by enhancing antigen presentation and induction of antibody production. Further, they can inhibit cell division and stimulate proliferation of memory T cells (Guidotti and Chisari 2001). Beside their immunomodulatory functions, type I interferons elicit direct antiviral activity against a broad range of viruses and IFN-α was shown to inhibit HBV on several

distinct levels. For instance, cells treated with IFN-α release factors inhibiting HBV entry by competing with viral binding to heparan sulphate proteoglycans (Xia et al. 2017a). IFN-α can also lead to epigenetic silencing of HBV cccDNA, thereby inhibiting viral transcription (Belloni et al. 2012). Further studies confirmed the IFN-α-triggered HBV repression by modulation of histones associated with cccDNA (Tropberger et al. 2015). Additionally, IFN-α leads to decay of HBV nucleic-acid containing capsids (Xu et al. 2010).

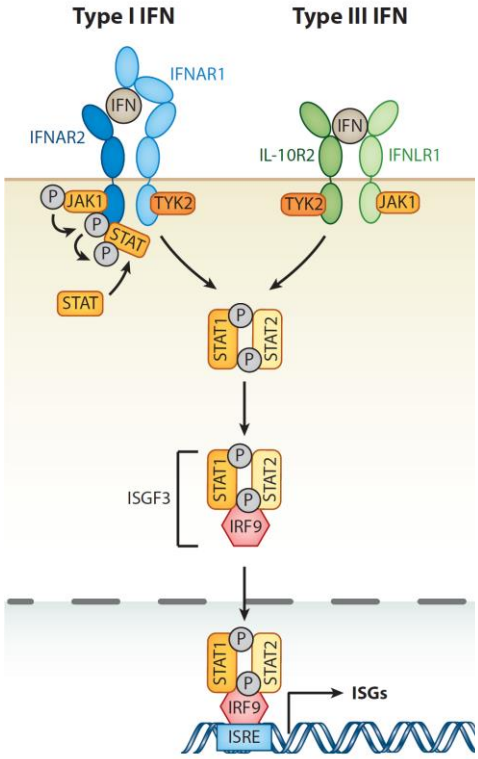

Figure 8: Type I interferon (IFN) signalling. Type I interferons bind to their receptor on the cell surface inducing JAK/STAT signalling. Formation of the complex interferon-stimulated gene factor 3 (ISGF3) enables target gene expression after translocation to the nucleus and binding to interferon-stimulated response elements (ISRE). Similar signalling is induced by type III interferons binding to interleukin-10 receptor 2 (IL-10R2) and interferon-lambda receptor 1 (IFNLR1) (Schneider et al. 2014).

1.3.2 Interferon-gamma (IFN-γ)

IFN-γ is the only representative of type II interferons. It is produced by cells of the immune system but nearly all cell types express the IFN-γ receptor (IFNGR) and can, thus, respond to it. Binding of IFN-γ to two IFNGR1 subunits causes additional binding of two IFNGR2 subunits. Following receptor activation, JAK1 and JAK2 kinases are phosphorylated resulting in dimerization of two phosphorylated STAT1 proteins. These homodimers enter the nucleus to induce target ISG transcription (figure 9) (Schneider et al. 2014). As IFN-α does, IFN-γ induces the expression of APOBEC3 proteins (Janahi and McGarvey 2013) and ISG20 (Gongora et al. 1997). More details on their antiviral role against HBV are given in the chapters below.

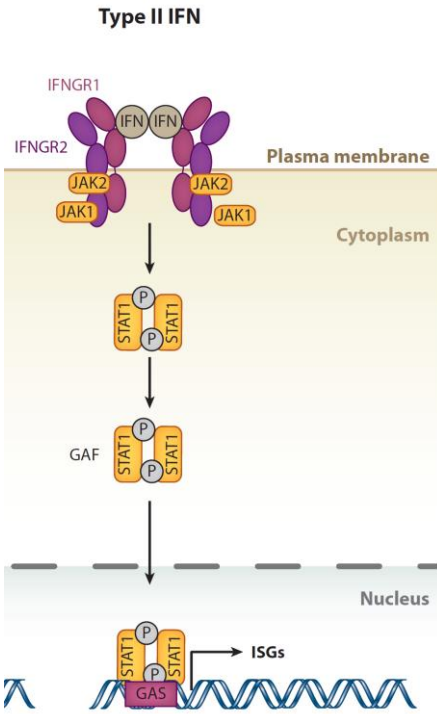

Figure 9: Type II interferon signalling. Type II interferons bind to their receptors triggering the JAK/STAT pathway. Phosphorylated STAT1 homodimers build the IFN-γ activation factor (GAF), that translocates to the nucleus, where it binds to gamma-activated sequence (GAS) promoter elements to induce target gene expression (Schneider et al. 2014).

Antiviral T-cell cytokines, such as IFN-γ, can control viral infection indirectly, by immunoregulatory activity, enhancing antigen presentation, triggering homing of T cells to the infected tissue or stimulating the cytolytic function of effector cells of the innate or adaptive immune response (Guidotti and Chisari 2001). IFN-γ is also capable of controlling HBV replication directly and can induce non-cytolytic HBV DNA decline (Guidotti et al. 1999, Phillips et al. 2010, Wieland, Spangenberg et al. 2004). Moreover, IFN-γ was shown to destabilize HBV RNAs (Heise et al. 1999), to inhibit viral protein translation by tryptophan deprivation (Mao et al. 2011) and to accelerate the decay of nucleic-acid containing HBV capsids (Xu et al. 2010).

1.3.3 Tumour necrosis factor-alpha (TNF-α)

TNF was originally found as tumour-destroying cytokine, where it got its name from. The TNF superfamily includes many members, e.g. TNF-α, FasL, CD40 ligand, OX40 ligand and lymphotoxins. TNF-α is secreted by activated T cells, monocytes, natural killer cells, mast cells, B cells and Kupffer cells in the liver. IFN-γ can increase its expression. Secreted TNF-α binds preferentially to TNF receptor 1 (TNFR1), which is expressed on all cell types despite erythrocytes. The second receptor TNFR2 is inducible and expressed particularly on endothelial and hematopoietic cells (Valaydon et al. 2016). In general and depending on cell type, status of the cell and cell cycle, TNFR1 activation leads to induction of apoptosis. This involves the adaptor proteins TNFR1-associated death domain (TRADD) and Fas-associated death domain (FADD) and is triggered by a

caspase cascade. In contrast, TNFR2 activation can promote cell survival. TNFR2 signalling involves cellular inhibitor of apoptosis protein (cIAP) and leads to nuclear translocation of the transcription factor NF-κB resulting in transcription of pro-survival genes (figure 10) (Faustman and Davis 2010, Valaydon et al. 2016).

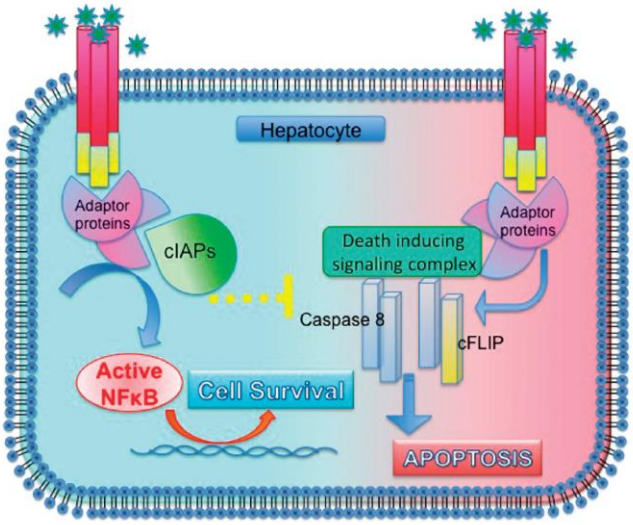

Figure 10: TNF-α induced pathways in hepatocytes. Recruitment of cIAP (cellular inhibitor of apoptosis) after receptor binding leads to upregulation of cell survival proteins. If cIAP is absent, cell death is induced (Valaydon et al. 2016).

To fulfil its antiviral function against HBV, TNF-α can induce the non-cytolytic disruption of HBV nucleocapsids via NF-κB signalling (Biermer et al. 2003). Furthermore, TNF-α destabilizes HBV RNAs together with IFN-γ (Guidotti et al. 1996). As T-cell cytokine, it mediates the non-cytolytic control of HBV replication (Phillips et al. 2010). Polymorphisms in the TNF-α gene are associated with the outcome of HBV infection, such as the 238A allele was linked with an increased risk to develop chronic hepatitis B in European populations (Zheng et al. 2012). Moreover, anti-TNF-α therapy, which is applied for treatment of inflammatory arthritis, can result in HBV reactivation in patients with chronic HBV infection who do not receive antiviral prophylaxis (Ye, Zhang et al. 2014).

1.3.4 Lymphotoxins (LT)

Lymphotoxins are cytokines belonging to the TNF superfamily that are involved in lymph-node development (Murphy and Weaver 2016). They are expressed by T cells, B cells, natural killer cells and lymphoid tissue-inducer cells. Lymphotoxin-beta (LTβ) is a transmembrane protein and forms membrane-anchored heterotrimers together with lymphotoxin-alpha (LTα), i.e. LTα1β2 and LTα2β1. Matrix metalloproteases can cleave these heterotrimers from the cellular surface, however. In contrast, LTα is secreted directly as soluble homotrimer. LTα and LTα2β1 activate TNFR1 or TNFR2, which are described above. In contrast, LTα1β2 signals via LTβR. LTβR stimulation triggers signalling via canonical or non-canonical NF-κB pathway. In the canonical NF-κB

signalling pathway, the complex of NEMO/IKKα/IKKβ is activated leading to phosphorylation and proteasomal degradation of the inhibitor of κB (IκB). This allows the heterodimer p50/RelA to enter the nucleus and induce gene expression involved for example in inflammation and cell proliferation. In contrast, the non-canonical signalling activates NF-κB-inducing kinase (NIK), which leads to phosphorylation of a homodimeric IKKα complex. This results in phosphorylation and proteasomal degradation of p100 into p52, which enters the nucleus as a heterodimer with RelB triggering target gene expression, important for instance in lymph-node development or B-cell survival (figure 11) (Wolf et al. 2010).

Lymphotoxins and LTβR were reported to be upregulated in HBV-induced hepatitis and hepatocellular carcinoma and sustained lymphotoxin signalling seems to be involved in hepatitis-induced carcinoma (Haybaeck, Zeller et al. 2009). However, depending on the cell type, LTβR agonisation can inhibit tumour growth in human colon carcinoma, mammary carcinoma and soft tissue sarcoma cells (Hu, Zimmerman et al. 2013).

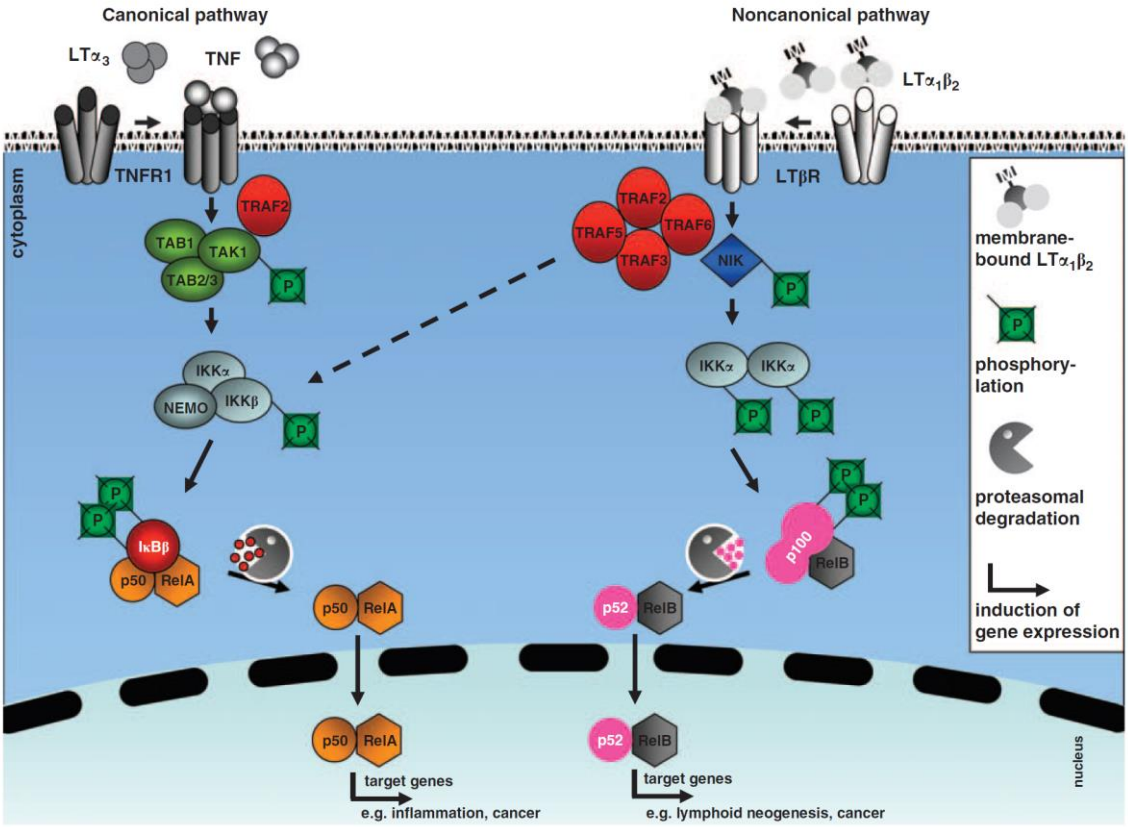

Figure 11: Canonical and non-canonical NF-κB signalling induced by lymphotoxins. Many agonists induce the canonical NF-κB pathway, here TNF and LTα3 are shown as examples (left part). LTα1β2 binding triggers non-canonical NF-κB signalling (right part) but can also induce the canonical NF-κB pathway (Wolf et al. 2010).

1.3.5 APOBEC3 deaminases as cytokine-induced effector proteins

APOBEC3 enzymes elicit antiviral activity against a broad range of DNA viruses and retroviruses (Stavrou and Ross 2015). These proteins are a family of cytidine deaminases converting cytosines to uracils in viral DNA (Janahi and McGarvey 2013). Several members of the APOBEC3 family can mutate HBV in this way. For instance, APOBEC3G (A3G) was shown to induce hypermutations on HBV rcDNA (Kitamura et al. 2013). In contrast to the cytoplasmic A3G, APOBEC3B (A3B) can locate in both cytoplasm and nucleus and it was reported to hypermutate HBV genomes too (Bonvin et al. 2006). A3B and APOBEC3A (A3A) can deaminate single-stranded DNA during replication (Hoopes, Cortez et al. 2016). A3A was reported to be involved in the degradation mechanism of foreign DNA, as depicted in figure 12: Interferon induces expression of A3A, which deaminates foreign DNA generating a substrate for uracil DNA glycosylase (UNG) 2. After uracil excision, apurinic/apyrimidinic site endonuclease (APEX) might possibly function as nuclease causing DNA degradation (Stenglein et al. 2010).

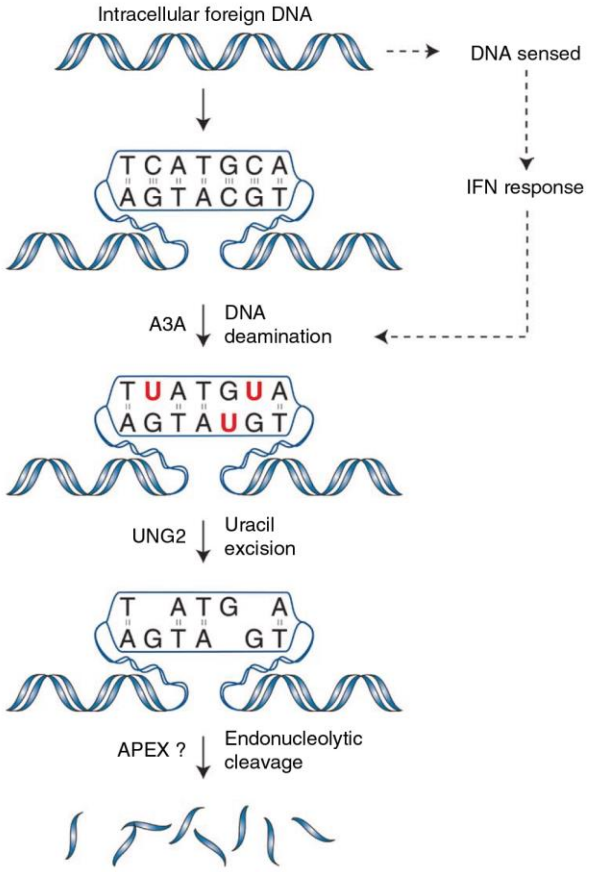

Figure 12: Degradation of foreign DNA involving deamination by A3A. Interferon-induced A3A deaminates foreign DNA leading to uracil excision by UNG2 (uracil DNA glycosylase 2) and DNA digestion possibly by APEX (apurinic/ apyrimidinic site endonuclease) (Stenglein et al. 2010).

1.3.6 ISG20 as interferon-induced effector nuclease

The interferon-induced ISG20 (Gongora et al. 1997) or HEM45 (HeLa Estrogen Modulated, band 45) (Pentecost 1998) is a 3' to 5' exonuclease, that can degrade single-stranded RNA and DNA (Nguyen et al. 2001). It belongs to the DEDDh subgroup of the DEDD exonuclease superfamily, which is characterized by three conserved aspartate (D), one conserved glutamate (E) and one conserved histidine (H) residue, and has three distinct exonuclease motifs named Exo I, Exo II and Exo III (Degols et al. 2007, Moser et al. 1997). ISG20 localizes to the nuclei and the cytoplasm of hepatocytes during response to IFN-α treatment (Lu et al. 2013).

ISG20 exerts antiviral activity against several viruses (Zheng et al. 2017), e.g. vesicular stomatitis virus, influenza virus, encephalomyocarditis virus (Espert et al. 2003) and human immunodeficiency virus type 1 (HIV-1) (Espert, Degols et al. 2005). Replication of HIV-1 was delayed by ISG20 when a catalytically active form was expressed (Espert, Degols et al. 2005). Recent studies showed that ISG20 expression itself can block HBV replication by degrading HBV RNA via its exonuclease activity (Leong, Funami et al. 2016, Liu et al. 2017, Ma et al. 2016). Through its binding to the ε stem-loop structure of HBV RNA, ISG20 can prevent pgRNA encapsidation even in its catalytically inactive form (Liu et al. 2017), thus providing several antiviral modes of action.

1.4 Aims of the study

So far, no curative treatment is available for chronic hepatitis B. A major problem in chronic HBV infection is the viral persistence mediated by the HBV cccDNA form in the nucleus of infected hepatocytes. Therefore, cccDNA is an important therapeutic target. Beside approaches which lead to direct killing of HBV-infected cells, non-cytolytic antiviral strategies targeting cccDNA gain increasing interest. The overall aim of this thesis was, thus, to obtain a detailed picture of the molecular mechanisms of non-cytolytic cccDNA loss through antiviral cytokine activity.

The first question addressed in this thesis was whether T-cell cytokines can reduce cccDNA in human hepatocytes without cytolysis, and by which mechanism this is achieved. A transwell co-culture system should be established to avoid killing through direct contact of T cells and HBV-infected target cells and to investigate the cytokine secretion of activated T cells together with the cytokine effects on HBV DNA and protein expression.

The aim of the second part of the thesis was to figure out whether the cytokine-induced DNA decline is specific for cccDNA or whether it can target any episomal DNA. For that purpose, a hepatoma cell line replicating HBV from an episomal construct should be studied regarding cytokine-induced deamination and decay of cccDNA and episomal DNA as well as protein interactions with cccDNA should be examined.

The third part of the thesis aimed at identifying the nuclease that is triggering cccDNA decay under treatment with cytokines IFN-α and IFN-γ. To this end, gene expression under interferon treatment in human hepatoma cells should be investigated and functional studies should be carried out to ascertain the nuclease involved in interferon-induced cccDNA reduction.

2 Results

According to the aims of the thesis, this part deals with three aspects of the control of HBV persistence, namely the non-cytolytic reduction of cccDNA by T-cell cytokines, the specificity of the treatment-induced cccDNA decline and the nuclease involved in interferon-triggered cccDNA loss in this mechanism.

2.1 Non-cytolytic reduction of HBV cccDNA by T-cell cytokines IFN-γ and TNF-α

In animal models, it has been suggested that T-cell cytokines contribute non-cytolytically to HBV clearance in acute, self-limiting hepatitis B (Guidotti et al. 1999, Wieland, Spangenberg et al. 2004). Further studies *in vitro* confirmed that T-cell cytokines IFN-γ and TNF-α are involved in the inhibition of HBV without cytolysis (Phillips et al. 2010). This part of the thesis, thus, examined the non-cytolytic effect of these T-cell cytokines on HBV cccDNA in human hepatoma cells focusing thereby on the mechanism of the reduction of cccDNA, the HBV persistence form.

2.1.1 Activated T cells secrete IFN-γ and TNF-α and induce cccDNA loss

First, to investigate non-cytolytic effects of T-cell cytokines directed against HBV in human hepatoma cells, a transwell co-culture system was established. This allows a separation of non-cytolytic T-cell functions from direct killing by cytotoxic T cells: Hepatoma cells expressing HBsAg on their surface (Huh7-S cells) or control cells (Huh7 cells) were seeded into the upper transwell chamber. On top of these cells, T cells were added which have a chimeric antigen receptor recognizing HBsAg (S-CAR) (Bohne et al. 2008). S-CAR T cells are activated by HBsAg on Huh7-S cells (figure 13A, left). Here, these S-CAR T cells were used as a model for HBV-specific T cells, that can be stimulated by the viral HBs leading to cytokine secretion and control of HBV replication (Bohne et al. 2008, Krebs, Böttinger et al. 2013). Activated T cells secreting cytokines were then transferred within the transwell-chamber to a cell culture vessel, where HepaRG cells were grown, differentiated and infected with HBV before. The secreted T-cell cytokines could pass through the pores of the transwell membrane and reached the HBV-infected target cells without direct contact of T cells and target cells. Thereby, cytokine-mediated, non-cytolytic effects of T cells on HBV could be studied (figure 13A, right) (Xia, Stadler et al. 2016).

In accordance with chimpanzee studies (Guidotti et al. 1999, Wieland, Spangenberg et al. 2004), we could confirm that patients with acute hepatitis B have elevated serum IFN-γ and TNF-α compared to patients with chronic hepatitis B or healthy donors (Xia, Stadler et al. 2016). Therefore, the secretion kinetics of IFN-γ and TNF-α by activated T

cells were determined first in the transwell system. ELISA experiments showed that only S-CAR T cells which were activated by co-culture with Huh7-S cells led to secretion of detectable amounts of IFN-γ and TNF-α. To determine the T-cell activation kinetics, supernatants from independent samples were analysed after two, four, eight, 16 and 24 hours of antigen stimulation. The results obtained by ELISA showed, that T cells started secretion of detectable amounts of IFN-γ and TNF-α after a minimum of 16 hours of antigen contact (figure 13B).

Transwells with activated S-CAR T cells for 16 hours were then transferred to HBV-infected dHepaRG cells. To test the minimal incubation time of activated T cells with target cells, which is necessary to get a loss of HBV cccDNA, transwells were removed after six, 12, 24, 36 or 48 hours of incubation. At the same time, cell culture supernatants were exchanged to remove secreted cytokines, so that stimulation of the HBV-infected target cells by cytokines was limited to the indicated time frames between six and 48 hours. HBV-infected dHepaRG cells were rested subsequently under standard culture conditions for a total of seven days to allow cytokine-induced effectors to elicit their antiviral functions. Results revealed that a 12-hour incubation time with activated T cells was sufficient to reduce cccDNA levels, reaching the maximal effect after 24 hours (figure 13C). Slightly delayed, also HBeAg (figure 13D) and total intracellular HBV DNA (figure 13E) were reduced by activated S-CAR T cells after 24 to 48 hours of incubation time.

In summary, this shows that activated T cells secrete IFN-γ and TNF-α and induce efficiently the reduction of HBV cccDNA, total intracellular HBV DNA and HBeAg levels (Xia, Stadler et al. 2016).

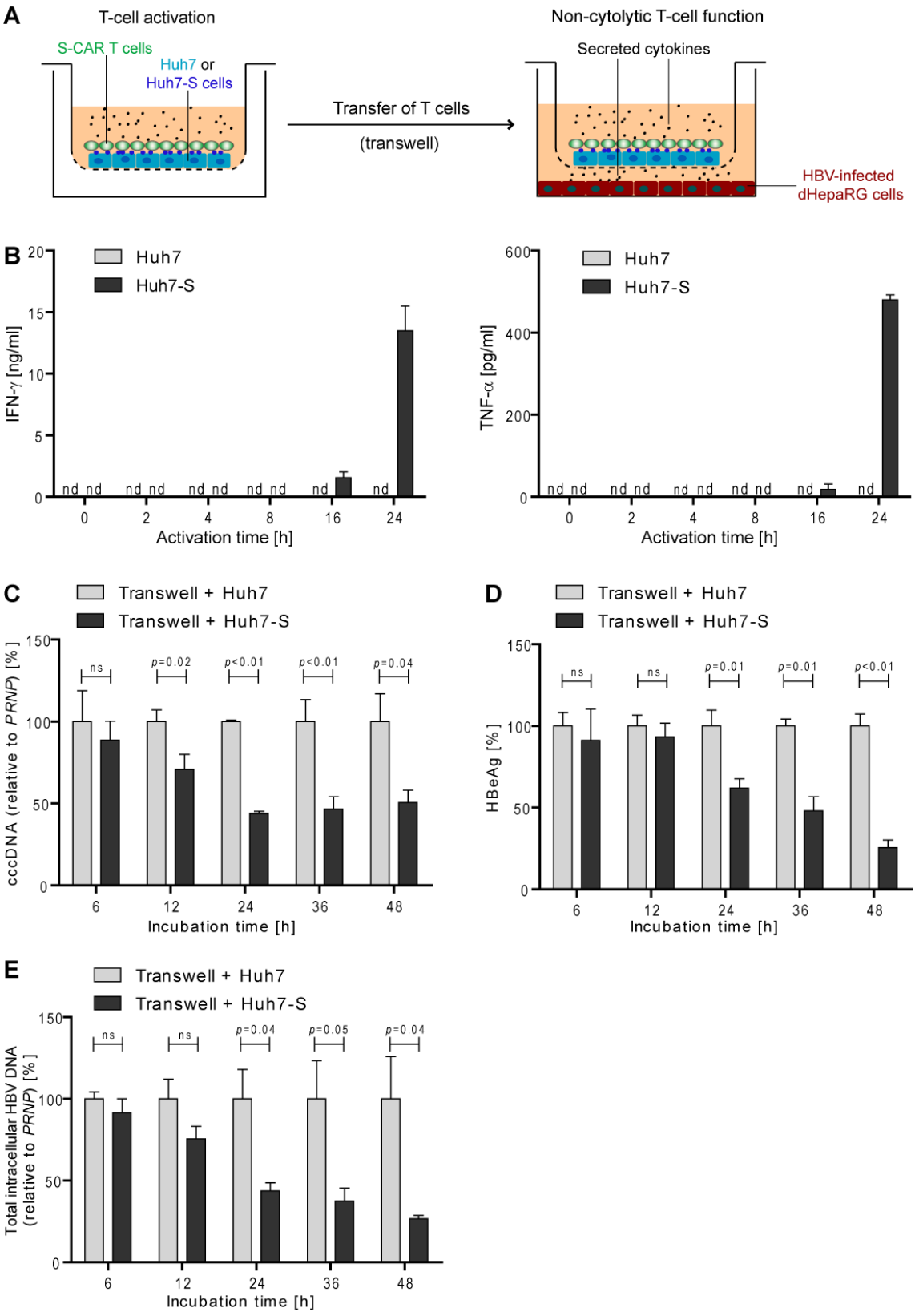

Figure 13: Cytokine secretion and non-cytolytic antiviral function of activated T cells. (A) HBsAg-specific (S-CAR) T cells were added in a transwell with either Huh7 or Huh7-S cells. Huh7-S cells activated S-CAR T cells by expression of HBsAg on the cellular surface, leading to

cytokine secretion. Transwells were transferred to cell culture vessels, where HBV-infected differentiated HepaRG (dHepaRG) cells were cultivated. T-cell cytokines could pass through the porous membrane of the transwell and elicit non-cytolytic, antiviral effects, whereby the transwell avoided direct contact of T cells with infected dHepaRG cells. **(B)** S-CAR T cells were activated by Huh7-S cells or kept with Huh7 cells as control for indicated time frames. Supernatants taken from different wells at each time point were analysed by ELISA to determine kinetics of IFN-γ and TNF-α secretion (n=3). **(C)** After 16 hours of activation, T cells within the transwells were transferred to HBV-infected dHepaRG cells (time point 0) and left there for the indicated incubation time to elicit their non-cytolytic functions. Amounts of cccDNA in HBV-infected dHepaRG cells, **(D)** HBeAg and **(E)** intracellular HBV DNA were determined at day seven by qPCR relative to *PRNP* (prion protein gene) or ELISA, respectively (n=3). Statistical analysis: Student's unpaired *t*-test with Welch's correction (ns: not significant, $p > 0.05$); nd: not detectable (Xia, Stadler et al. 2016).

2.1.2 Decline of cccDNA is mediated by T-cell cytokines IFN-γ and TNF-α

To ascertain the cytokines that mediate the non-cytolytic antiviral activity of T cells, neutralizing antibodies were applied in the transwell co-culture system. In this experimental setup, S-CAR T cells were stimulated by purified HBs (also termed HBsAg), which was used for coating of transwells, or kept without HBsAg as control. Stimulation of T cells without cytokine neutralization (no neutralizing antibodies) reduced cccDNA levels to approximately 20 % of the control level (without T-cell activation). IFN-γ neutralization rescued about two-thirds of this cccDNA decline. TNF-α neutralizing antibodies had a minor but still significant effect on blocking the reduction of cccDNA triggered by activated T cells. Both IFN-γ and TNF-α neutralizing antibodies together restored cccDNA levels to more than 80 % of control (figure 14A). Analogously, IFN-γ or TNF-α neutralization impaired HBeAg reduction and combination of both neutralizing antibodies restored HBeAg levels efficiently to over 80 % of control level (figure 14B) (Xia, Stadler et al. 2016).

As further potential T-cell effector cytokines (Murphy and Weaver 2016), lymphotoxins were neutralized by antibodies. Baminercept is a recombinant LTβR protein that can block LTα1β2 and LTα2β1 signalling. Etanercept as a recombinant TNF-receptor p75 protein can neutralize TNF-α and LTα3 signalling but can also block receptor binding of LTα1β2 and LTα2β1 cytokines. Baminercept addition to stimulated T cells in the transwell system did not alter cccDNA nor HBeAg levels. Etanercept blocked T-cell-mediated reduction of cccDNA and HBeAg to a small but significant extent. However, IFN-γ neutralization was still responsible for the major effects on restoration of cccDNA and HBeAg levels (figure 14C-D).

Altogether, neutralization experiments confirmed that IFN-γ and TNF-α are the key factors of cytokine-triggered, non-cytolytic cccDNA decline through activated T cells (Xia, Stadler et al. 2016).

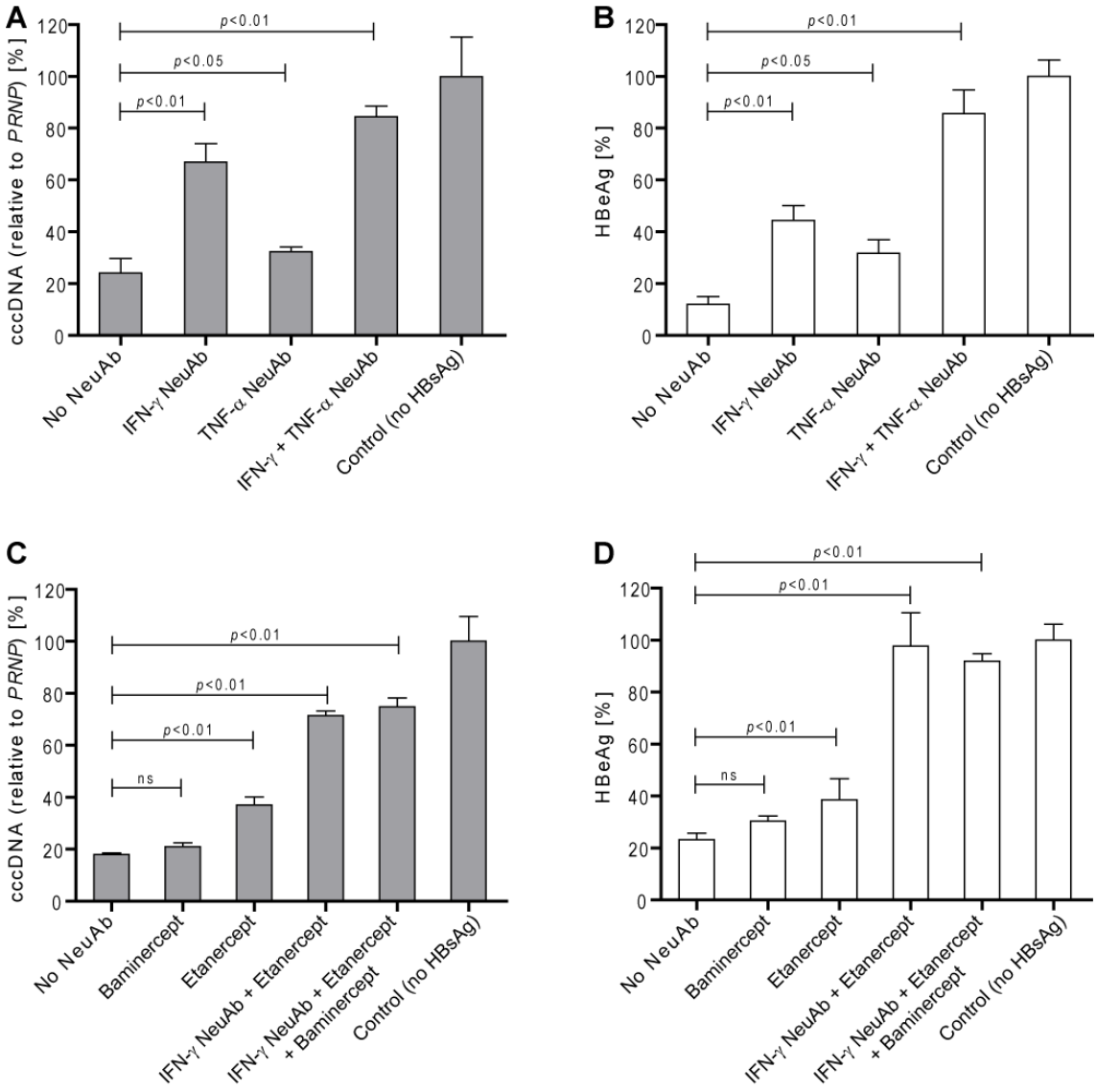

Figure 14: Neutralization of T-cell derived cytokines. (A) HBsAg-stimulated S-CAR T cells were kept in the transwell system and antibodies for neutralizing IFN-γ (IFN-γ NeuAb) and TNF-α (TNF-α NeuAb) were added to the cell culture medium. cccDNA levels from HBV-infected dHepaRG cells and **(B)** HBeAg levels were determined (n=3) (cooperation with Yuchen Xia). **(C, D)** Analogously, antibodies neutralizing LTβR-binding cytokines (Baminercept) or lymphotoxins and TNF-α (Etanercept) were applied in the transwell setting and **(C)** cccDNA and **(D)** HBeAg from HBV-infected dHepaRG cells were measured after seven days of transwell co-culture (n=3). No NeuAb: HBsAg-stimluated S-CAR T cells without application of neutralizing antibodies. No HBsAg: Control samples with unstimulated S-CAR T cells. Statistical analysis: Student's unpaired *t*-test with Welch's correction (ns: not significant, $p > 0.05$) (Xia, Stadler et al. 2016).

2.1.3 Cytokine-induced A3A and A3B are essential for cccDNA deamination and decay

We reported previously that IFN-α treatment and LTβR activation lead to cccDNA decline and that induction of cytosine deaminases A3A and A3B is essential herein (Lucifora, Xia et al. 2014). To examine whether the cccDNA loss induced by T-cell cytokines IFN-γ and TNF-α is mediated by a similar mechanism, expression of A3A and A3B and knockdown of these deaminases were studied in dHepaRG cells. For this purpose, purified cytokines were applied without the use of activated T cells to link the seen effects directly to the cytokines. As expected, both IFN-γ and TNF-α reduced HBeAg levels of HBV-infected dHepaRG cells substantially. At the same time, application of IFN-γ and TNF-α did not affect viability of HBV-infected dHepaRG cells, since lactate dehydrogenase (LDH) release into the supernatant as a marker for cell death was not increased compared to untreated control cells (figure 15A).

To see whether A3A and A3B are induced by IFN-γ and TNF-α treatment, the expression of these deaminases was investigated in HBV-infected dHepaRG cells. *A3A* mRNA levels were measured by qRT-PCR, showing that *A3A* expression is induced by IFN-γ treatment. Knockdown by siRNA lowered *A3A* levels largely below control levels (figure 15B). *A3B* was upregulated by both IFN-γ and TNF-α and knockdown by siRNA reduced *A3B* levels strongly in treated and untreated samples (figure 15C).

Next, deamination by cytokine-induced A3A and A3B was examined by differential DNA denaturation-PCR (3D-PCR). 3D-PCR is a method to amplify DNA sequences selectively at low denaturing temperatures if they were exposed to deamination before. Since DNA deamination results in formation of uracils from cytosines, amplification (e.g. by qPCR) leads to CG-to-TA conversions or so-called hypermutations. These AT-rich sequences have a lower melting temperature due to a reduced number of hydrogen bonds and can, thus, be detected with lower denaturing temperatures than the unmodified, original sequence (Suspene et al. 2005). Here, cccDNA amplicons from previous qPCR were used as templates in 3D-PCR to undergo cccDNA modifications. If cccDNA was deaminated, qPCR should produce AT-rich cccDNA amplicons, which can be detected in 3D-PCR. Indeed, with a control siRNA, both IFN-γ and TNF-α led to a lower permitted denaturing temperature in 3D-PCR suggesting induction of deamination and cccDNA modification. Knockdown of A3A and A3B inhibited cytokine-induced deamination almost completely as shown by highly similar cccDNA amplification patterns in 3D-PCR (figure 15D).

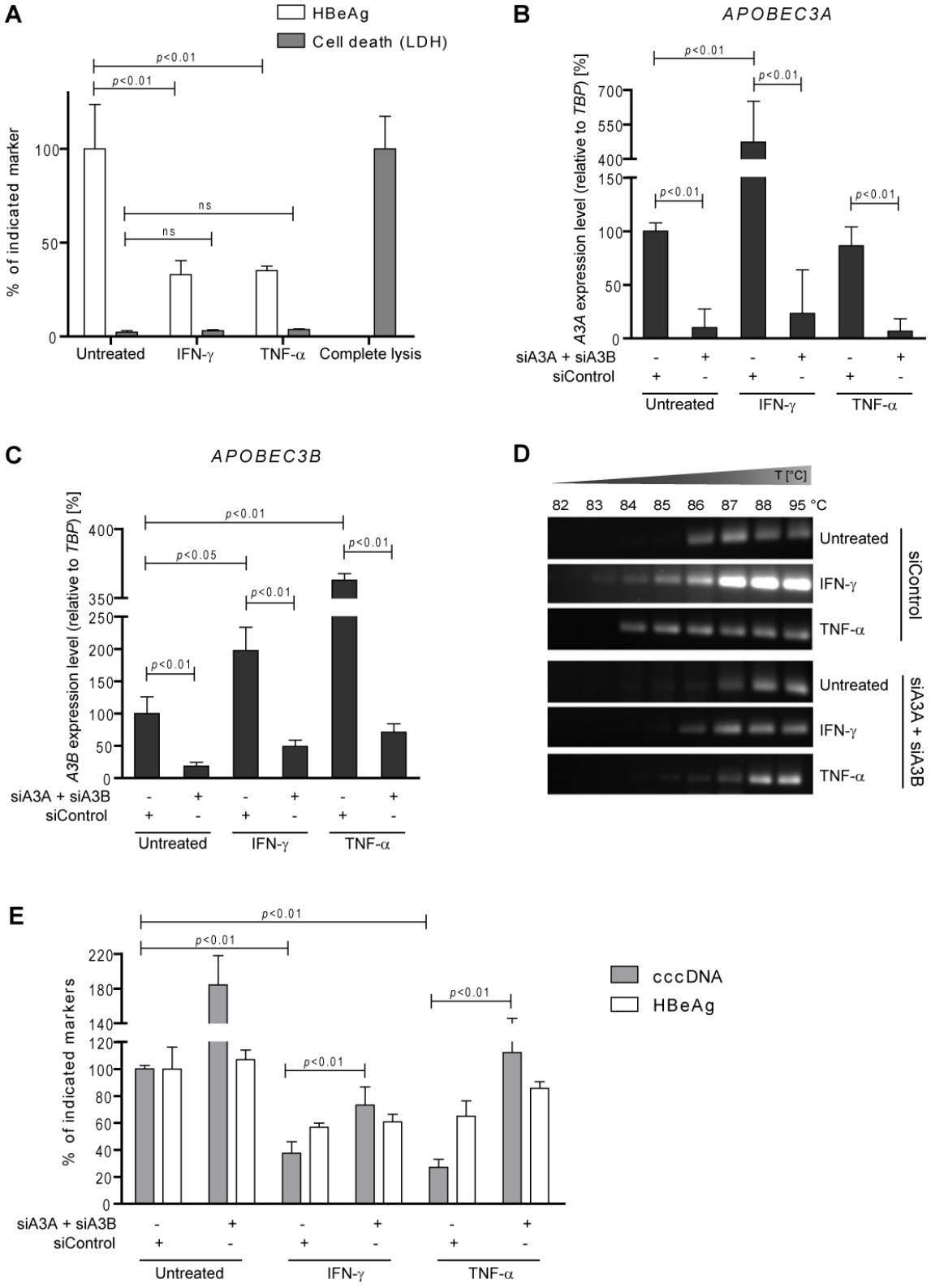

Figure 15: Deamination and cccDNA loss through cytokine-induced A3A and A3B. HBV-infected dHepaRG cells were treated with 200 U/ml IFN-γ or 800 U/ml TNF-α and **(A)** HBeAg was measured by ELISA seven days after treatment. LDH release assay was applied to the same samples to determine cell death (n=3). **(B, C)** HBV-infected dHepaRG cells were transfected with

siRNA against A3A and A3B (siA3A + siA3B) or control siRNA, treated with 200 U/ml IFN-γ or 800 U/ml TNF-α and analysed for **(B)** *A3A* and **(C)** *A3B* mRNA levels by qRT-PCR relative to *TBP* (TATA-box binding protein gene). **(D)** In analogous experiments, 3D-PCR was used to amplify AT-rich cccDNA amplicons to determine DNA deamination and **(E)** cccDNA and HBeAg were analysed by qPCR relative to *PRNP* or by ELISA, respectively. Statistical analysis: Student's unpaired *t*-test with Welch's correction (ns: not significant, $p > 0.05$) (cooperation with Yuchen Xia) (Xia, Stadler et al. 2016).

Accordingly, cccDNA levels from HBV-infected dHepaRG cells were reduced by treatment with IFN-γ and TNF-α using a control siRNA, and siRNA-mediated knockdown of A3A and A3B blocked cccDNA loss induced by IFN-γ or TNF-α treatment significantly. Remarkably, also the cccDNA level in untreated samples was higher when A3A and A3B were blocked. HBeAg levels displayed similar tendencies as cccDNA under IFN-γ or TNF-α treatment and changed slightly under A3A- and A3B-knockdown (figure 15E).

Altogether, these data show that A3A and A3B, induced by IFN-γ and TNF-α, are essential for cytokine-triggered deamination and decline of HBV cccDNA (Xia, Stadler et al. 2016).

2.2 Specificity of treatment-induced cccDNA loss

As demonstrated in the previous part, T-cell cytokines IFN-γ and TNF-α lead to non-cytolytic loss of cccDNA (Xia, Stadler et al. 2016), similar as IFN-α treatment and LTβR activation do (Lucifora, Xia et al. 2014). Therefore, the question of the following part was, whether this cytokine-mediated mechanism is specific for HBV cccDNA or whether any episomal DNA can be targeted.

2.2.1 Treatment-induced decay and deamination targets cccDNA but not episomal DNA

To have a cell culture system with nuclear episomes besides cccDNA, HepaRG-pEpi-H1.3 cells were used. These are HepaRG cells that carry an episomal construct including a 1.3-fold overlength HBV genome (pEpi-H1.3) in the nuclei (Stadler 2013). In these cells, HBV should be able to replicate from the viral genome on the episome allowing the quantification of the HBV markers HBeAg, total intracellular HBV DNA and cccDNA from the same samples in which the episome pEpi-H1.3 is measured. In this particular case, qPCR for total intracellular HBV DNA measures mainly rcDNA and minor amounts of cccDNA but includes also a small portion of pEpi-H1.3. HepaRG-pEpi-H1.3 cells were differentiated and treated for 11 days. Noteworthy, fully

differentiated HepaRG-pEpi-H1.3 (dHepaRG-pEpi-H1.3) cells enabled detection of HBeAg, total intracellular HBV DNA, cccDNA as well as pEpi-H1.3, whereby cccDNA and pEpi-H1.3 levels kept stable in untreated cells over the whole period of 11 days (figure 16A-D). In parallel, these cells were treated with IFN-γ, TNF-α, IFN-α or the LTβR agonist BS1. All treatments led to diminished HBeAg secretion compared to untreated cells, detectable after four days of treatment (figure 16A). Analogously, total intracellular HBV DNA (i.e. mainly rcDNA) was reduced by all treatments after four days (figure 16B). With slower kinetics, cccDNA reduction was measured resulting in a clear difference to control levels under all treatments after 11 days (figure 16C). Interestingly, pEpi-H1.3 levels stayed unaltered over the whole period of 11 days, unaffected from cytokine treatments (figure 16D) (Lucifora, Xia et al. 2014, Xia, Stadler et al. 2016).

Next, deamination and consequent AT-content of cccDNA amplicons was compared to that of episomal pEpi-H1.3 amplicons. As expected, T-cell cytokines IFN-γ and TNF-α as well as IFN-α and BS1 treatment led to lower permitted denaturing temperatures of cccDNA amplicons in 3D-PCR, indicating a higher AT-content and prior deamination (figure 16E). In contrast, amplicons from treated pEpi-H1.3 could not be amplified at lower denaturing temperatures than untreated controls, thus indicating that the episomal construct pEpi-H1.3 was not deaminated under cytokine treatments (figure 16F).

In summary, these results suggested that treatment-induced deamination and DNA decline is specifically affecting cccDNA but not any episomal DNA (Lucifora, Xia et al. 2014, Xia, Stadler et al. 2016).

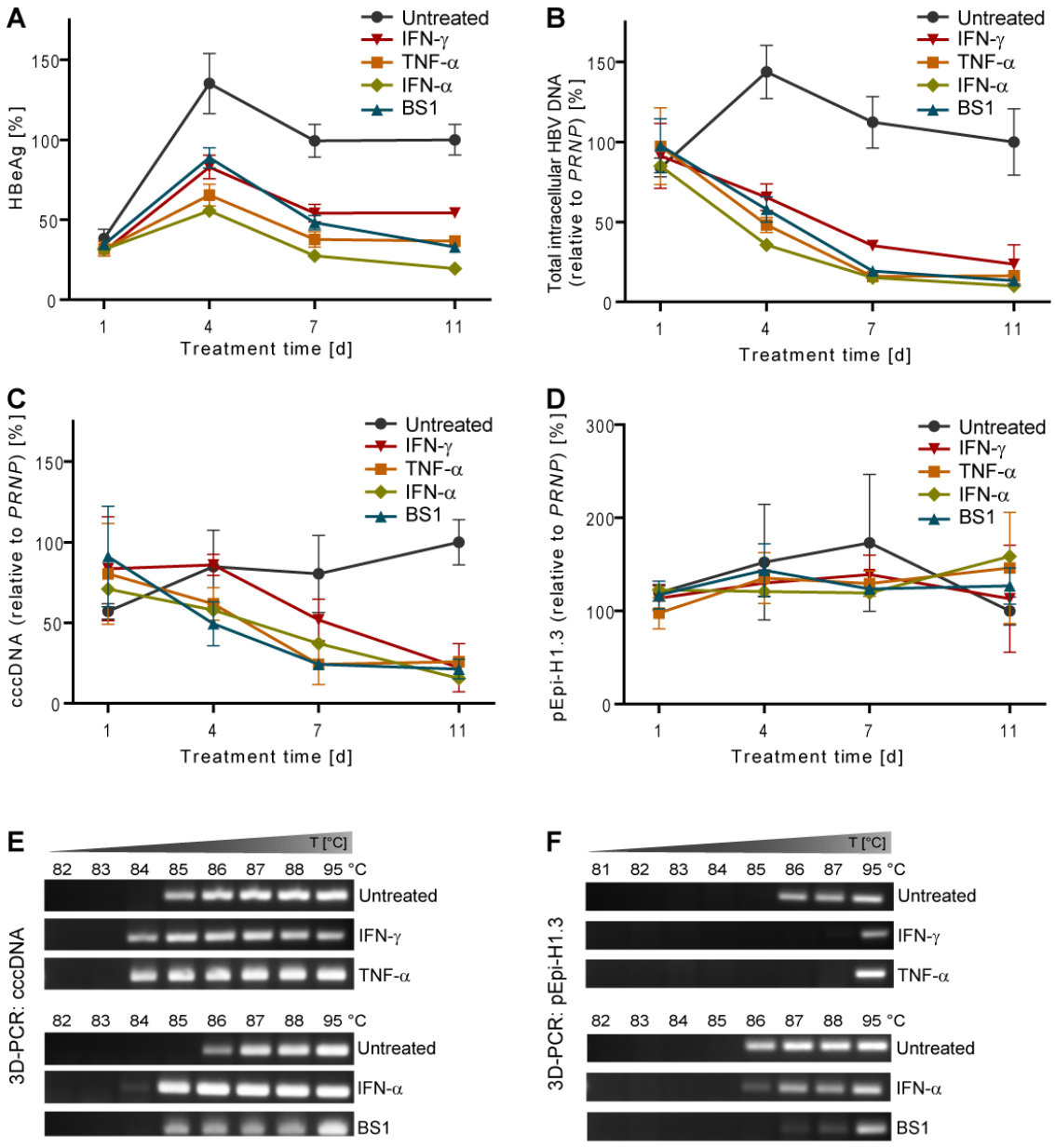

Figure 16: Treatment effects on cccDNA and episomal DNA. dHepaRG-pEpi-H1.3 cells, expressing HBV from an episomal construct (pEpi-H1.3), were treated with 200 U/ml IFN-γ, 800 U/ml TNF-α, 500 U/ml IFN-α or 0.5 µg/ml BS1 for 11 days. **(A)** HBeAg was determined by ELISA, **(B)** total intracellular HBV DNA, **(C)** cccDNA and **(D)** pEpi-H1.3 by qPCR relative to *PRNP* (n=3); values from untreated control samples at day 11 were set as 100 %. **(E)** 3D-PCR was applied to amplicons from cccDNA qPCR from time point four days (upper panel) or time point one day (lower panel). **(F)** Similar 3D-PCR was carried out using amplicons from pEpi-H1.3 qPCR from time point one day as template (Lucifora, Xia et al. 2014, Xia, Stadler et al. 2016).

2.2.2 A3A and A3B induce hypermutations on cccDNA

All applied treatments – IFN-γ, TNF-α, IFN-α and BS1 – induce cytosine deaminases A3A or A3B, which are essential for deamination and cccDNA purging as shown above and previously (Lucifora, Xia et al. 2014, Xia, Stadler et al. 2016). Therefore, the effect of overexpression of these two enzymes was studied in cell culture experiments. HepG2H1.3 cells, a hepatoma cell line replicating HBV from a 1.3-fold overlength genome integrate (Jost et al. 2007, Protzer et al. 2007), were transfected with a plasmid for overexpression of A3A (pLenti6.3-A3A) or a respective control plasmid. 3D-PCR showed clearly lower permitted denaturing temperature in cccDNA samples during A3A overexpression as compared to controls (figure 17A). Selected amplification products from 3D-PCR were recovered and sequenced. Following analyses revealed decreased numbers of guanines and increased numbers of adenines under A3A overexpression while cytosine and thymine content did not change. Since the plus strand of the database DNA sequence (wildtype) was used for sequence comparison, these G-to-A hypermutations indicated augmented deamination of minus-strand HBV DNA (figure 17B) (Stadler 2013).

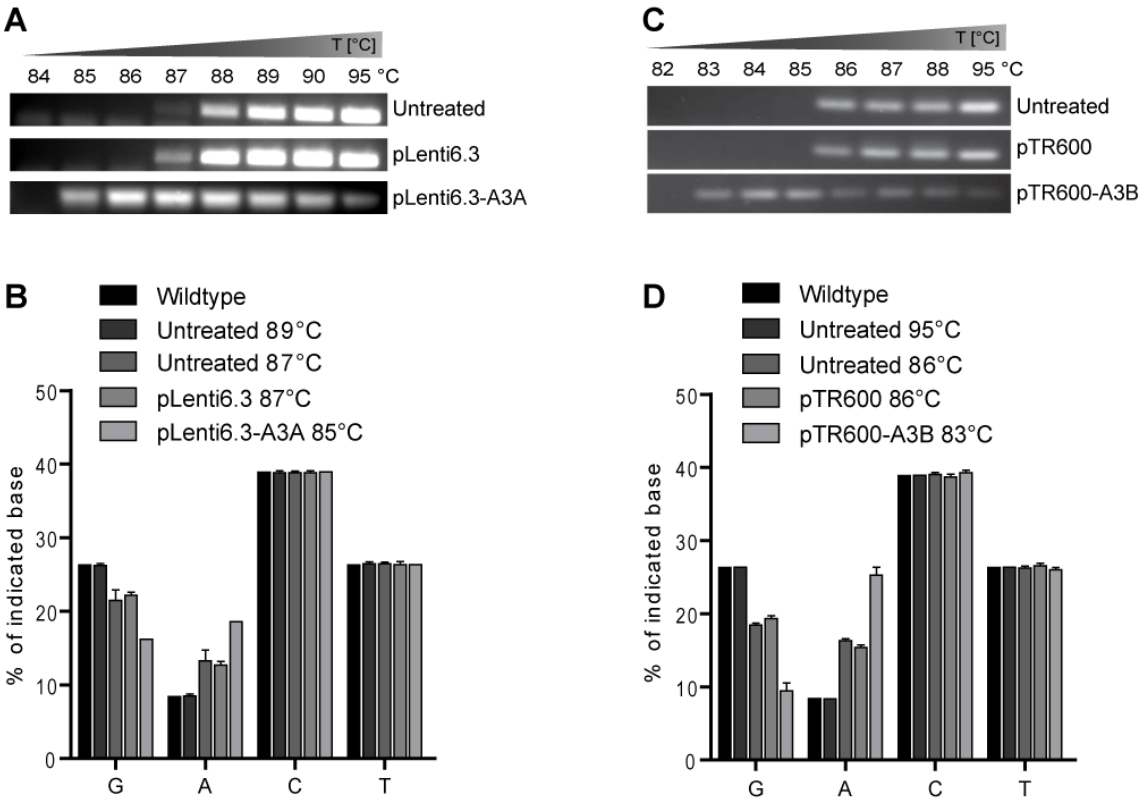

Figure 17: Overexpression of A3A and A3B. (A) HepG2H1.3 cells were transfected with a plasmid for A3A overexpression (pLenti6.3-A3A) or a control plasmid (pLenti6.3) during the seeding procedure and cultured in differentiation medium after reaching confluency. 3D-PCR with

cccDNA amplicons as template was carried out five days after transfection and **(B)** selected amplification products were sequenced to get the nucleotide composition (n=3-6) (Stadler 2013). **(C)** For A3B overexpression, HepG2H1.3 cells were transfected with an according plasmid (pTR600-A3B) during seeding and cultured in differentiation medium after reaching confluency. 3D-PCR using cccDNA amplification products as templates was done five days after transfection and **(D)** selected amplicons from different temperatures were analysed regarding nucleotide composition (n=3-5) (Lucifora, Xia et al. 2014).

Accordingly, overexpression of A3B by plasmid transfection (pTR600-A3B) in HepG2H1.3 cells allowed amplification from cccDNA amplicon templates at lower denaturing temperatures than controls, indicating increased deamination under A3B overexpression (figure 17C). Again, sequence analyses of selected products from 3D-PCR demonstrated increased G-to-A conversions under A3B expression, revealing a deamination preference for minus-strand HBV DNA (figure 17D).

Together, these results illustrate that A3A and A3B expression themselves lead to hypermutations on HBV cccDNA displayed by augmented G-to-A conversions (Lucifora, Xia et al. 2014).

2.2.3 A3A and HBV core protein bind to cccDNA

Since cytokine-induced decline and hypermutations proved to be specific for cccDNA and deamination was mediated by APOBEC3 proteins (Lucifora, Xia et al. 2014, Stadler 2013, Xia, Stadler et al. 2016), an interesting question was how these deaminases are targeted to cccDNA. Earlier studies showed that the viral HBV core protein associates with A3G (Turelli, Mangeat, Jost et al. 2004), another member of the APOBEC3 family deaminases (Janahi and McGarvey 2013), and with cccDNA (Bock et al. 2001). HBV core protein was therefore a candidate to mediate the targeting of nuclear APOBEC3 proteins to cccDNA and to determine thereby potentially the specificity for HBV cccDNA. In such a case, both HBV core protein and APOBEC3 deaminase should bind to cccDNA or be at least close to it. Thus, chromatin immunoprecipitation (ChIP) experiments were performed with dHepG2H1.3 cells, which were transfected with an A3A-expressing plasmid (pLenti6.3-A3A). Immunoprecipitation with antibodies against histone H3, HBV core protein as well as A3A allowed pull down of approximately 20-30 % of input cccDNA (figure 18A). In dHepG2H1.3-A3A cells, which replicate HBV from an integrate and constantly express A3A (Lucifora, Xia et al. 2014, Stadler 2013), A3A-mediated pull down of cccDNA was confirmed by ChIP (figure 18B). On the contrary, ChIP using an antibody against A3A did not result in increased precipitation of genomic DNA as compared to control samples in dHepG2H1.3-A3A cells (figure 18C).

Together, these results suggest that HBV core protein and A3A associate with cccDNA, potentially by a direct interaction, but A3A does not bind to genomic DNA (Lucifora, Xia et al. 2014).

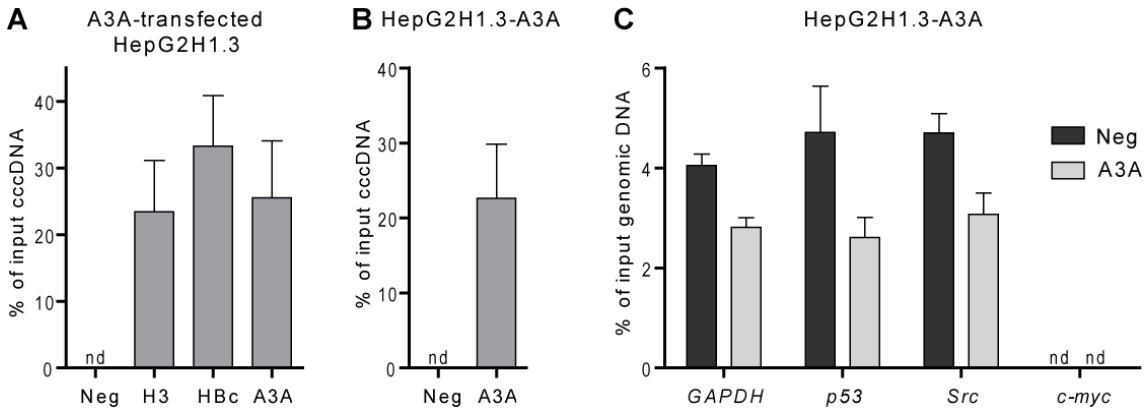

Figure 18: Chromatin immunoprecipitation (ChIP). (A) dHepG2H1.3 cells were transfected with pLenti6.3-A3A for A3A expression and immunoprecipitation was carried out using protein A/G beads only as negative control (Neg), antibodies against histone H3, A3A or HBV core protein (HBc) two days after transfection. cccDNA amounts were determined relative to input amounts by qPCR (n=3). **(B)** dHepG2H1.3-A3A cells, constantly expressing A3A, were used for ChIP with protein A/G beads only as negative control (Neg) and an antibody against A3A. cccDNA amounts were determined relative to input amounts by qPCR (n=3). **(C)** ChIP-samples from dHepG2H1.3-A3A cells were analysed by qPCR for genomic DNA using primers for *GAPDH*, tumour suppressor *p53*, cellular/sarcoma tyrosine kinase (*Src*) and myelocytomatosis (*c-myc*) (n=3). nd: not detectable (Lucifora, Xia et al. 2014).

2.3 Identification of ISG20 as the nuclease in interferon-induced decline of cccDNA

Deamination by APOBEC3 proteins is a prerequisite step in cytokine-induced loss of cccDNA and all here studied interferons induce the expression of A3A (Lucifora, Xia et al. 2014, Xia, Stadler et al. 2016). However, due to its biochemical properties as deaminase (Jarmuz et al. 2002), A3A is supposedly not able on its own to cut nuclear HBV DNA and an additional nuclease is needed for final DNA degradation. Therefore, the last part of this thesis aimed at identifying the nuclease which is involved in interferon-mediated cccDNA purging.

2.3.1 A3A leads to deamination but is not sufficient for cccDNA reduction

First, it was tested whether A3A expression is indeed not sufficient for cccDNA decline and other host factors need to be induced, even in the presence of basally expressed proteins of the host cell. To this end, HepaRG cells with tetracycline-inducible overexpression of A3A (HepaRG-TR-A3A cells) were used. HepaRG-TR-A3A cells kept the ability to differentiate into biliary- and hepatocyte-like cells, which are susceptible for HBV infection, after four weeks of standard cell culture (figure 19A) (Stadler 2013).

Tetracycline-inducible expression of A3A was confirmed after two and seven days on mRNA levels by qRT-PCR (figure 19B) and analogously on protein levels by Western blot (figure 19C).

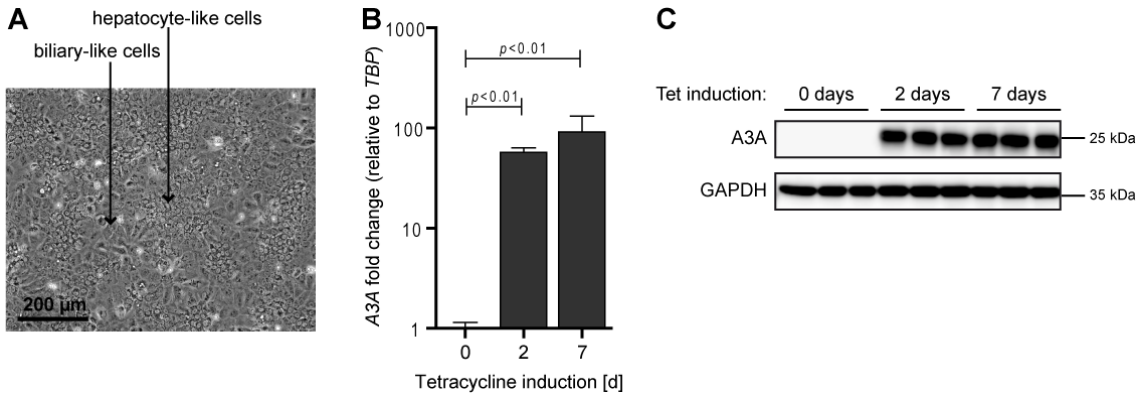

Figure 19: Characterization of HepaRG-TR-A3A cells. (A) Differentiation of HepaRG-TR-A3A cells into hepatocyte- and biliary-like cells was confirmed by microscopy (Stadler 2013). **(B)** Expression of A3A was induced by treatment with 0.005 mg/ml tetracycline (Tet) and checked by qRT-PCR (n=8) and **(C)** Western blot using an anti-V5 antibody for detection of A3A. Statistical analysis: Student's unpaired *t*-test with Welch's correction (ns: not significant, $p > 0.05$).

Next, the effect of A3A expression on cccDNA in infected and differentiated HepaRG-TR-A3A (dHepaRG-TR-A3A) cells was studied. A3A expression alone, IFN-α treatment or the combination of A3A expression and IFN-α treatment led each to lower denaturing temperatures in 3D-PCR as compared to untreated control (figure 20A). Amplicons at low denaturing temperatures were recovered and sequenced (figure 20B). Analysis of the nucleotide composition revealed increased G-to-A conversions under all treatments compared to the untreated control (figure 20C). As described above, this indicated augmented deamination of nuclear, minus-strand HBV DNA under A3A expression, IFN-α treatment or the combination of both.

To see whether HBV markers are affected analogously, HBV cccDNA, total intracellular HBV DNA and HBeAg were measured by qPCR or ELISA, respectively. As expected, IFN-α treatment – whether alone or combined with A3A expression – reduced all viral markers. However, A3A expression alone did not affect total intracellular HBV DNA, cccDNA nor HBeAg levels (figure 20D).

Altogether, these results show that A3A expression alone leads to deamination but is not sufficient to reduce cccDNA without additional interferon treatment.

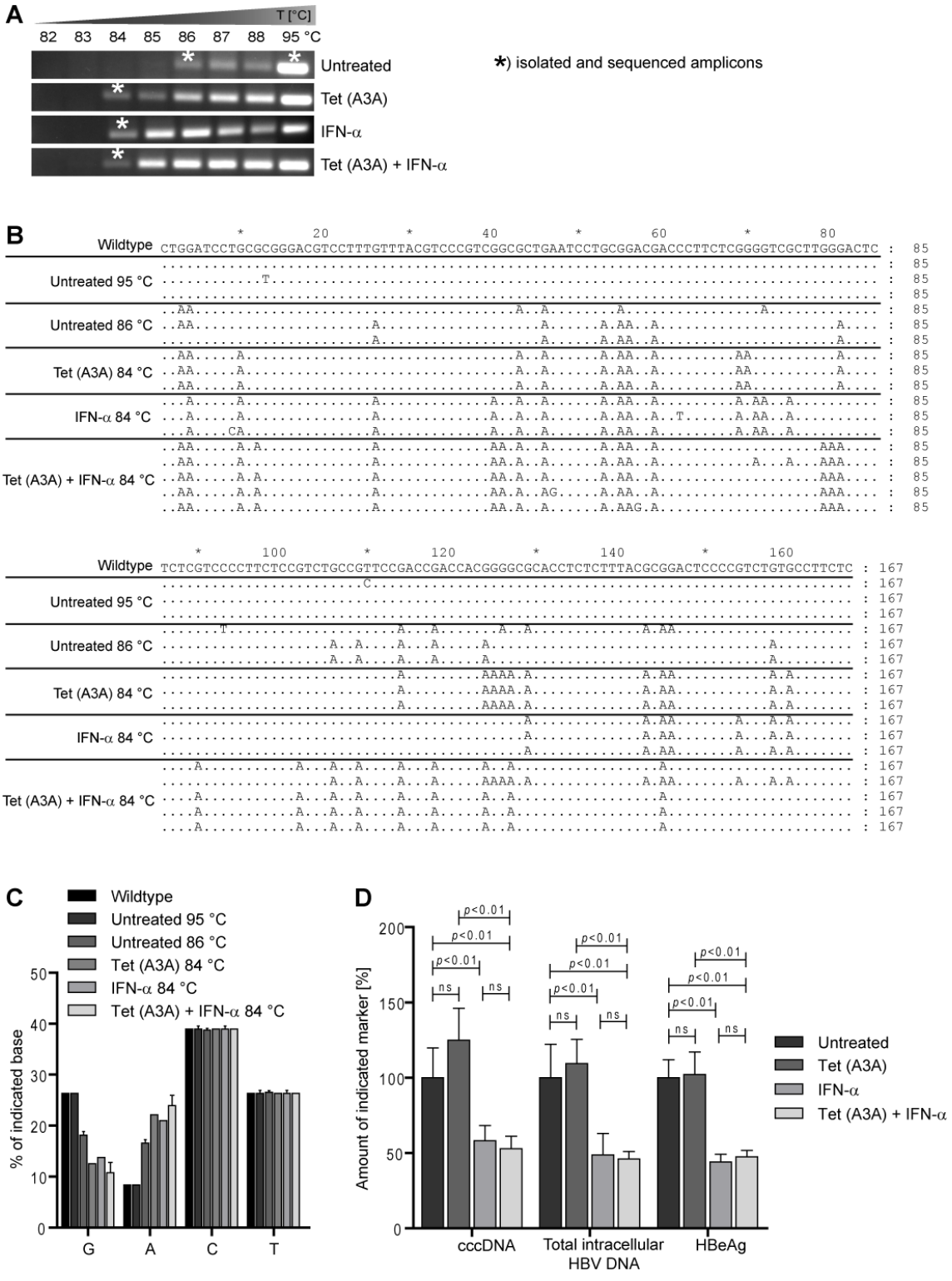

Figure 20: Deamination under A3A expression without cccDNA loss. dHepaRG-TR-A3A cells were treated nine days post-infection (dpi) with 0.005 mg/ml tetracycline (Tet (A3A)) or/and 300 U/ml IFN-α for nine days. **(A)** 3D-PCR shows differential denaturation patterns. Marked amplicons were **(B)** sequenced (n=3-5). **(C)** Nucleotide composition is displayed for sequenced amplicons in comparison to wildtype HBV sequence (n=3-5). **(D)** HBV markers were measured by qPCR relative to *PRNP* or by ELISA for HBeAg (n=6). Statistical analysis: Student's unpaired *t*-test with Welch's correction (ns: not significant, $p > 0.05$).

2.3.2 Interferons upregulate expression of the nuclease ISG20

Because IFN-α is needed in addition to A3A expression to reduce cccDNA, the consequent hypothesis was, that IFN-α induces at least one more factor enabling DNA degradation. To identify this factor, a gene expression analysis in HBV-infected dHepaRG-TR-A3A cells was carried out and A3A expression alone and A3A expression in combination with IFN-α treatment were compared each to untreated controls after six and 72 hours of treatment. As expected, influence of A3A expression on gene expression profiles was minor but IFN-α up- or downregulated many genes at both time points. Figure 21A and 21B show, therefore, the top 50 differentially expressed genes after six hours or 72 hours of treatment, respectively. Among these genes, *ISG20* was the only one with assigned nuclease activity.

Since the non-cytolytic loss of cccDNA under IFN-α supposedly requires a nuclease (Lucifora, Xia et al. 2014), analysis was focused on all upregulated genes with known nuclease activity under IFN-α treatment in A3A-expressing cells. For that purpose, complete datasets of differentially expressed genes under additional IFN-α treatment were compared to datasets from samples without IFN-α treatment, considering normalization to untreated controls before. Since complete datasets were used and all upregulated genes with annotated nuclease activity were extracted, these analyses delivered more hits: After six hours of treatment, increased mRNA levels of *ISG20*, *PNPT1*, *XRN1*, *RAD9A* and *PELO* were found and after 72 hours of *ISG20* and *PNPT1* (figure 22A).

All *ISG20* (Lu et al. 2013), *RAD9A* (Yoshida et al. 2003) and *PELO* (Shamsadin et al. 2000), but not *PNPT1* (Chen et al. 2007) and *XRN1* (Nagarajan et al. 2013), code for enzymes indeed located in the nucleus, making them suitable candidates for cccDNA decay. Thus, expression of these genes was further studied by qRT-PCR. This confirmed the upregulation of *ISG20,* which was also the candidate with strongest fold change in microarray analysis, with maximum effect nine hours after IFN-α treatment. *RAD9A* and *PELO*, however, were not significantly upregulated in IFN-α-treated, HBV-infected dHepaRG cells in qRT-PCR analysis (figure 22B).

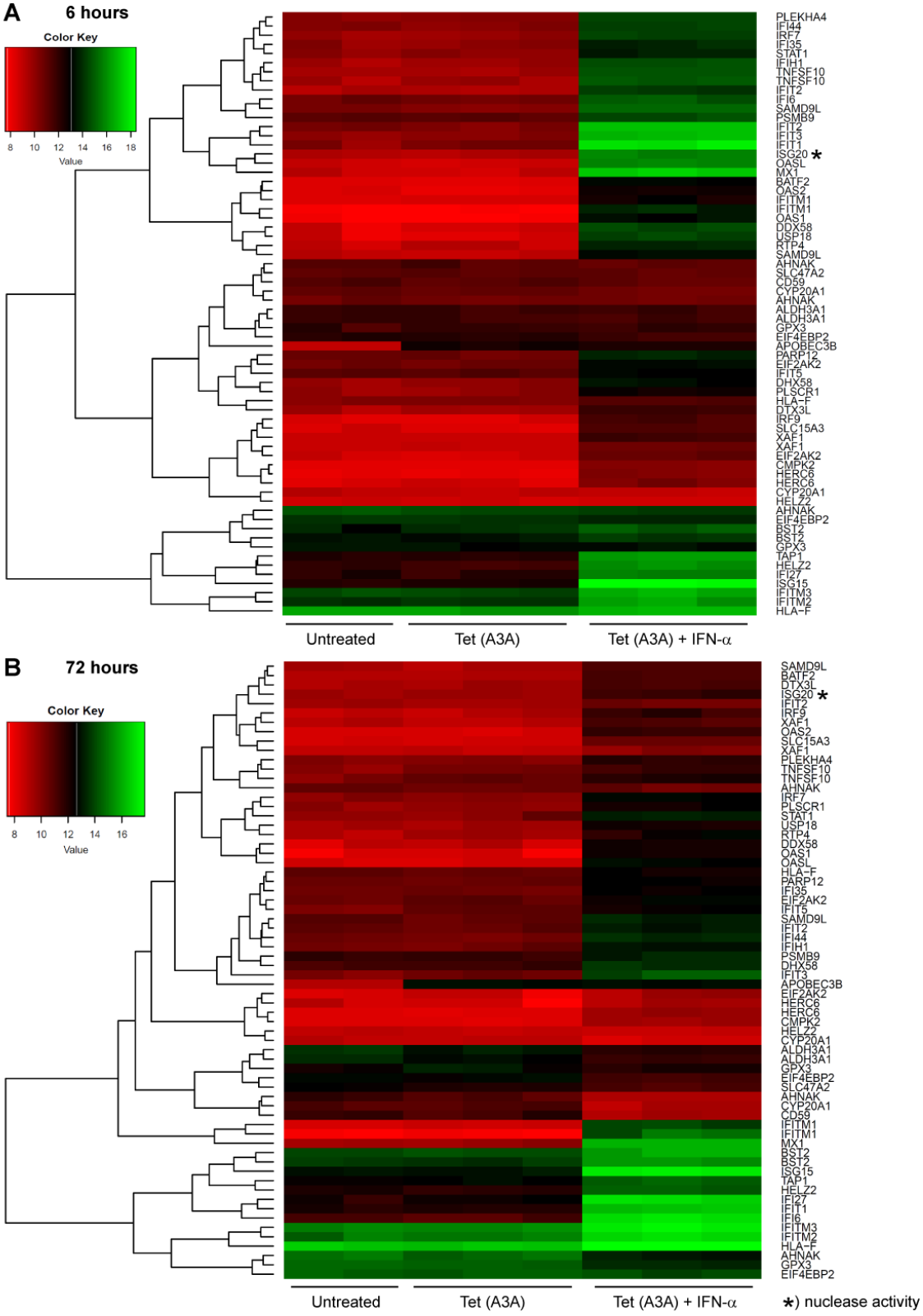

Figure 21: Gene expression analysis. dHepaRG-TR-A3A cells were treated seven days after HBV infection with 0.005 mg/ml tetracycline alone (Tet (A3A)) or combined with 300 U/ml IFN-α (Tet (A3A) + IFN-α). Agilent gene expression microarray data is displayed for the top 50 differentially expressed genes with two to three replicates per treatment condition after **(A)** six hours or **(B)** 72 hours of treatment. Asterisks mark genes with annotated nuclease activity (cooperation with Julia Heß and Kristian Unger).

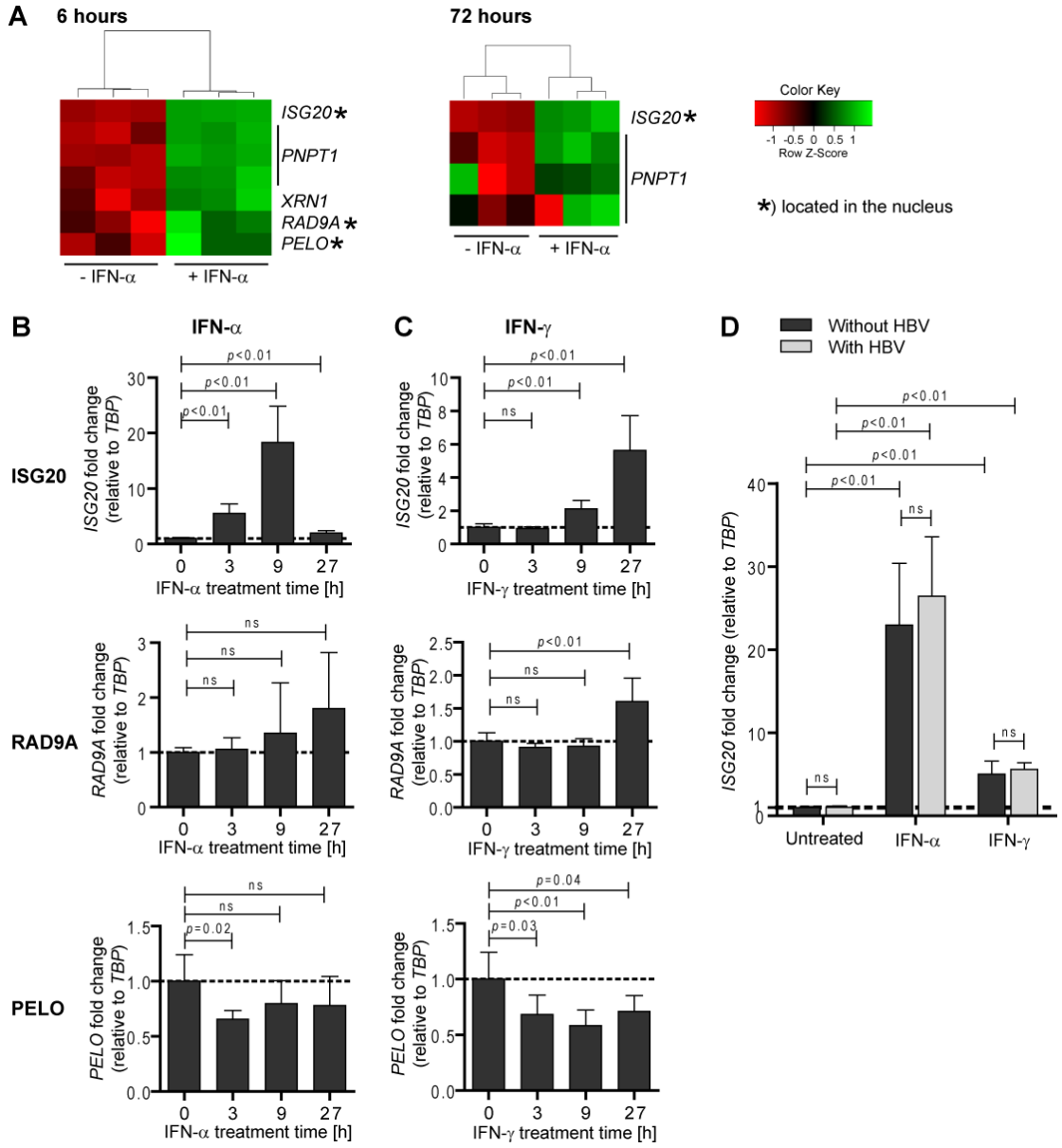

Figure 22: Gene expression analysis under interferon treatment. (A) A3A-expressing dHepaRG-TR-A3A cells were treated seven dpi with 300 U/ml IFN-α (+ IFN-α) or left without (- IFN-α). Microarray data was analysed for upregulated nucleases (cooperation with Julia Heß and Kristian Unger). **(B)** dHepaRG cells were treated nine dpi with IFN-α or **(C)** IFN-γ. Gene expression was analysed by qRT-PCR (n=6). **(D)** dHepaRG cells were treated seven dpi with IFN-α for six hours or IFN-γ for 24 hours (n=7). Statistical analysis: Student's unpaired *t*-test with Welch's correction (ns: not significant, $p > 0.05$).

IFN-α as type I interferon mediates transcriptional activation of its target genes via the JAK/STAT pathway. The type II interferon IFN-γ triggers similar signalling cascades (Schneider et al. 2014) resulting in the same effect on HBV cccDNA when applied to HBV-infected hepatocytes as described above (Xia, Stadler et al. 2016). Thus, the transcriptional regulation of the candidate nucleases (i.e. *ISG20*, *RAD9A* and *PELO*)

under IFN-γ treatment was examined. The results showed that *ISG20* and to a minor extend *RAD9A* were upregulated under IFN-γ treatment with slightly different kinetics compared to IFN-α treatment. No upregulation of *PELO* under IFN-γ was detected (figure 22C).

Since *ISG20* was upregulated under both IFN-α and IFN-γ, the influence of HBV infection on gene expression of this nuclease was checked. HBV infection did not alter mRNA levels of *ISG20* neither without treatment nor under IFN-α and IFN-γ treatment (figure 22D).

Overall, results demonstrated that both type I and type II interferons upregulate the expression of the nuclease ISG20 in dHepaRG cells.

2.3.3 ISG20 is expressed in acute hepatitis B and in co-infections

Intracellular expression of ISG20, which is the strongest upregulated nuclease in the present analyses (84-fold after six hours and 4-fold after 72 hours by microarray, 6-fold to 26-fold by qRT-PCR), correlates with positive response to IFN-α treatment in patients with chronic hepatitis B (Lu et al. 2013, Xiao et al. 2012). Namely, the part of patients with chronic hepatitis B who responded well to IFN-α, defined by a return to normal ALT levels, HBeAg seroconversion and undetectable HBV DNA in PCR after IFN-α treatment, showed increased ISG20 expression as compared to non-responders (Lu et al. 2013). Moreover, ISG20 is induced in livers of chimpanzees with acute hepatitis B during viral clearance (Wieland et al. 2004). Due to these correlations to HBV elimination, ISG20 was considered a reasonable candidate for DNA degradation in the mechanism of interferon-induced loss of cccDNA. Further, an augmented ISG20 expression during acute hepatitis B in patients was expected. To test this hypothesis, liver tissue samples from hepatitis patients were stained for ISG20 by immunohistochemistry. Indeed, strong ISG20 staining was visible in acute hepatitis B samples (figure 23A). This was reflected in a quantitative analysis by a significantly higher percentage of ISG20 positive area per sample in acute hepatitis B compared to control samples (figure 23B).

In contrast to acute hepatitis B, chronic HBV infection is characterized by persistence of HBsAg and HBV DNA (Trépo et al. 2014). If ISG20 degrades cccDNA leading to HBV elimination in acute hepatitis B, its expression should be hampered in chronic hepatitis B. Therefore, liver tissue samples from patients with chronic hepatitis B were stained in parallel in immunohistochemistry for ISG20. As expected, chronic hepatitis B samples showed similar staining as controls without increased ISG20 expression in opposition to acute hepatitis B samples (figure 23A). Again, this was reflected by the measurement of the ISG20 positive area per sample, which was considerably lower in chronic than in acute hepatitis B samples and equal to control levels (figure 23B).

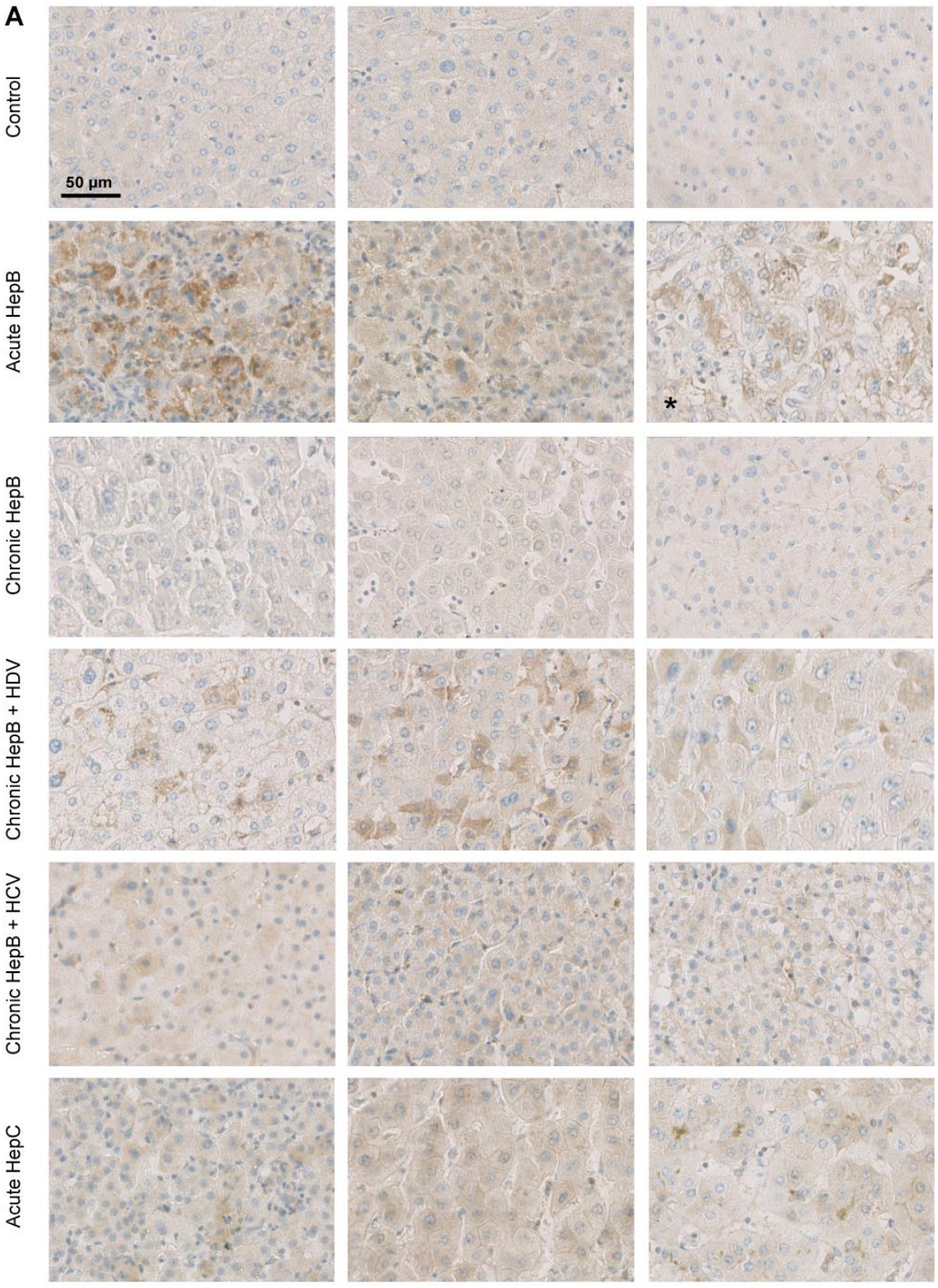

*) fulminant case

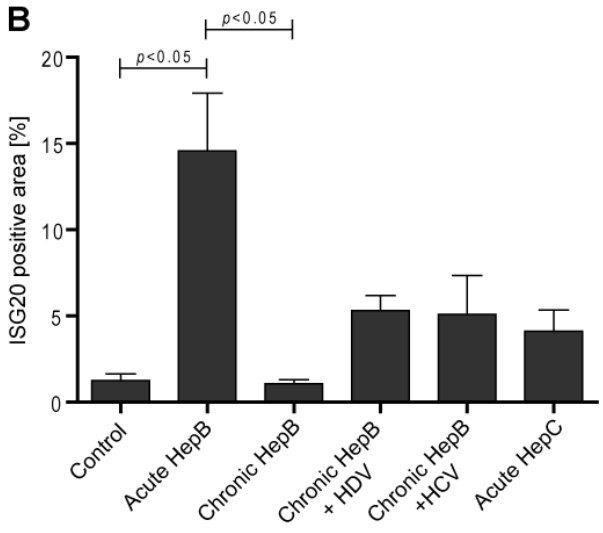

Figure 23: ISG20 expression in acute and chronic hepatitis. (A) Liver tissue samples from patients with acute or chronic hepatitis B (HepB), superinfection with hepatitis D virus (HDV), coinfection with hepatitis C virus (HCV) or acute hepatitis C (HepC) were stained for ISG20 by immunohistochemistry. For each clinical entity, stainings of sections from three different patients are shown (cooperation with Felix Lasitschka). **(B)** ISG20 positive area was determined in % of total recognizable tissue area, data was analysed by one-way ANOVA (cooperation with Marc Ringelhan).

Generally, immune responses in chronic hepatitis B are impaired (Protzer et al. 2012). To see whether the immune system can be triggered by additional stimuli during chronic HBV infection and whether this restores ISG20 expression, samples from co-infections were studied. Liver tissues from patients with hepatitis D virus (HDV) co-infection, which induces an innate immune response and expression of interferon-stimulated genes in hepatocytes of humanized mice (Giersch et al. 2015), were investigated. Individual cells in chronic hepatitis B samples with HDV superinfection showed clear ISG20 staining (figure 23A). Overall, the percentage of ISG20 positive area under HDV superinfection tended to be increased compared to control or chronic hepatitis B only samples (figure 23B).

Moreover, samples from patients with chronic hepatitis B and coinfection with hepatitis C virus (HCV) were examined. HCV activates an interferon-mediated innate immune response in the course of infection (Heim and Thimme 2014, Su, Pezacki et al. 2002). HCV coinfection in chronic hepatitis B showed a stronger ISG20 staining in immunohistochemistry than control or chronic hepatitis B only samples. Similarly, ISG20 expression was increased in acute hepatitis C samples (figure 23A). Again, the portion of ISG20 positive area tended to be elevated for both HCV coinfection and acute hepatitis C samples (figure 23B).

In summary, ISG20 is expressed during acute hepatitis B, acute hepatitis C or in chronic hepatitis B upon superinfection with HDV or coinfection with HCV *in vivo* and thus suggests that ISG20 is a key downstream molecule in interferon-mediated cccDNA purging.

2.3.4 ISG20 knockdown abolishes interferon-induced loss of cccDNA

For functional investigations, ISG20 knockdowns via short hairpin RNA (shRNA) or small interfering RNA (siRNA) targeting ISG20 were established in dHepaRG cells. shRNA-constructs were delivered by adenoviral vectors. To test their efficiency and toxicity, dHepaRG cells were transduced with a range in multiplicity of infection (MOI) from one to 20 using a green fluorescent protein (GFP)-expressing adenoviral vector and observed over a period of 17 days. Fluorescence microscopy revealed GFP-expression beginning four days after transduction with a substantial increase from MOI one to MOI three but only marginal differences towards higher MOIs. Interestingly, mainly hepatocyte-like but not biliary-like cells showed GFP signals (figure 24A). In parallel, cell death was monitored over time by LDH release assay. Cell death was lower than 10 % over the whole period of 17 days and no titre-dependent increase of toxicity was observed (figure 24B). Due to absence of toxicity and a good efficiency, an MOI of three was used for adenoviral transduction in further experiments.

Analogously, efficiency and toxicity of adenoviral transduction of dHepG2H1.3-A3A cells was tested. Efficiency determined by GFP-expressing cells was similar as for dHepaRG cells, increasing with higher MOIs but showing already satisfying GFP expression with an MOI of three. However, all MOIs provoked toxicity 10 days after transduction in LDH release assay (data not shown). Therefore, experiments in these cells were restricted to a maximum of seven days after transduction and an MOI of three was used due to absence of early toxicity but good transduction efficiency.

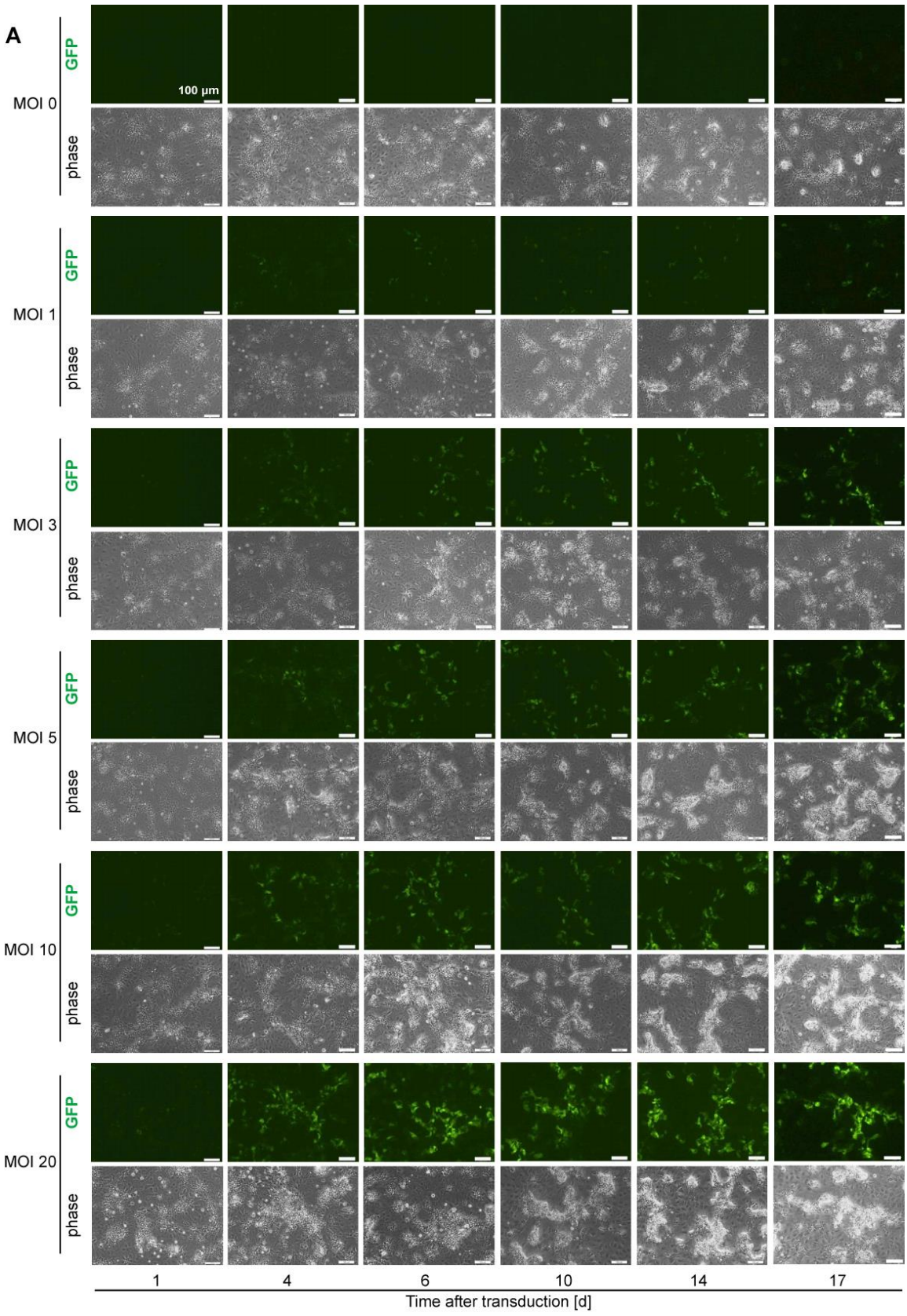
A
MOI 0
MOI 1
MOI 3
MOI 5
MOI 10
MOI 20
GFP
phase
100 µm
1
4
6
10
14
17
Time after transduction [d]

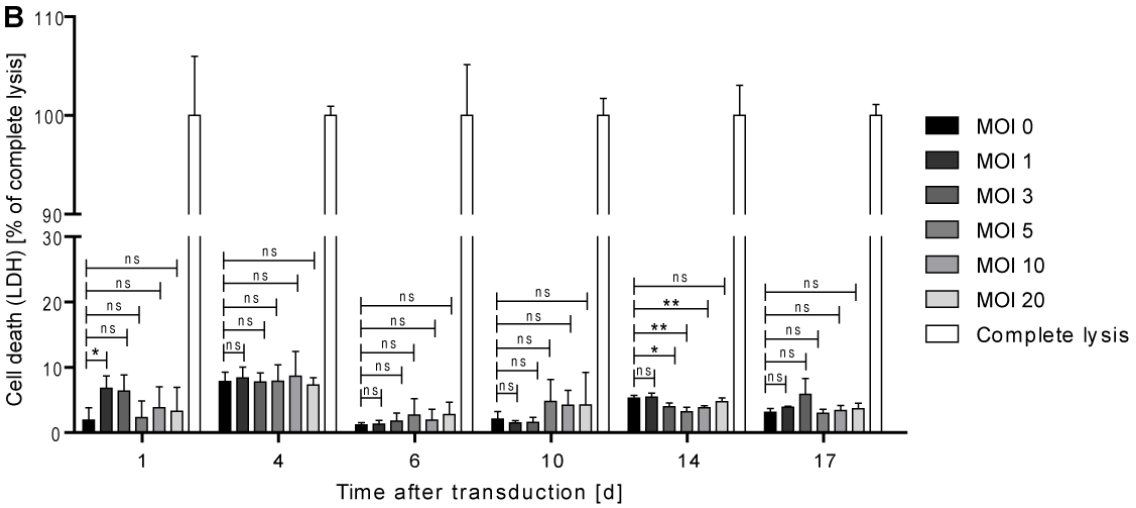

Figure 24: Efficiency and toxicity of adenoviral transduction of dHepaRG cells. dHepaRG cells were transduced with a green fluorescent protein (GFP)-expressing adenoviral vector with a range in multiplicity of infection (MOI) from one to 20 and analysed over 17 days. **(A)** Fluorescence microscopy pictures were taken at different timepoints to investigate the efficiency of adenoviral transduction of dHepaRG cells. **(B)** LDH release assay was applied to measure the amount of cell death over time. Statistical analysis: Student's unpaired *t*-test with Welch's correction (ns: not significant, $p > 0.05$; * $p = 0.02$; ** $p < 0.01$).

First, for knockdown of ISG20, HBV-infected dHepaRG cells were transduced with adenoviral vectors for expression of shRNA against ISG20 and the effects of interferon treatment were investigated after 12 days. Under control conditions, IFN-α and IFN-γ reduced cccDNA levels clearly. However, shRNA-mediated ISG20 knockdown significantly diminished the loss of cccDNA under IFN-α treatment and completely abolished cccDNA reduction under IFN-γ treatment (figure 25A). Total intracellular HBV DNA was reduced under IFN-α as well as IFN-γ treatment but, remarkably, this interferon-mediated decline was not affected at all by ISG20 knockdown (figure 25B). Similarly, HBeAg levels were diminished under IFN-α and IFN-γ but shRNA-mediated knockdown of ISG20 had no influence on HBeAg amounts, whether under interferon treatments or control conditions (figure 25C).

Moreover, HBV-infected dHepaRG cells were transfected with siRNA targeting ISG20 and HBV markers were analysed after three days of interferon treatment. Application of siRNA decreased IFN-α-induced ISG20 to control amounts and lowered the basal expression of ISG20 (figure 25D). Concurrently, IFN-α reduced cccDNA under control conditions but when ISG20-specific siRNA was added, cccDNA level under IFN-α treatment was brought back to 100 % (figure 25E). Again, IFN-α induced the reduction of total intracellular HBV DNA as well as HBeAg and these effects were not rescued by ISG20 knockdown via siRNA (figure 25F).

Altogether, the results demonstrate that ISG20 knockdown abolishes the interferon-triggered loss of cccDNA without affecting HBV DNA and HBeAg levels, suggesting that ISG20 is directly involved in interferon-induced reduction of cccDNA.

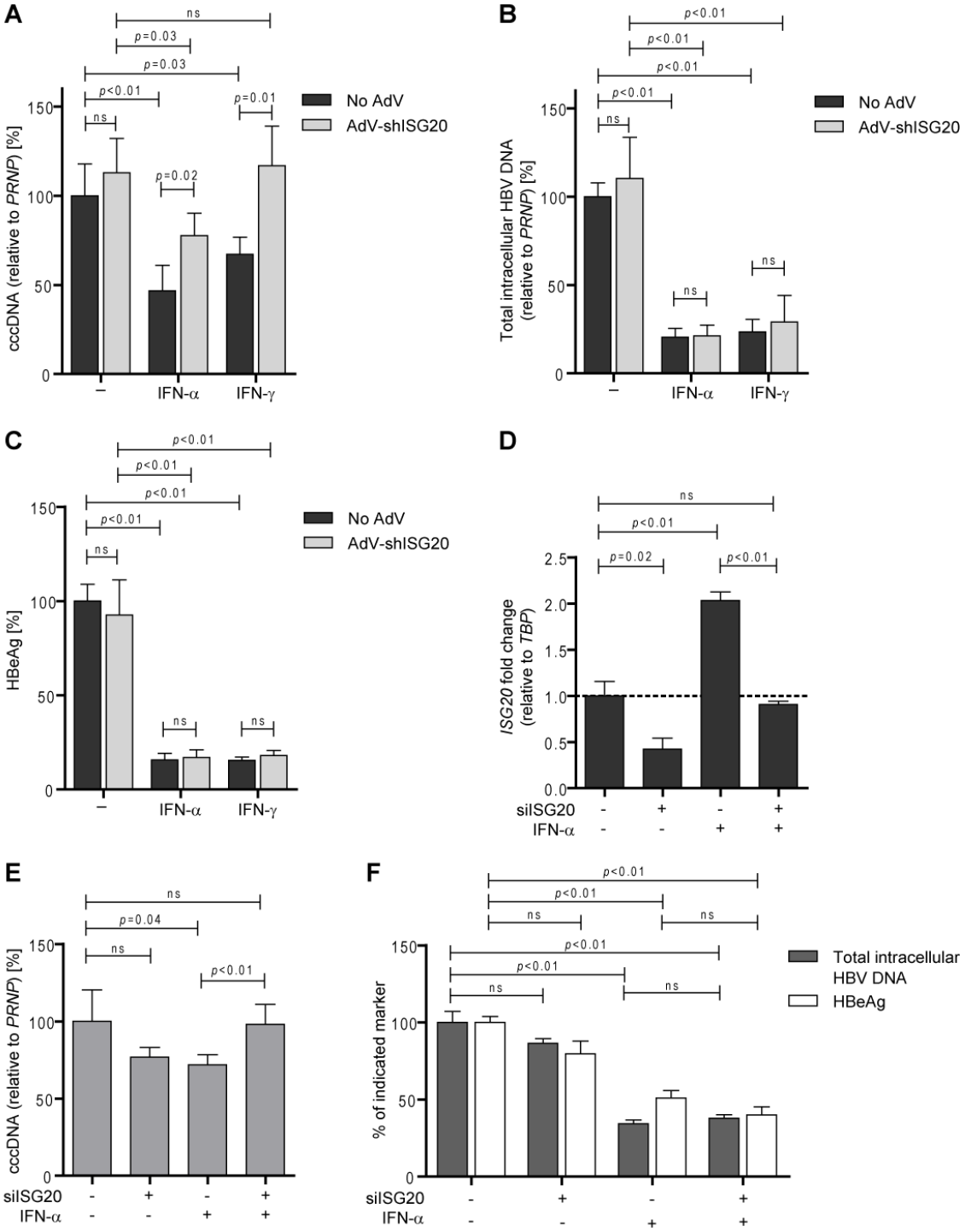

Figure 25: Knockdown of ISG20. (A) HBV-infected dHepaRG cells were transduced with adenoviral vectors for expression of short hairpin RNA (AdV-shISG20) or used without adenoviral transduction (No AdV) as control and treated two days later with IFN-α or IFN-γ. After 12 days,

T5-digested cccDNA, **(B)** intracellular HBV DNA and **(C)** HBeAg were measured (n=4-8). **(D)** HBV-infected dHepaRG cells were transfected with small interfering RNA targeting ISG20 (siISG20) or control siRNA and treated one day later with IFN-α for three days. *ISG20* mRNA (n=3) as well as **(E)** T5-digested cccDNA, **(F)** intracellular HBV DNA and HBeAg were measured (n=5-6). T5: T5 exonuclease, used for improving accuracy of cccDNA qPCR (for details see method section). Statistical analysis: Student's unpaired *t*-test with Welch's correction (ns: not significant, $p > 0.05$).

2.3.5 ISG20 overexpression together with A3A is sufficient for cccDNA reduction

Finally, overexpression of ISG20 was studied by adenoviral transduction of different hepatoma cells. When ISG20 was overexpressed in dHepaRG cells by adenoviral transduction, highly elevated *ISG20* mRNA levels were detected (figure 26A). Western blot confirmed the expression of ISG20 in transduced dHepaRG cells on protein level (figure 26B).

To investigate the effect on HBV markers, HBV-infected dHepaRG-TR-A3A cells were transduced and A3A expression was induced by tetracycline addition to have single A3A or ISG20 expression and the simultaneous expression of both proteins. cccDNA levels were not significantly altered by neither A3A nor ISG20 expression alone. However, the combination of both enzymes led to a significant reduction of cccDNA to less than 50 % of the non-transduced, untreated control (figure 26C). Analogously, total intracellular HBV DNA was reduced by concerted A3A and ISG20 expression but not A3A expression alone. In this case though, already ISG20 expression itself led to a slight decrease of HBV DNA, but this effect was significantly enhanced by additional A3A expression (figure 26D).

Similarly, ISG20 was overexpressed in dHepG2H1.3-A3A cells. Since dHepG2H1.3-A3A cells constantly express A3A, they allow to investigate the effects of combined A3A and ISG20 expression on HBV in an additional, HBV-replicating cell line. *ISG20* mRNA levels were clearly increased after transduction of dHepG2H1.3-A3A cells with an ISG20-overexpression construct compared to controls (figure 26E). In comparison to A3A expression alone, additional ISG20 overexpression led to a reduction of cccDNA (figure 26F).

In summary, these data confirm that A3A expression alone is not sufficient for cccDNA loss but combined overexpression with ISG20 leads to cccDNA decline in different hepatoma cell lines. Remarkably, concerted action of A3A and ISG20 suffices to reduce HBV cccDNA potently without the need of further cytokine treatment.

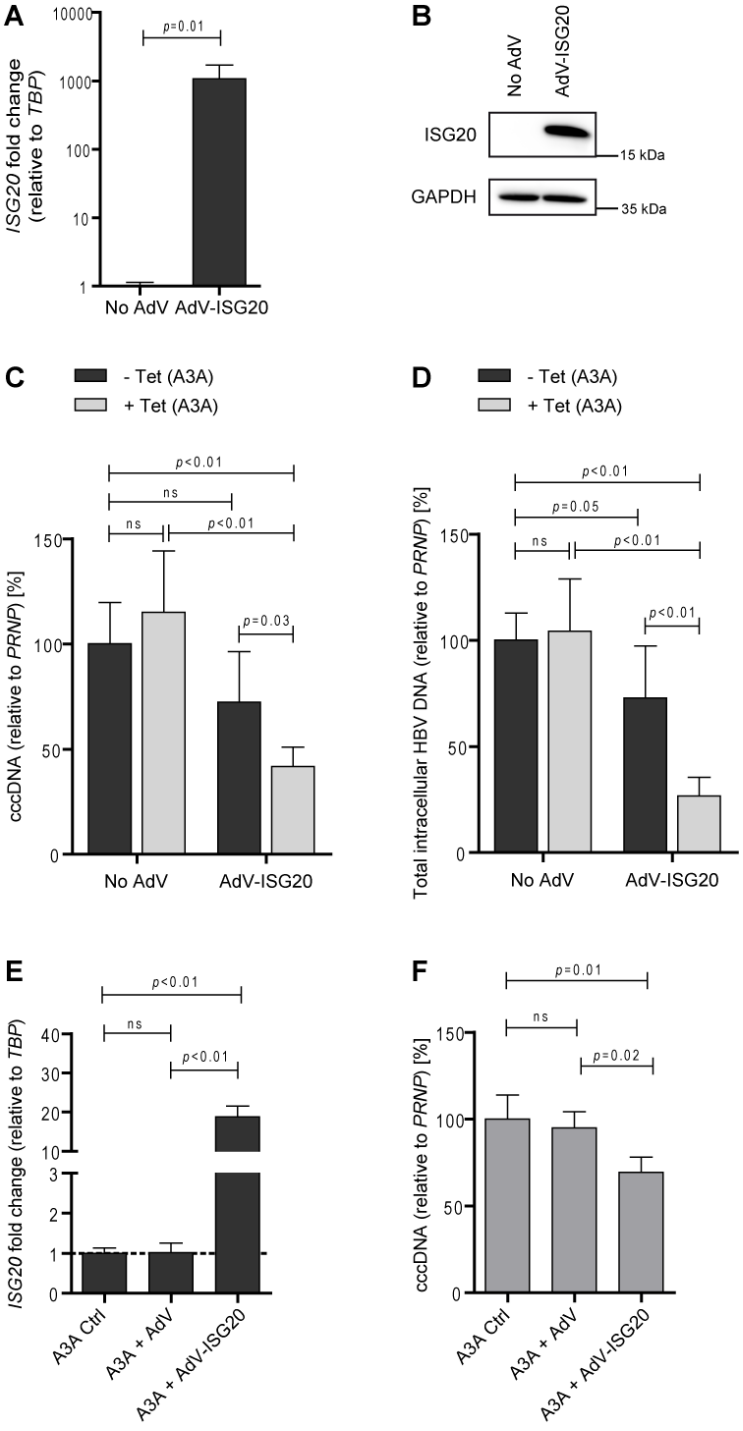

Figure 26: Overexpression of ISG20. (A) dHepaRG cells were transduced with adenoviral vectors for expression of ISG20 (AdV-ISG20) and *ISG20* mRNA levels were determined 24 hours later (n=6). **(B)** Expression of ISG20 was confirmed by Western blot three days after transduction. **(C)** dHepaRG-TR-A3A cells were transduced seven dpi for ISG20 overexpression (AdV-ISG20), treated with tetracycline to induce A3A expression (+ Tet (A3A)) for one week and analysed for T5-digested cccDNA and **(D)** intracellular HBV DNA (n=5-6). **(E)** dHepG2H1.3-A3A cells, which constantly express A3A (A3A Ctrl), were transduced 10 days after differentiation with an empty adenoviral vector (AdV) or an adenoviral vector for ISG20 expression (AdV-ISG20). One day after transduction, *ISG20* levels were determined by qRT-PCR (n=4). **(F)** T5-digested cccDNA was measured in dHepG2H1.3-A3A cells seven days after transduction (n=4). Statistical analysis: Student's unpaired *t*-test with Welch's correction (ns: not significant, $p > 0.05$).

3 Discussion

Current treatments for chronic hepatitis B can control HBV replication but cannot eliminate the virus completely due to its persistence mediated by the cccDNA form of HBV (Lucifora and Protzer 2016, Revill et al. 2016). Therefore, cccDNA is a major therapeutic target and thus, mechanisms of cytokine-induced cccDNA loss were investigated in this thesis (published in Xia, Stadler et al. (2016), Lucifora, Xia et al. (2014) and Xia et al. (2017b)). Mainly, non-cytolytic processes and the molecular effectors induced in the host cell were studied, as discussed in the following chapters.

3.1 Non-cytolytic reduction of HBV cccDNA by T-cell cytokines IFN-γ and TNF-α

Complete clearance of HBV apparently needs killing of infected hepatocytes by cytotoxic T cells. However, T-cell cytokines might support viral eradication in a non-cytolytic manner (Guidotti and Chisari 2001, Guidotti et al. 1999, Wieland, Spangenberg et al. 2004). This thesis demonstrates that activated T cells reduce HBV cccDNA, the viral persistence form, in human hepatoma cells without cytolysis. In this process, T-cell cytokines IFN-γ and TNF-α are the key players for cytokine-induced HBV inhibition by inducing the expression of deaminases A3A and A3B, which lead together with further host cell enzymes to cccDNA purging (Xia, Stadler et al. 2016). IFN-γ was shown earlier to trigger the inhibition of HBV replication by accelerating the decay of replication-competent nucleocapsids (Xu et al. 2010). Further, TNF-α induces NF-κB signalling leading to interference with HBV nucleocapsid integrity without cell lysis (Biermer et al. 2003). Beside affecting HBV nucleocapsid formation or stability, T-cell cytokines lead to the destabilization of HBV RNAs (Guidotti et al. 1996, Heise et al. 1999) and IFN-γ mediates inhibition of viral protein translation by tryptophan deprivation (Mao et al. 2011). Thus, T-cell cytokines can inhibit HBV on post-transcriptional level but also by directly affecting the nuclear cccDNA pool (Xia, Stadler et al. 2016), thereby controlling HBV persistence.

3.1.1 IFN-γ and TNF-α as the main T-cell cytokines mediating cccDNA loss

In this study, blocking of both IFN-γ and TNF-α by neutralizing antibodies restored cccDNA and HBeAg levels in the presence of activated, cytokine-secreting T cells to more than 80 % of control levels. However, a small portion of cccDNA could not be recovered by neutralization of IFN-γ and TNF-α (Xia, Stadler et al. 2016) and, hence, additional mechanisms must be involved in non-cytolytic reduction of cccDNA. A possible explanation for this cccDNA decline is the secretion of further antiviral T-cell cytokines. To identify these, potential T-cell effector cytokines found in cytokine-screening assays (Xia, Stadler et al. 2016) could be neutralized in transwell co-culture experiments. Moreover, it should be considered that activated T-cells might trigger the secretion of

antiviral cytokines by the hepatocytes themselves and that possibly the concerted action of several cytokines is needed, making it difficult to pinpoint the single ones. In this thesis, lymphotoxins were neutralized because they might function as T-cell effector cytokines (Murphy and Weaver 2016) and because LTβR activation leads to cccDNA reduction (Lucifora, Xia et al. 2014). Neutralization of LTβR-binding cytokines by addition of Baminercept did not influence cccDNA and HBeAg loss by T-cell cytokines. Together with the effect of Etanercept, which was comparable to that of TNF-α neutralization (Xia, Stadler et al. 2016), this leads to the conclusion that lymphotoxins are not involved in the reduction of HBV markers by secreted T-cell cytokines. Anyway, the major effect was achieved by neutralizing IFN-γ in all measurements (Xia, Stadler et al. 2016). In summary, IFN-γ and TNF-α account for the main impact and appear, thus, as the key T-cell cytokines triggering cccDNA reduction.

3.1.2 Impact of T-cell cytokines IFN-γ and TNF-α on controlling HBV infection in patients

Since IFN-γ and TNF-α appeared in neutralization experiments as the main cytokines inducing cccDNA decline upon T-cell activation (Xia, Stadler et al. 2016), the question arose whether secretion of these cytokines correlated with acute, resolving but not chronic hepatitis B and might be involved in HBV clearance in patients. Patients with acute hepatitis B, which is characterized by a strong and polyfunctional T-cell response (Bertoletti and Ferrari 2012, Said and Abdelwahab 2015), show indeed higher IFN-γ and TNF-α levels in serum samples than healthy donors or patients with chronic hepatitis B (Xia, Stadler et al. 2016), who have a weak, oligoclonal and exhausted T-cell response (Bertoletti and Ferrari 2012, Protzer et al. 2012). Consistently, Dimitropoulou *et al.* also showed decreased levels of IFN-γ in patients with chronic active HBV infection compared to inactive carriers and a negative correlation of IFN-γ levels with serum HBV load in chronic hepatitis B patients (Dimitropoulou et al. 2013). Additionally, a polymorphism of the IFN-γ gene is associated with low level production of IFN-γ and susceptibility to develop chronic hepatitis B (Ben-Ari et al. 2003). The 238A allele of TNF-α, which diminishes the TNF-α promoter activity (Kaluza, Reus et al. 2000), is associated with an increased risk of chronic hepatitis B in European populations (Zheng et al. 2012). Furthermore, anti-TNF-α therapy for treatment of inflammatory arthritis can lead to HBV reactivation in patients with chronic HBV infection (Ye, Zhang et al. 2014). In summary, these studies underline the clinical importance of IFN-γ and TNF-α for controlling HBV infection in patients and further emphasize the finding that they are the main T-cell cytokines for cccDNA purging.

3.1.3 Non-cytolytic cccDNA reduction

The non-cytolytic effects of T-cell cytokines on HBV cccDNA were investigated here in different experimental setups *in vitro*. To avoid killing of HBV-infected target cells by

direct contact with T cells, a transwell co-culture system was applied allowing separation of effector and target cells (Phillips et al. 2010, Xia, Stadler et al. 2016). Still, release of perforin and granzyme B by antigen-stimulated T cells could theoretically lead to cell death (Thome and Tschopp 2001) and thereby diminish levels of HBV markers. However, this seems unlikely because ALT levels as marker for hepatocyte damage were increased when T cells were directly co-cultured with HBV-infected target cells but not when T cells were kept in transwells (Xia, Stadler et al. 2016). Further, T-cell cytokines themselves could induce cell lysis and thereby cccDNA loss, e.g. TNF-α induces depending on the metabolic state of the target cell pro-survival signalling or cell death by caspase-8-mediated apoptosis or necroptosis (Valaydon et al. 2016). However, this can be ruled out as dHepaRG cells were treated with IFN-γ and TNF-α and cell viability was confirmed to be unaltered by five independent assays (LDH release assay as shown in this thesis, ALT measurement, XTT assay, cleaved caspase 3 staining and measurement of mitochondrial DNA by qPCR) (Xia, Stadler et al. 2016). In conclusion, these data demonstrate that the observed HBV cccDNA reduction is mediated by T-cell cytokines IFN-γ and TNF-α in a non-cytolytic fashion.

3.1.4 Cytokine signalling diminishes cccDNA independent of rcDNA reimport

On the one hand, cell division during proliferation of HBV-infected hepatocytes might lead to cccDNA clearance (Lutgehetmann, Volz et al. 2010). On the other hand, recycling of rcDNA-containing nucleocapsids from the cytoplasm to the nucleus can amplify the cccDNA pool efficiently, at least in the DHBV model (Köck et al. 2010). Both mechanisms interfere with a stable cccDNA pool in the nucleus of HBV-infected cells and would, thus, hamper to draw conclusions on cccDNA decline under cytokine treatment. Therefore, most experiments in this thesis were carried out in dHepaRG cells, which support long-term persistence of HBV without cccDNA amplification (Hantz et al. 2009). Supporting the results from dHepaRG cells, HBV-infected primary human hepatocytes (PHH), which cannot proliferate after isolation *in vitro*, also showed cccDNA decline under IFN-γ and TNF-α treatment (Xia, Stadler et al. 2016). Additionally, HBV-infected dHepaRG cells were pre-treated with entecavir, which inhibits viral reverse transcription and, thus, rcDNA formation. Levels of rcDNA were largely diminished under entecavir treatment but cccDNA levels were not affected. When entecavir was combined with IFN-γ or TNF-α, cccDNA declined indicating that the cytokines directly affect cccDNA levels independent from cytoplasmic rcDNA levels and excluding the possibility of rcDNA recycling (Xia, Stadler et al. 2016). In addition, knockdown experiments using siRNA against A3A and A3B restored cccDNA levels under IFN-γ and TNF-α treatment, thereby excluding that cccDNA was lost mainly by cell division. Interestingly, cccDNA levels increased already in untreated cells after knockdown of A3A and A3B. This indicates a basal expression and activity of APOBEC3 deaminases. Surprisingly, HBeAg levels under the same experimental conditions are not affected by A3A and A3B knockdown (Xia, Stadler et al. 2016). This could be explained by a higher number of cccDNA molecules but impaired

protein expression or transcription from cccDNA, probably regulated by epigenetic silencing (Pollicino et al. 2006). In summary, these results indicate that cytokines diminish cccDNA directly and independent of reimport of rcDNA-containing nucleocapsids.

3.1.5 Physiological relevance of non-cytolytic T-cell cytokines in comparison to T-cell killing

Although there is no final proof for the physiological role of non-cytolytic antiviral effects of T cells, there are many hints for their relevance in diverse aspects of HBV infection. While the process of cccDNA purging through T-cell cytokines takes four to seven days, only a short incubation time of 12 hours with cytokine-secreting T cells was needed to initiate this process, as shown in transwell experiments in this thesis. According to the function of cccDNA as transcription template, decrease of total intracellular HBV DNA and HBeAg levels was slightly delayed (Xia, Stadler et al. 2016). The rapid induction of cccDNA decay makes it plausible that cytokine-induced effects play an important role in non-cytolytic cccDNA purging before T-cell killing starts. In line with this concept, different studies demonstrated non-cytolytic cccDNA reduction before hepatocytes are lysed by cytotoxic T cells (Guidotti et al. 1999, Wieland, Spangenberg et al. 2004).
Exhaustion of T cells occurs in a hierarchical manner by losing killing capacity prior to the capacity to secrete TNF-α and IFN-γ (Wherry 2011). Therefore, non-cytolytic, cytokine-mediated T-cell functions might play also a role late in HBV infection when T cells start losing their cytotoxic effector functions but still secrete effector cytokines.
Furthermore, the liver is a large organ and the number of virus-specific T cells seems low compared to the number of target hepatocytes (Guidotti and Chisari 2001). In this case, secretion of non-cytolytic T-cell cytokines may be essential to support the antiviral response. Accordingly, livers of transgenic mice were harmed only slightly after transfer of HBV-specific T cells but the antiviral effect of the T cells on HBV RNA levels was much stronger, making it unlikely that T cells function solely via killing of infected cells (Guidotti et al. 1994, Guidotti and Chisari 2001). Altogether, it seems likely that T cells elicit non-cytolytic antiviral effects that are relevant in different stages of HBV infection.

3.1.6 Therapeutic implications of non-cytolytic T-cell functions

Since current treatments for chronic hepatitis B cannot eradicate the virus and a cure is rarely achieved (Revill et al. 2016, Xia and Protzer 2017), treatment alternatives are needed. The present work provides evidence for non-cytolytic functions of T cells by cytokine-triggered decline of cccDNA, the HBV persistence form (Xia, Stadler et al. 2016). This stimulates the development of therapeutic strategies to restore a proper T-cell response in chronic hepatitis B. The sole use of IFN-γ and TNF-α for systemic therapy seems less promising as PEGylated IFN-α is already approved as drug but was reported to have response rates of less than 10 % as determined by HBsAg seroconversion (Janssen et al. 2005) and is limited by severe systemic side effects

(Janssen et al. 2005, Trépo et al. 2014). Therefore, it appears more attractive to use HBV-specific T cells, which might be more effective because of their non-cytolytic as well as cytolytic antiviral effects. Moreover, HBV-specific T cells may elicit their antiviral functions close to the HBV-infected target cells after receptor binding with a high local cytokine concentration. This could be achieved by injection of T cells engineered to target HBV-infected cells as it has been suggested for S-CAR T cells (Bohne et al. 2008, Krebs, Böttinger et al. 2013). Adoptively transferred and HBV-specific T cells are promising tools to inhibit HBV in the liver by cytolytic and non-cytolytic means (Guidotti et al. 1996). New strategies also include redirection of T cells by bifunctional engineered antibodies or therapeutic vaccination to boost the immune response against HBV (Revill et al. 2016), all with the aim to control and finally cure HBV infection.

3.2 Specificity of treatment-induced cccDNA loss

T-cell cytokines IFN-γ and TNF-α (Xia, Stadler et al. 2016) as well as IFN-α treatment and LTβR activation (Lucifora, Xia et al. 2014) trigger the non-cytolytic loss of HBV cccDNA. The present study demonstrates that this treatment-induced DNA reduction is specific for cccDNA and does not target other episomal DNA: While cytokine-induced deamination and decline affects HBV cccDNA, pEpi-H1.3 is neither deaminated nor reduced (Lucifora, Xia et al. 2014, Xia, Stadler et al. 2016). The construct pEpi-H1.3, which was used as model for episomal HBV DNA, is based on a vector that replicates episomally in eukaryotic cells and is maintained at low copy number and stably in the cells over more than 100 generations (Piechaczek et al. 1999). It includes a 1.3-fold overlength HBV genome, which enables HBV replication in HepaRG cells from transfected pEpi-H1.3. The HBV genome on pEpi-H1.3 is identical to cccDNA in sequence but linear (Lucifora, Xia et al. 2014, Stadler 2013). Moreover, overexpression of A3A and A3B deaminases, which are essential in cytokine-induced cccDNA purging (Lucifora, Xia et al. 2014, Xia, Stadler et al. 2016), induces hypermutations on cccDNA as shown here (Lucifora, Xia et al. 2014, Stadler 2013). Both A3A and HBV core protein associate with cccDNA as demonstrated in this thesis supporting the hypothesis that HBV core protein targets nuclear APOBEC3 deaminases to cccDNA (Lucifora, Xia et al. 2014), thereby determining the cccDNA specificity as discussed below.

3.2.1 Role of the HBV core protein for cccDNA targeting

If HBV core protein is responsible for bringing APOBEC3 deaminases to their target sites on cccDNA, these proteins are expected to co-localize on cccDNA and interact with each other. In line with ChIP experiments in this thesis demonstrating that HBV core protein and A3A associate with cccDNA (Lucifora, Xia et al. 2014), different studies showed that HBV core protein binds to cccDNA (Bock et al. 2001, Guo, Li et al. 2011, Pollicino et al. 2006). Furthermore, fluorescence microscopy showed co-localization of A3B and A3A with HBV core protein in different hepatoma cells or human hepatocytes. Additionally,

A3A can interact with HBV core protein, as indicated by co-immunoprecipitation experiments, proximity ligation assay (PLA), fluorescence resonance energy transfer (FRET) analysis and molecular modelling (Lucifora, Xia et al. 2014). Similarly, HBV core protein can bind to A3G as demonstrated by co-immunoprecipitation experiments (Turelli, Mangeat, Jost et al. 2004) and FRET analyses (Lucifora, Xia et al. 2014) as well as to APOBEC3C as shown by co-immunoprecipitation (Baumert et al. 2007), further pointing out that HBV core protein can interact with APOBEC3 deaminases. Taking this together, it is conceivable that HBV core protein binds nuclear APOBEC3 deaminases and mediates thereby the targeting of APOBEC3 enzymes to HBV cccDNA.

In the scenario of HBV-core-mediated targeting of nuclear APOBEC3 deaminases to cccDNA, the question arises whether HBV core protein can distinguish cccDNA from episomal HBV DNA and determine cccDNA specificity in doing so. In contrast to well described HBV-core-protein binding to cccDNA (this thesis, Bock et al. 2001, Guo, Li et al. 2011, Lucifora, Xia et al. 2014, Pollicino et al. 2006), ChIP experiments to study HBV-core binding to pEpi-H1.3 were not successful so far. Thus, it still needs to be determined, whether HBV core protein specifically binds cccDNA but not pEpi-H1.3 and whether this prevents cytokine-induced deamination and degradation of the episomal construct. Further, it remains elusive whether other mechanisms may influence HBV-core-protein binding or APOBEC3 deaminase activity, such as the methylation status of cccDNA (Guo, Li et al. 2011, Guo et al. 2009) and pEpi-H1.3 (Piechaczek et al. 1999), the epigenetic organisation of cccDNA (Pollicino et al. 2006, Rivière et al. 2015, Tropberger et al. 2015) or additional viral or host factors binding to cccDNA.

3.2.2 Absence of deamination of genomic DNA by APOBEC3 proteins

Deregulated APOBEC3 protein expression is suspected to be involved in genomic DNA deamination and cancer formation, e.g. A3A was reported to lead to genomic DNA damage during replication (Green et al. 2016). A3B was suggested as source for deamination-induced mutations in breast cancer (Burns et al. 2013). However, no DNA alterations were detected in HBV-infected human hepatocytes or differentiated hepatoma cells under cytokine treatment by 3D-PCR experiments, analysis of abasic sites and deep sequencing of several human genes (Lucifora, Xia et al. 2014). Additionally, A3A did not bind to genomic DNA in ChIP experiments as shown here (Lucifora, Xia et al. 2014), even when HBV core protein was present, which was described to interact with genomic DNA (Guo, Kang, Lei et al. 2012). This is consistent with data demonstrating that the human protein TRIB3 protects genomic DNA from cytosine deamination by A3A (Aynaud et al. 2012). Taken together, APOBEC3 deaminases seem not to attack genomic DNA under these experimental settings, probably due to a host guardian protein protecting genomic DNA.

3.2.3 Fate of deaminated HBV DNA: repair versus degradation

Overexpression of A3A and A3B results in hypermutations on HBV cccDNA without further treatment as demonstrated in this thesis and reported before (Lucifora, Xia et al. 2014, Stadler 2013). Additionally, A3A and A3B knockdown experiments shown here lead to an increase of cccDNA levels above the level of the untreated control (Xia, Stadler et al. 2016), as discussed previously. This indicates that nuclear HBV DNA can be targeted by A3A or A3B without the need to induce an additional factor and that a basal activity of APOBEC3 deaminases is operative in infected cells. Accordingly, untreated control samples in sequencing experiments in this thesis show already increased G-to-A hypermutations in comparison to the wildtype HBV sequence from the database (Lucifora, Xia et al. 2014, Stadler 2013). Similarly, varying deamination of pEpi-H1.3 was detected by 3D-PCR with even less deamination in some treated compared to untreated samples although pEpi-H1.3 levels measured by qPCR were not altered in the present study. This might be explained by the instability of deaminated DNA in the nucleus due to host repair mechanisms (Krokan et al. 2014). Noteworthy, cccDNA could be repaired *in tubo* by a repair enzyme mix after deamination had been induced (Lucifora, Xia et al. 2014), indicating that lacking recognition by the host repair machinery cannot be the reason for cccDNA loss. Thus, it seems likely that cytokine treatments leading to cccDNA decline induce an additional factor which enables to switch from cccDNA repair (Kitamura et al. 2013) to degradation (Stenglein et al. 2010).

3.2.4 Epigenetic impact on the accessibility of cccDNA

A3A and A3B were shown to deaminate single-stranded DNA during DNA replication (Hoopes, Cortez et al. 2016). One possibility for A3A and A3B to get access to single-stranded cccDNA is given during viral transcription, when cccDNA as the template is rendered single-stranded. This active transcription might also determine susceptibility of cccDNA for cytokine-induced reduction in general: Even after cytokine treatment for 11 days a portion of cccDNA was left as measured by qPCR in this thesis (Lucifora, Xia et al. 2014, Xia, Stadler et al. 2016). It is conceivable that only transcriptionally active cccDNA molecules can be targeted by cytokine-induced enzymes leading to cccDNA purging. Transcriptionally inactive cccDNA molecules, in contrast, may not be susceptible to deamination by A3A or A3B because they stay double-stranded, accounting for the residual cccDNA not degraded. Transcription from cccDNA was shown to be regulated epigenetically (Belloni et al. 2009, Lucifora, Arzberger et al. 2011, Pollicino et al. 2006). Thus, also histone acetylation status could influence cytokine-mediated cccDNA decline. Furthermore, methylation of cccDNA (Guo, Li et al. 2011, Guo et al. 2009) might affect its susceptibility for cytokine-induced decay and be responsible for the resistance of some cccDNA molecules. However, the nature of the leftover cccDNA remains to be determined. Anyhow, functional cure of hepatitis B is seen currently as a more realistic goal than complete elimination of cccDNA. Functional cure is characterized by HBsAg loss, undetectable serum HBV DNA but persisting,

transcriptionally inactive cccDNA, which allows to stop treatments (Revill et al. 2016). Cytokine-triggered reduction of cccDNA combined with transcriptional silencing of the remaining cccDNA molecules might help to achieve this goal.

3.3 Identification of ISG20 as the nuclease in interferon-induced decline of cccDNA

Although IFN-α and IFN-γ can induce the loss of HBV cccDNA (Lucifora, Xia et al. 2014, Xia, Stadler et al. 2016), the nuclease involved in this mechanism remained unknown. My results strongly indicate that ISG20 is the nuclease in interferon-triggered cccDNA purging. Elevated *ISG20* mRNA levels were detected under IFN-α and IFN-γ treatment, confirming previous studies (Gongora et al. 1997, Liu et al. 2017). Furthermore, ISG20 expression was highly increased during acute but not chronic hepatitis B. Knockdown of ISG20 blocked interferon-induced loss of cccDNA. Moreover, ISG20 overexpression together with A3A overexpression was sufficient to reduce cccDNA levels, indicating its importance in interferon-induced cccDNA decline. ISG20 is a 3' to 5' exonuclease that can degrade single-stranded RNA and DNA (Nguyen et al. 2001) and is found in nuclei and cytoplasm of hepatocytes in response to IFN-α treatment (Lu et al. 2013). In accordance with its known DNase activity and the nuclear distribution, the present results reveal that ISG20 is the downstream nuclease which finally cleaves damaged cccDNA.

3.3.1 Damaged cccDNA as substrate for ISG20

Since ISG20 acts on single-stranded substrates (Nguyen et al. 2001), the degradation of cccDNA might depend on the transcriptionally active status, which renders cccDNA single-stranded, similarly to the cccDNA status required for APOBEC3 deamination as discussed above. The fact that ISG20 is an exonuclease (Nguyen et al. 2001) implies that its HBV DNA substrate has been damaged previously, i.e. uracils introduced by APOBEC3 deaminases were removed and DNA strand breaks occurred. Accordingly, ISG20 expression alone is not sufficient to diminish cccDNA levels in the experiments shown here. However, concerted expression of ISG20 and A3A reduces cccDNA. Since A3A deaminates cytosines to uracils, it seems reasonable that cellular factors expressed constitutively remove the uracils from DNA leading to the formation of apurinic/apyrimidinic (AP) sites and induce strand breaks resulting in a damaged cccDNA that is a substrate for ISG20. In line with this, AP sites are formed during cccDNA purging induced by IFN-α treatment or LTβR activation (Lucifora, Xia et al. 2014). AP sites can be generated by the glycosylase UNG, which was shown to be involved in cccDNA loss after deamination by activation-induced cytidine deaminase (AID) (Chowdhury et al. 2013, Qiao et al. 2016). However, we could not prove a participation of UNG in interferon-induced cccDNA reduction so far, leaving the identity of the additionally involved proteins open. Nevertheless, it seems reasonable that deamination

by APOBEC3 proteins is followed by further enzymatic steps generating damaged cccDNA, which is degraded by ISG20.

3.3.2 Reduction of cccDNA through ISG20 is independent of nuclear reimport

Recent studies show that expression of ISG20 can inhibit HBV replication by diminishing HBV RNAs, whereby the exonuclease activity of ISG20 is required (Leong, Funami et al. 2016, Liu et al. 2017, Ma et al. 2016). Consistent with these data, total intracellular HBV DNA was reduced, when ISG20 was expressed in dHepaRG-TR-A3A cells. Because intracellular HBV DNA consists mainly of cytoplasmic rcDNA, which is exclusively located inside capsids and supposedly protected from any nuclease attack, its reduction is likely due to degradation of pgRNA by ISG20 (Leong, Funami et al. 2016, Liu et al. 2017) or inhibition of pgRNA encapsidation by ISG20 (Liu et al. 2017). In the present experiments, siRNA- and shRNA-mediated knockdowns of ISG20 could neither rescue the reduction of HBV DNA nor HBeAg under interferon treatment. The ongoing antiviral effect of interferon in these cases can be explained by additional antiviral effects, such as IFN-α-mediated epigenetic silencing of cccDNA resulting in transcriptional inhibition (Belloni et al. 2012, Tropberger et al. 2015) or accelerated decay of HBV nucleic-acid containing capsids by IFN-α and IFN-γ (Xu et al. 2010). In contrast to rcDNA, cccDNA reduction was rescued by ISG20 knockdown. The loss of cccDNA observed after interferon treatment was abolished or strongly diminished by a knockdown of ISG20. This demonstrates that interferon-induced ISG20 can directly deplete the nuclear cccDNA pool, independent from a potential reimport of newly reverse-transcribed rcDNA. In addition, dHepaRG cells lack cccDNA amplification by nuclear capsid reimport or reinfection (Hantz et al. 2009), further strengthening the notion that ISG20-mediated cccDNA loss under interferon treatment is not an artefact of reduced cytoplasmic rcDNA levels but interferon-induced ISG20 affects cccDNA levels directly.

3.3.3 Potential involvement of additional nucleases in cccDNA decay

In the experiments presented, shRNA-mediated knockdown of ISG20 abolished IFN-γ-induced cccDNA loss completely, but IFN-α-mediated reduction was only partially reversed. The weaker ISG20-knockdown effect under IFN-α treatment might reflect an incomplete knockdown because induction of *ISG20* transcription by IFN-α is much stronger than that by IFN-γ. Another possible explanation is a compensation by other nucleases, which assist the function of ISG20. Stenglein *et al.* hypothesized that the nuclease APEX degrades foreign DNA (Stenglein et al. 2010), although a knockdown of APEX did not affect IFN-γ-mediated reduction of cccDNA in our experiments (Xia, Stadler et al. 2016). Gene expression analysis by microarray displayed the induction of further IFN-α-induced nucleases: *PNPT1* encodes for human polynucleotide phosphorylase (hPNPase), an RNase localized to the mitochondrial intermembrane space (Chen et al. 2007), making it an unsuitable candidate for nuclear HBV DNA degradation. The

exoribonuclease XRN1 is clearly upregulated by IFN-α and IFN-γ, but is a cytoplasmic RNase (Nagarajan et al. 2013). RAD9A is a DNase with preference for single over double strands (Bessho and Sancar 2000) and localizes to the nucleus (Yoshida et al. 2003). However, it is only weakly induced in dHepaRG cells under interferon as indicated by a gene expression analysis. PELO (protein pelota homolog) has a nuclear localization signal (Shamsadin et al. 2000) but localizes also to the cytoskeleton and might degrade aberrant mRNAs (Burnicka-Turek, Kata et al. 2010) and it is not upregulated by interferons as shown by qRT-PCR here. In this respect, it remains open which and whether an additional nuclease supports interferon-mediated decay of cccDNA.

3.3.4 Impact of ISG20 on HBV clearance in patients

An important aspect is the role of ISG20 for HBV elimination *in vivo*. Studies with chimpanzees demonstrated that ISG20 is expressed in the liver of acutely infected animals during viral clearance (Wieland et al. 2004), suggesting that ISG20 is involved in the elimination of HBV. Accordingly, increased ISG20 staining in liver tissue samples from patients with acute hepatitis B was detected in our study. In chronic HBV infection, the level of ISG20 is as low as in control samples. Concurrently, *in situ* hybridization showed increased mRNA amounts of A3A and A3B in acute but not in chronic hepatitis B (Xia, Stadler et al. 2016). These findings might be explained by a strong, polyfunctional T-cell response during acute hepatitis B (Bertoletti and Ferrari 2012, Said and Abdelwahab 2015), whereby the non-cytolytic T-cell cytokines IFN-γ and TNF-α lead to cccDNA reduction (Xia, Stadler et al. 2016), supposedly via induction of APOBEC3 deaminases and ISG20. In contrast, the T-cell response in chronic hepatitis B is weak, oligoclonal and exhausted (Bertoletti and Ferrari 2012, Protzer et al. 2012) lacking IFN-γ and TNF-α secretion (Xia, Stadler et al. 2016). Superinfection with HDV or co-infection with HCV during chronic hepatitis B, however, restores ISG20 induction in liver tissue samples. The induced immune responses by HDV (Giersch et al. 2015) or HCV (Heim and Thimme 2014, Su, Pezacki et al. 2002) are most likely responsible for it. This is in accordance with studies, which show that IFN-α treatment response in chronic hepatitis B patients correlates with ISG20 expression (Lu et al. 2013, Xiao et al. 2012). Altogether, clinical data strongly indicate that ISG20 is critically involved in HBV elimination *in vivo*. It is plausible, thus, that ISG20 acts as DNase targeting the HBV persistence form cccDNA during viral clearance.

3.3.5 Decline of cccDNA by concerted expression of A3A and ISG20

In AID-mediated loss of cccDNA, the overexpression of the deaminase AID seems sufficient to get a reduction of cccDNA levels (Chowdhury et al. 2013, Qiao et al. 2016). In contrast, no decrease of cccDNA levels was detected here when only A3A was overexpressed, indicating that a further inducible factor plays a crucial role enabling DNA degradation (Stenglein et al. 2010). Indeed, when ISG20 is co-expressed, cccDNA is diminished in cell culture experiments. Although dHepG2H1.3-A3A cells were

differentiated for 10 days to reduce reimport of rcDNA from cytoplasm (Protzer et al. 2007) and stabilize cccDNA pools, it cannot be ruled out that the observed effects of concerted A3A and ISG20 expression in this cell culture system are due to constant A3A overexpression and cccDNA refill by reimport mechanisms. Therefore, these data were confirmed in dHepaRG-TR-A3A cells, where cccDNA reimport is absent (Hantz et al. 2009). In that experimental model, combined A3A and ISG20 expression was found to be sufficient to reduce cccDNA levels to less than 50 % of control without further treatment. Even though this finding needs validation *in vivo*, it opens possibilities for therapeutic intervention by triggering specifically A3A and ISG20 expression or direct delivery of A3A and ISG20 to hepatocytes avoiding side effects (Janssen et al. 2005) by systemic IFN-α administration.

3.4 Conclusions

Collectively, the following mechanism of action is proposed for cytokine-triggered, non-cytolytic HBV cccDNA decline: Activated T cells secrete the cytokines IFN-γ and TNF-α, which are the key factors of non-cytolytic T-cell function. These cytokines as well as IFN-α treatment and LTβR activation induce the expression of cytosine deaminases A3A and A3B in HBV-infected hepatocytes. In the nucleus of the infected cell, A3A and A3B target cccDNA specifically by interaction with HBV core protein. Subsequent DNA deamination leads to formation of uracils, which are supposedly excised by host uracil glycosylases (Lucifora, Xia et al. 2014, Xia, Stadler et al. 2016). Additional host proteins might participate in damaging HBV DNA. Finally, the interferon-induced nuclease ISG20 degrades damaged DNA, leading to loss of cccDNA without cytolysis (figure 27).

This thesis provides strong evidence for the non-cytolytic control of cccDNA, the HBV persistence form, induced by cytokines and elucidates the molecular mechanisms behind this. The molecular investigation of the underlying mechanisms identified the crucial host effector proteins and revealed that expression of the deaminase A3A together with the nuclease ISG20 is sufficient to reduce cccDNA levels, thereby opening potential for implementation in therapy of chronic hepatitis B.

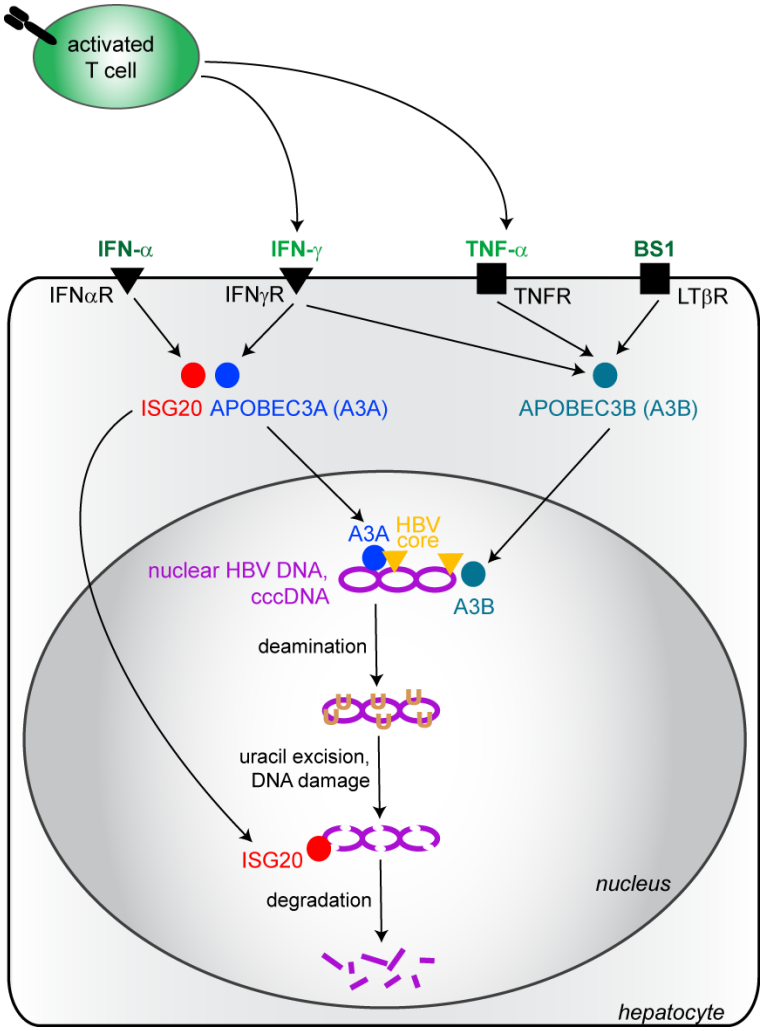

Figure 27: Proposed mechanism for cytokine-induced, non-cytolytic HBV cccDNA decline. Details are given in the main text.

4 Materials and methods

In the following chapters, used materials and applied methods are described. Parts of the here established or optimized methods are published as indicated (Lucifora, Xia et al. 2014, Xia et al. 2017b, Xia, Stadler et al. 2016).

4.1 Materials

This section gives an overview of the used laboratory materials, machines and software applications.

4.1.1 Cell lines

Used cell lines belong to the laboratory stock of AG Protzer, Institute of Virology, Munich.

Name	Description
HEK293	Human embryonic kidney cells, transformed with fragments of adenovirus type 5 DNA (Graham et al. 1977)
HepaRG	Human hepatoma cells, can be differentiated into hepatocyte- and biliary-like cells, susceptible to HBV infection (Gripon et al. 2002)
HepaRG-pEpi-H1.3	HepaRG cells with HBV-replicating episomes (Stadler 2013)
HepaRG-TR-A3A	HepaRG cells with inducible overexpression of A3A (Stadler 2013)
HepG2.2.15	HBV-producing hepatoblastoma cell line (Sells et al. 1987)
HepG2H1.3	Human hepatoma cells replicating HBV from a 1.3-fold genome integrate (Jost et al. 2007, Protzer et al. 2007)
HepG2H1.3-A3A	HepG2H1.3 cells with constant A3A overexpression (Stadler 2013)
Huh7	Human hepatoma cell line (Nakabayashi et al. 1982)
Huh7-S	Huh7 cells expressing the small HBsAg, generated by Oliver Quitt (Xia, Stadler et al. 2016)
E. coli Stbl3	Chemical competent *Escherichia coli* cells (Invitrogen, Carlsbad, USA)

4.1.2 Cell culture media

	William's E standard	William's E differentiation	William's E transwell
William's E medium	500 ml	500 ml	500 ml
FBS (fetal bovine serum) Fetalclone II	10 %	10 %	10 %
Penicillin/streptomycin	100 U/ml	100 U/ml *	100 U/ml
Glutamine	2 mM	2 mM	2 mM
Human insulin	0.023 U/ml	0.023 U/ml	0.023 U/ml
Hydrocortisone	4.7 µg/ml	4.7 µg/ml	-
Gentamicin	80 µg/ml	80 µg/ml *	80 µg/ml
DMSO		1.8 %	1.8 %

	DMEM full	DMEM differentiation
Dulbecco's Modified Eagle's Medium	500 ml	500 ml
Heat-inactivated fetal calf serum (FCS)	10 %	1 %
Penicillin/streptomycin	100 U/ml *	100 U/ml *
Glutamine	2 mM	2 mM
Non-essential amino acids	1 x	1 x
Sodium pyruvate	1 mM	1 mM
DMSO		1.74 %

*) omitted in antibiotic-free medium

	HBV production medium
William's E medium	500 ml
Heat-inactivated FCS	5 %
Penicillin/streptomycin	100 U/ml
Glutamine	2 mM
Non-essential amino acids	1 x
Sodium pyruvate	1 mM
Hydrocortisone	4.7 µg/ml
DMSO	1 %

4.1.3 Oligonucleotides for PCR

Oligonucleotides were purchased from Microsynth AG, Balgach, Switzerland; primers for *GAPDH* promoter region used in ChIP experiments were included in the Pierce Agarose ChIP Kit. A3A-V5 primers were used to measure overexpressed A3A, A3A primers for endogenous A3A mRNA levels.

Name	Sequence
3'-HBxin	AAGTGCACACGGTYYGGCAGAT
5'-HBxin	ATGGCTGCTARGCTGTGCTGCCAA
3'-pEpiOut	GGAGGTGTGGGAGGTTTTT
5'-pEpiXOut	CGCAAATATACATCGTTTCCAT
A3A fw	AAGGGACAAGCACATGGAAG
A3A rev	TGTGTGGATCCATCAAGTGTC
A3A-V5 fw	ACTAGATGAGCACAGCCAAGC
A3A-V5 rev	CCGAGGAGAGGGTTAGGGATA
A3B fw	CGCCAGACCTACTTGTGCTA
A3B rev	GCCACAGAGAAGATTCTTAGCC
cccDNA 2251+	AGCTGAGGCGGTATCTA
cccDNA 92-	GCCTATTGATTGGAAAGTATGT

c-myc-L	TCGAGAAGGGCAGGGCTTCTCAGAGGCTTG
c-myc-R	GGCGATATGCGGTCCCTACTCCAAGGAGCT
HBV DNA 1745	GGAGGGATACATAGAGGTTCCTTGA
HBV DNA 1844	GTTGCCCGTTTGTCCTCTAATTC
ISG20 fw	GATGCCGGCTTGGAGTTAGA
ISG20 rev	GACCCTCAGAGATGCTGCC
Kan-L	GGCAGGATCTCCTGTCATCT
Kan-R	CATCAGCCATGATGGATACTTTC
p53-L	GAGTGCAGTGGCACGATTT
p53-R	GAATCGCTTTCAGCTCAGGA
PELO fw	CCTCACTGACAGGGATGGAAGA
PELO rev	GAGTGGTGGCGAGTCCTTTA
PRNP fw	TGCTGGGAAGTGCCATGAG
PRNP rev	CGGTGCATGTTTTCACGATAGTA
RAD9A_1 fw	GAGAGCTGGGCAGTGTTGG
RAD9A_1 rev	CCTTGCCGAGCACCTTCA
Src-L	TGTGTGTGTGAGAAAACACAAAAT
Src-R	TCAGTCCTCCCAGGATGTTC
TBP_1 fw	TATAATCCCAAGCGGTTTGC
TBP_1 rev	CTGTTCTTCACTCTTGGCTCCT

4.1.4 Kits

Product	**Supplier**
AllPrep DNA/RNA Kit	Qiagen, Valencia, CA, USA
ChIP Kit ab500	Abcam, Cambridge, UK
CytoTox-ONE Homogeneous Membrane Integrity Assay	Promega Corporation, Madison, WI, USA
DIG Luminescent Detection Kit	Roche, Mannheim, Germany
Gateway LR Clonase II Enzyme Mix	Invitrogen, Carlsbad, CA, USA
GeneJET Gel Extraction Kit	Fermentas, St. Leon-Rot, Germany
GeneJET Plasmid Miniprep Kit	Thermo Scientific, Schwerte, Germany
Human IFN-γ ELISA MAX Standard Sets	Biolegend, San Diego, CA, USA
Human TNF ELISA Set (BD OptEIA)	BD Biosciences, San Diego, CA, USA
LightCycler 480 SYBR Green I Master mix	Roche, Mannheim, Germany
NucleoSpin RNA isolation Kit	Macherey-Nagel, Düren, Germany
NucleoSpin Tissue Kit	Macherey-Nagel, Düren, Germany
Pierce Agarose ChIP Kit	Thermo Scientific, Schwerte, Germany
PuReTaq Ready-To-Go PCR beads	GE Healthcare, Munich, Germany
SuperScript III First-Strand Synthesis SuperMix for qRT-PCR	Invitrogen, Carlsbad, CA, USA
TA Cloning Kit	Invitrogen, Karlsruhe, Germany

4.1.5 Antibodies

Name	Supplier	Catalogue number	Application (dilution)
A3A	Acris, Herford, Germany	AP31973PU-N	ChIP (1:50)
Anti-mouse	Sigma-Aldrich, Steinheim, Germany	A0168	Western blot (1:10,000)
Anti-rabbit	Sigma-Aldrich, Steinheim, Germany	A0545	Western blot (1:10,000)
Baminercept	Biogen Idec, Boston, MA, USA	BG9924	Cytokine neutralization (5 µg/ml)
Etanercept/Enbrel	Immunex, Seattle, WA, USA		Cytokine neutralization (10 µg/ml)
GAPDH	Acris, Herford, Germany	ACR001PT	Western blot (1:5,000)
HBV core (HBcAg)	Dako, Glostrup, Denmark	B0586	ChIP (1:20)
Histone H3	Abcam, Cambridge, UK	ab1791	ChIP (5 µg/reaction)
Human TNF-α neutralizing	Cell Signaling, Danvers, MA, USA	7321	Cytokine neutralization (500 ng/ml)
ISG20	Abcam, Cambridge, UK	ab154393	Western blot (1:500)
ISG20 H-50	Santa Cruz Biotechnology, Santa Cruz, CA, USA	sc-66937	Immunohistochemistry (1:200)
LEAF purified anti-human IFN-γ	Biolegend, San Diego, CA, USA	507513	Cytokine neutralization (20 µg/ml)
V5-tag	Abcam, Cambridge, UK	ab27671	Western blot (1:5,000)

4.1.6 Plasmids

Plasmid pLenti6.3/V5-GW/lacZ was obtained from Invitrogen (Karlsruhe, Germany), pLenti6.3-A3A was generated for CMV-promoter-driven overexpression of A3A as described (Stadler 2013). Plasmids pTR600 and pTR600-A3B for A3B-overexpression were kindly provided by Carsten Münk (Ooms et al. 2012).

4.1.7 Chemicals and reagents

Chemical or reagent	Supplier
Accell human ISG20 siRNA SMARTpool	GE Healthcare Dharmacon, Lafayette, USA
Accell non-targeting pool siRNA	GE Healthcare Dharmacon, Lafayette, USA
Accell SMARTpool APOBEC3A siRNA	GE Healthcare Dharmacon, Lafayette, USA
Accell SMARTpool APOBEC3B siRNA	GE Healthcare Dharmacon, Lafayette, USA
Agar-agar	Roth, Karlsruhe, Germany
Agarose	Peqlab, Erlangen, Germany

Amersham ECL Prime Western Blotting Detection Reagent	GE Healthcare Life Sciences, Freiburg, Germany
Ampicillin	Roth, Karlsruhe, Germany
APS	Roth, Karlsruhe, Germany
Blasticidin S HCl	Invitrogen, Carlsbad, USA
BS1	Biogen Idec, Boston, USA
Collagen R	Serva Electrophoresis, Heidelberg, Germany
CsCl	Roth, Karlsruhe, Germany
DharmaFECT 1 siRNA Transfection Reagent	GE Healthcare Dharmacon, Lafayette, USA
DMSO	Sigma-Aldrich, Steinheim, Germany
Dulbecco's Modified Eagle's Medium	Gibco/Invitrogen, Carlsbad, USA
Ethanol	Roth, Karlsruhe, Germany
Ethidium bromide	Merck, Darmstadt, Germany
FBS Fetalclone II, Hyclone	GE Healthcare Life Sciences, Freiburg, Germany
FCS (heat-inactivated)	Gibco/Invitrogen, Carlsbad, USA
Fish (herring) sperm DNA	Invitrogen, Carlsbad, USA
Formaldehyde	Roth, Karlsruhe, Germany
Geneticin (G418)	Thermo Fisher Scientific, Scotland, UK
Gentamicin	Ratiopharm, Ulm, Germany
Glutamine	Sigma-Aldrich, Steinheim, Germany
Glycine	Roth, Karlsruhe, Germany
HBsAg, recombinant	Rhein Biotech, Düsseldorf, Germany
Human TNF-α	Miltenyi Biotec, Bergisch Gladbach, Germany
Hydrocortisone	Pfizer, New York, USA
IFN-α (interferon alpha-2a/Roferon-A)	Roche, Vienna, Austria
IFN-γ (interferon gamma-1b/ Imukin)	Boehringer Ingelheim, Vienna, Austria
Insulin (Insuman Rapid)	Sanofi Aventis, Frankfurt, Germany
IPTG	Thermo Scientific, Rockford, USA
Isopropanol	Roth, Karlsruhe, Germany
LDS Sample Buffer, Non-Reducing (4X)	Thermo Scientific, Rockford, USA
Lipofectamine 2000	Life Technologies, Carlsbad, USA
Methanol	Roth, Karlsruhe, Germany
Milk powder	Roth, Karlsruhe, Germany
M-PER Mammalian Protein Extraction Reagent	Thermo Scientific, Rockford, USA
NaCl	Roth, Karlsruhe, Germany
NaN_3	Serva Electrophoresis, Heidelberg, Germany
NaOH	Roth, Karlsruhe, Germany

Non-essential amino acids 100x	Gibco/Invitrogen, Carlsbad, USA
OptiMEM	Gibco/Invitrogen, Carlsbad, USA
Page Ruler Plus Prestained protein ladder	Thermo Scientific, Waltham, USA
PBS	Gibco/Invitrogen, Carlsbad, USA
PEG6000	Merck, Hohenbrunn, Germany
Penicillin/streptomycin	Gibco/Invitrogen, Carlsbad, USA
Pierce RIPA buffer	Thermo Scientific, Rockford, USA
Polyacrylamide	Roth, Karlsruhe, Germany
Protease inhibitor (Complete)	Roche, Mannheim, Germany
RotiSafe	Roth, Karlsruhe, Germany
SDS	Roth, Karlsruhe, Germany
SmartLadder DNA (small fragment)	Eurogentec, Liege, Belgium
Sodium citrate	Roth, Karlsruhe, Germany
Sodium pyruvate	Gibco/Invitrogen, Carlsbad, USA
Sucrose	Roth, Karlsruhe, Germany
T5 exonuclease	New England Biolabs, Ipswich, USA
TEMED	Roth, Karlsruhe, Germany
Tetracycline	Applichem, Darmstadt, Germany
Tris base	Roth, Karlsruhe, Germany
Tris HCl	Roth, Karlsruhe, Germany
Trypan blue	Gibco/Invitrogen, Carlsbad, USA
Trypsin	Gibco/Invitrogen, Carlsbad, USA
Tryptone	Roth, Karlsruhe, Germany
Tween 20	Roth, Karlsruhe, Germany
William’s medium E	Gibco/Invitrogen, Carlsbad, USA
X-gal	Sigma-Aldrich, Steinheim, Germany
Yeast extract	Roth, Karlsruhe, Germany
Zeocin	Life Technologies, Carlsbad, USA

4.1.8 Laboratory equipment and consumables

Product	**Supplier**
Amersham Hybond PVDF membrane	GE Healthcare Life Sciences, Freiburg, Germany
Amersham nylon membrane Hybond N+	GE Healthcare Life Sciences, Freiburg, Germany
BEP (HBeAg measurement)	Siemens Molecular Diagnostics, Marburg, Germany
Cell culture flasks and plates	TPP, Trasadingen, Switzerland

Cell culture incubator HERAcell 150i	Thermo Scientific, Rockford, USA
Centricon Plus-70	Merck Millipore, Billerica, USA
Centrifuge 5417C / 5417R	Eppendorf, Hamburg, Germany
Cryo vials	Greiner Bio One, Kremsmünster, Austria
Dot blot device	GE Healthcare Life Sciences, Freiburg, Germany
ELISA 96well plates Nunc	Thermo Scientific, Rockford, USA
Falcon tubes 15ml, 50ml	Greiner Bio One, Kremsmünster, Austria
Fluorescence microscope CKX41	Olympus, Hamburg, Germany
Freezing container	Thermo Fisher Scientific, Waltham, USA
Fusion Fx7 (chemiluminescence detection; UV light system)	Peqlab, Erlangen, Germany
Gel chambers (agarose gel electrophoresis)	Peqlab, Erlangen, Germany
Gel chambers (SDS-PAGE)	Bio-Rad, Hercules, USA
Heating block	Eppendorf, Hamburg, Germany
Hemocytometer	Brand, Wertheim, Germany
Hyperflask	Corning, Amsterdam, The Netherlands
Light Cycler 480 II	Roche, Mannheim, Germany
Light Cycler 96	Roche, Mannheim, Germany
Nanodrop Photometer	Implen, Munich, Germany
Pipette “Accu-jet pro”	Brand, Wertheim, Germany
Pipette filter tips	Starlab, Ahrensburg, Germany
Pipette tips 2 - 50ml	Greiner Bio One, Kremsmünster, Austria
Pipettes	Eppendorf, Hamburg, Germany
PVDF membrane	Bio-Rad, Hercules, USA
qPCR 96-well plates	4titude, Berlin, Germany
Reaction tubes	Eppendorf, Hamburg, Germany
Reflotron ALT stripes	Roche, Mannheim, Germany
Reflotron Reflovet Plus (ALT reader)	Roche, Mannheim, Germany
Sterile filters 0.45µm	Merck, Millipore, Billerica, USA
Sterile hood	Heraeus, Hanau, Germany
Tecan plate reader Infinite F200	Tecan, Männedorf, Switzerland
Transwells 0.4 µm	Corning, Amsterdam, The Netherlands
Ultracentrifuge Beckman SW40 rotor	Beckman Coulter, Brea, USA
Western Blotting Chamber (Transblot SD Semi-Dry)	Bio-Rad, Hercules, USA
Western Blotting Chamber (Wet Blot)	Bio-Rad, Hercules, USA
Whatman paper	Bio-Rad, Hercules, USA

4.1.9 Software

Software name	Supplier
GeneDoc	Pittsburgh Supercomputing Center, Pittsburgh, USA
Graph Pad Prism 5.01	Graph Pad, La Jolla, USA
ImageJ	NIH, Bethesda, USA
LightCycler 480 Software 1.5.1.62	Roche, Mannheim, Germany
MEGA 5	Arizona State University, Tempe, USA
MUSCLE	EMBL-EBI, Cambridgeshire, UK
Windows 7/8/10, MS Office	Microsoft, Redmond, USA

4.2 Methods

In the following, the applied methods are described in order of their appearance in the results section.

4.2.1 Cell culture and treatments

All used human cells were cultured under standard cell culture conditions (37 °C, 5 % CO_2, 95 % humidity) and cell culture experiments were carried out with mycoplasma-negative cells under sterile conditions. For subculturing, cells were washed with 1x PBS, detached from cell culture flasks by incubation with 1x trypsin at 37 °C for five to ten minutes and resuspended in cell culture medium. HepaRG cells and derived cell lines were passaged weekly or every second week with a maximum dilution of 1:6, HEK293, Huh7- and HepG2-based cells were split every three to four days with a maximum dilution of 1:10. HepG2-based cells were kept in collagen-coated cell culture vessels (incubation of vessels with 1:10-diluted collagen for at least 30 minutes at 37 °C and washed with 1x PBS). For seeding of a defined cell number, an aliquot of the cell suspension was diluted 1:2 with trypan blue and living cells were counted using a hemocytometer (average number per quadrant multiplied with dilution factor 2 and 10^4 to get number of cells per ml). For freezing, cell suspension was centrifuged at 300 g for 10 minutes, cell pellet was diluted in freezing medium (respective standard cell culture medium with a total of 20 % FCS and 10 % DMSO) and put within cryovials into a freezing container at -80 °C. After a minimum of one day, frozen cells were transferred to the liquid nitrogen tank. For thawing of cells, vials were brought quickly from liquid nitrogen to 37 °C using a water bath. Thawed cells were resuspended, transferred to a new tube for centrifugation (300 g, 10 min), pellet was diluted in fresh, prewarmed cell culture medium and put into an appropriate cell culture flask.

HepaRG cells and derived cell lines were seeded and grown for two weeks in William's E standard medium and then differentiated for another two weeks in William's E differentiation medium as described in literature (Gripon et al. 2002). Only fully differentiated HepaRG (dHepaRG) cells were used for HBV infection. HepaRG-TR-A3A cells for tetracycline-inducible overexpression of A3A were generated previously (Stadler 2013). Briefly, the sequence of *A3A* was amplified from cDNA from IFN-γ-treated, dHepaRG cells and cloned into plasmid pLenti4-TO between a tetracycline-regulated CMV-promoter and a V5-tag. Using this plasmid, lentiviral vectors were produced and HepaRG-TR cells, which express the tetracycline repressor (TR), were transduced in cooperation with Julie Lucifora as described (Lucifora, Arzberger et al. 2011). HepaRG-TR-A3A cells were cultured as regular HepaRG cells except for the addition of selection antibiotics (300 µg/ml zeocin, 10 µg/ml blasticidin) for the transgenes at the time point of splitting. HepaRG-pEpi-H1.3 cells were generated by transfection of an episomal, HBV-replicating construct pEpi-H1.3 as described (Lucifora, Xia et al. 2014, Stadler 2013). HepaRG-pEpi-H1.3 cells were treated as regular HepaRG cells except for addition of 600 µg/ml geneticin at the time point of splitting to maintain the episomal construct and two weeks of additional differentiation to stabilize cccDNA amounts. HepG2H1.3, HepG2H1.3-A3A, Huh7, Huh7-S and HEK293 cells were cultured in DMEM full medium. HepG2H1.3-A3A cells, constantly expressing A3A under a CMV-promoter, were generated previously by lentiviral transduction (Lucifora, Xia et al. 2014, Stadler 2013). HepG2H1.3 and HepG2H1.3-A3A cells were seeded and grown to confluency in one to three days and differentiated then for 10 days before start of experiments using DMEM differentiation medium unless differently indicated. Huh7-S cells, expressing the small HBsAg, were generated by Oliver Quitt as described (Xia, Stadler et al. 2016) and passaged in the presence of 10 µg/ml blasticidin. The dHepaRG and derived cells were treated with 300 U/ml IFN-α or 500 U/ml IFN-α where indicated, 200 U/ml IFN-γ, 800 U/ml TNF-α, 0.5 µg/ml BS1 or 5 µg/ml tetracycline.

4.2.2 T-cell transwell co-culture system

To separate HBV-infected target cells and T cells, a transwell co-culture system (0.4 µm) was used. HBV-infected dHepaRG cells were kept in the lower chamber. The upper transwells were coated in initial experiments with 5 µg/ml recombinant HBsAg at 37 °C for two hours for stimulation of S-CAR T cells (cooperation with Yuchen Xia) (Xia, Stadler et al. 2016). After further optimization for this thesis, Huh7-S cells were used within the transwells for a more physiological activation of S-CAR T cells. $1.45x10^5$ Huh7 or Huh7-S cells were seeded per transwell and one day later $1x10^6$ S-CAR T cells were added to each transwell. From the timepoint of T-cell addition to the system, cell culture medium was changed to William's E transwell medium (Xia, Stadler et al. 2016). S-CAR T cells were generated and provided by Antje Malo as described (Xia, Stadler et al. 2016). For neutralization of T-cell cytokines, 20 µg/ml anti-human IFN-γ antibody, 500 ng/ml TNF-α neutralizing antibody, 5 µg/ml Baminercept (recombinant LTβR-Fc fusion protein) or

10 µg/ml Etanercept/Enbrel (recombinant TNF-receptor p75-Fc fusion protein) were used (Xia, Stadler et al. 2016).

4.2.3 Enzyme-linked immunosorbent assay (ELISA)

Cell culture supernatants were analysed for IFN-γ and TNF-α amounts by ELISA following the manufacturer's instructions. Absorbance was measured with a plate reader by Tecan.

4.2.4 HBV production and infection

HBV-producing HepG2.2.15 cells were seeded to a hyperflask and medium was changed to HBV production medium three to four days after. Medium was then renewed three times every three to four days and the last three supernatants were collected. HBV-containing medium was filtered through a 0.45 µm filter and concentrated in centrifugal filter devices (Centricon Plus-70) with an exclusion limit of 100 kDa in repeated centrifugation steps with 3,500 g at 4 °C for 30 to 60 minutes. In the end, concentrated virus was harvested by reverting the centrifugal device and two centrifugation steps with 2,000 g for 10 minutes each. Collected HBV stock was frozen in aliquots at -80 °C. Titre was determined by density gradient centrifugation followed by dot blot analysis: Each 500 µl CsCl in different concentrations (1.4 g/l, 1.3 g/l, 1.2 g/l), 20 % sucrose, 1 ml 1x PBS, 50 µl HBV stock and 1 ml 1x PBS were added in layers to a 5 ml-tube. Ultracentrifugation at 55,000 rpm, 10 °C for 17 hours with deceleration without brake was carried out. Harvested gradient (6 drops per well) was blotted together with an HBV DNA standard (denatured at 99 °C, 10 min) onto a nylon membrane. After PBS washing, membrane was dried, denatured (3 min, 0.4 M NaOH) and renatured (4 min, 2x SSC). Dried membrane was baked at 80 °C for one hour and developed: Prepared fish sperm DNA (99 °C, 10 min) was diluted 1:100 in prewarmed Church buffer and incubated with the membrane at 65 °C for two to four hours. 5 µl of DIG-labelled HBV-probe (99 °C, 5 min) were added to blocking buffer and membrane and incubated at 65 °C overnight. After three washing steps (2x SSC, 0.1 % SDS; 2x SSC, 0.1 % SDS; 1x SSC, 0.1 % SDS) for five minutes at 65 °C each, membrane was developed using the DIG Luminescent Detection Kit following manufacturer's instructions. These HBV stocks were used at a multiplicity of infection (MOI) of 600. Later, HBV stocks were provided by Jochen Wettengel through heparin affinity chromatography and sucrose gradient ultracentrifugation as described (Xia, Stadler et al. 2016). These HBV stocks were used at an MOI of 100 (regular dHepaRG cells) to 300 (dHepaRG-TR-A3A cells). HBV infection was performed in William's E differentiation medium with 5 % PEG6000 at 37 °C for 16 to 24 hours. After removing the infection medium, cells were washed three times with 1x PBS and cultured further in William's E differentiation medium. Experiments

with HBV-infected dHepaRG cells were started seven to 10 dpi unless otherwise indicated.

4.2.5 DNA extraction

Cellular DNA was extracted using the NucleoSpin Tissue Kit following the standard protocol for cultured cells but with an additional pre-lysis step at 56 °C (1-3 h), an elongated drying step (2 min) and incubation with prewarmed elution buffer for approx. five minutes.

4.2.6 Measurement of HBV markers and pEpi-H1.3

Total intracellular HBV DNA (primers: HBV 1745, HBV 1844), cccDNA (primers: cccDNA 92-, cccDNA 2251+), episomal pEpi-H1.3 (primers: Kan-L, Kan-R) and *PRNP* as a reference gene (primers: PRNP fw, PRNP rev) were determined by qPCR on a LightCycler 480 Real-time PCR system and data was analysed by advanced relative quantification considering primer efficiency and normalization to the reference gene. Per reaction, 4 µl extracted DNA were mixed with 0.5 µl forward primer (20 µM), 0.5 µl reverse primer (20 µM) and 5 µl LightCycler 480 SYBR Green I Master mix. During this study, cccDNA qPCR was optimized by prior digestion of extracted DNA with a T5 exonuclease, which removes linear DNA, rcDNA or nicked DNA but spares cccDNA, increasing the selectivity for cccDNA as described (Xia et al. 2017b). Where indicated, T5 exonuclease digestion was done before cccDNA qPCR: 8.5 µl extracted DNA were mixed with 1 µl NEB buffer 4 and 0.5 µl T5 exonuclease, incubated at 37 °C for 30 minutes with subsequent heat inactivation at 99 °C for 5 minutes and diluted 1:4 with water (Xia et al. 2017b). Secreted HBeAg was measured with a commercial immunoassay (BEP).

Total intracellular HBV DNA and *PRNP* were measured with following qPCR program:

	T [°C]	t [sec]	Ramp [°C/sec]	Acquisition mode	Cycles
Denaturation	95	300	4.4		1
Amplification	95	25	4.4		
	60	10	2.2		40
	72	30	4.4	single	
Melting	95	1	4.4		
	65	60	2.2		1
	95		0.11	continuous: 5/°C	
Cooling	40	30	2.2		1

Temperature profile for cccDNA amplification was:

	T [°C]	t [sec]	Ramp [°C/sec]	Acquisition mode	Cycles
Denaturation	95	600	4.4		1
Amplification	95	15	4.4		50
	60	5	2.2		
	72	45	4.4		
	88	2	4.4	single	
Melting	95	1	4.4		1
	65	15	2.2		
	95		0.11	continuous: 5/°C	
Cooling	40	30	2.2		1

Cycling program for pEpi-H1.3 was the program “GE_C3”:

	T [°C]	t [sec]	Ramp [°C/sec]	Acquisition mode	Cycles
Denaturation	95	300	4.4		1
Amplification	95	15	4.4		45
	60	10	2.2		
	72	25	4.4	single	
Melting	95	10	4.4		1
	65	60	2.2		
	95		0.11	continuous: 5/°C	
Cooling	40	1	2.2		1

4.2.7 Differential DNA denaturation PCR (3D-PCR) and sequence analysis

Cytosine deamination leads to the formation of uracils resulting in CG-to-TA conversions and therefore lower melting temperatures of double-stranded DNA allowing differential amplification of AT-rich sequences at low denaturing temperatures (Suspene et al. 2005). Therefore, 3D-PCR was applied to investigate deamination of nuclear HBV DNA as described (Xia et al. 2017b). In summary, 1/50-diluted products from cccDNA qPCR were used as template in nested PCR with the primers 5’-HBxin and 3’-HBxin with a temperature gradient in denaturing temperature. For pEpi-H1.3, first PCR was a qPCR with the primers 5’-pEpiXOut and 3’-pEpiOut and program “GE_C3” as described above. Diluted amplification products were used for a second, nested PCR with the primers 5’-HBxin and 3’-HBxin as for cccDNA. Nested PCRs were composed of 0.5 µl forward primer (20 µM), 0.5 µl reverse primer (20 µM), 1 µl diluted template DNA and 23 µl water added to “PuReTaq Ready-To-Go PCR beads”. Amplification was performed on a LightCycler 96 system with a gradient in denaturing temperature: (92-82 °C) for 5 min;

then (92-82 °C for 1 min; 60 °C for 30 sec; 72 °C for 30 sec) x35; 72 °C for 10 min. Amplification with the same program but a denaturing temperature of 95 °C was used as positive control. Amplicons from 3D-PCR were visualised on a 2 %-agarosegel and selected amplicons were extracted for sequence analysis.

DNA was extracted from gel with GeneJET Gel Extraction Kit following the provided protocol but with shaking at 800 rpm in step 3, addition of isopropanol in step 4 and incubation with prewarmed elution buffer in step 9 (65 °C, 5 min). Purified DNA was cloned into a sequencing vector using TA Cloning Kit following the protocol and using 1 µl of pCR2.1 vector (25 ng/µl) and 2 µl of purified PCR product. Competent *E. coli* Stbl3 cells were transformed with ligation product as suggested by the TA Cloning Kit-protocol but 2.5 µl ligation product were used, mixing was done without stirring with the pipette tip and vials were shaken approx. 30 minutes. Bacteria were grown on LB plates with 100 µg/ml ampicillin and additionally 40 µl X-gal (4 %) and 4 µl IPTG (1 M) at 37 °C. The day after, white colonies were selected and propagated in LB medium with 50 µg/ml ampicillin overnight at 37° C and 225 rpm. Grown bacteria were harvested by centrifugation (5000 g, 10 min) and plasmids were extracted using the GeneJET Plasmid Miniprep Kit according to the protocol but with drying for two minutes and incubation before elution for more than two minutes. Samples were brought to a concentration between 30 and 100 ng/µl and sent for sequencing to GATC Biotech (Konstanz, Germany). Insert sequences were analysed by multiple sequence alignment with “MUSCLE” (Edgar 2004) including the wild type (WT) sequence of HBV from the databank of the Institute of Virology, Munich. The alignment was processed with the software “GeneDoc” and nucleotide compositions were calculated with “MEGA 5” (Tamura et al. 2011).

4.2.8 Cytotoxicity assay: LDH release assay

“CytoTox-ONE Homogeneous Membrane Integrity Assay” was used to measure cell death by means of LDH release into the supernatant according to the manufacturer’s instructions.

4.2.9 Knockdowns of A3A, A3B and ISG20 by siRNA

For A3A and A3B knockdown, dHepaRG cells were transfected with 2 µl Lipofectamine 2000 reagent and 40 pmol siRNA (Accell SMARTpool APOBEC3A siRNA, Accell SMARTpool APOBEC3B siRNA or Accell non-targeting pool siRNA) per well of a 12-well plate according to the supplied protocol in antibiotic-free William’s E differentiation medium. For ISG20 knockdown, dHepaRG cells were transfected overnight in antibiotic-free William’s E differentiation medium with 0.75 µl DharmaFECT 1 siRNA Transfection Reagent per well of a 12-well plate according to the manufacturer’s instructions and

20 nM Accell human ISG20 siRNA SMARTpool or 20 nM Accell non-targeting pool siRNA.

4.2.10 RNA extraction and quantitative reverse transcription PCR (qRT-PCR)

RNA was extracted according to manufacturer's instructions with the NucleoSpin RNA isolation Kit, for HBV-infected samples incubation time of DNA digestion was increased to 45 minutes and elution volume was generally reduced to 40 µl. Reverse transcription into cDNA was carried out using "SuperScript III First-Strand Synthesis SuperMix for qRT-PCR" following the provided protocol with following modifications: 5 µl RT reaction mix were mixed with 1 µl RT enzyme mix and 4 µl extracted RNA to a final volume of 10 µl; 0.5 µl RNaseH were added and cDNA was diluted 1:10 with PCR-grade water. Diluted cDNA was used with LightCycler 480 SYBR Green I Master mix in qPCR with the program "GE_C3" as described above for pEpi-H1.3. qPCRs ran on a LightCycler 480 system and data was analysed by advanced relative quantification considering primer efficiency and normalization to a reference gene.

4.2.11 Plasmid transfection

HepG2H1.3 cells were transfected with the plasmids pLenti6.3, pLenti6.3-A3A, pTR600 and pTR600-A3B. Transfection in suspension during the seeding procedure was carried out in antibiotic-free DMEM full medium, medium was changed one day after transfection to DMEM full medium and cells were further cultured as indicated for the individual experiments. When cells were differentiated before experiment start as indicated, dHepG2H1.3 cells were transfected overnight in antibiotic-free DMEM differentiation medium. 3.5 µl Lipofectamine 2000 reagent and 1 µg plasmid-DNA per well of a 12-well plate were used according to manufacturer's instructions.

4.2.12 Chromatin immunoprecipitation (ChIP)

Transfected dHepG2H1.3 cells and dHepG2H1.3-A3A cells were prepared for ChIP using the ChIP Kit ab500 according to manufacturer's instructions but without shearing of DNA and reverse cross-link or Pierce Agarose ChIP Kit following the supplied protocol, respectively. Non-sheared or non-digested DNA for cccDNA or DNA digested with MNase for genomic DNA were analysed by qPCRs. Protocol for cccDNA qPCR is described above and genomic DNA (*GAPDH*, *p53*, *Src, c-myc* promoter regions) was measured using LightCycler 480 SYBR Green I Master mix in qPCR with the program "GE_C3" as described above for pEpi-H1.3. qPCRs ran on a LightCycler 480 system and data was analysed by absolute quantification considering primer efficiency.

4.2.13 Sodium dodecyl sulphate-polyacrylamide gel electrophoresis (SDS-PAGE) and Western blot analyses

SDS-PAGE was prepared as follows including isopropanol overlay of separation gel during polymerization:

Separation gel	**12.5 %**
Acrylamide (40 %)	3.1 ml
Tris (1.5 M, pH 8.8)	2.5 ml
H_2O	4.3 ml
SDS (10 %)	165 µl
TEMED	10 µl
APS (10 %)	50 µl
total volume	10 ml

Collection gel	**5 %**
Acrylamide (40 %)	187.5 µl
Tris (0.5 M, pH 6.8)	600 µl
H_2O	1.7 ml
SDS (10 %)	25 µl
TEMED	2 µl
APS (10 %)	25 µl
total volume	2.5 ml

Protein lysates were cooked (99 °C, 5 min, 800 rpm) and spun down and separated together with 5 µl of prestained protein ladder (Page Ruler Plus) by SDS-PAGE (running buffer: 3 g/l Tris base, 14.4/l g glycine, 1 g/l SDS).

For A3A Western blot, cells were lysed in M-PER Mammalian Protein Extraction Reagent with protease inhibitors and mixed with a loading dye (LDS Sample Buffer, Non-Reducing (4X)) before protein separation in a 12.5 %-SDS-PAGE. Proteins were blotted onto a methanol-activated PVDF membrane in a semi-dry manner (transfer buffer: 3 g/l Tris base, 14.4/l g glycine, 20 % methanol) for two hours at 20 Volt. After blocking with 5 % milk, blots were incubated in primary antibody solution (0.5 % milk, 0.05 % PBS-T, diluted primary antibody) at 4°C overnight. After three times washing (0.05 % PBS-T) for 10 minutes, membranes were kept for two hours in secondary antibody solution (0.5 % milk, 0.05 % PBS-T, diluted secondary antibody) at room temperature and the blots were developed after three times washing using Amersham ECL Prime Western Blotting Detection Reagent.

For ISG20 Western blot, cells were lysed in Pierce RIPA buffer with protease inhibitors. Proteins were separated in a 12 %-SDS-PAGE and blotted onto a methanol-activated PVDF membrane (Bio-Rad) in a wet blot procedure (transfer buffer: 3 g/l Tris base, 14.4/l g glycine, 20 % methanol) with 300 mA for 1.5 hours. After blocking with 3 % milk in TBS-T, blots were incubated in primary antibody solution (1 % milk, 0.1 % TBS-T, 0.04 % NaN_3, diluted primary antibody) at 4°C overnight. After three times washing (0.1 % TBS-T) for 10 minutes, membranes were kept for one hour in secondary antibody solution (1 % milk, 0.1 % TBS-T, diluted secondary antibody) at room temperature and the blots were developed after three times washing using Amersham ECL Prime Western Blotting Detection Reagent.

4.2.14 Microarray-based gene expression analysis

Total RNA was extracted from cell culture samples using the AllPrep DNA/RNA Kit according to manufacturer's instructions. Further steps were carried out by Julia Heß and Kristian Unger (Research Unit Radiation Cytogenetics, Helmholtz Zentrum München, Neuherberg, Germany): RNA integrity was assessed using the 2100 Bioanalyzer (Agilent Technologies, Santa Clara, CA, USA) in combination with the RNA 6000 Nano Kit (Agilent Technologies). All samples showed a RIN of > 8.5. Global gene expression profiling was performed using SurePrint G3 Human Gene Expression 8x60k microarrays (v2, AMADID 039494, Agilent Technologies) according to the manufacturer's protocol with an input of 25 ng of total RNA (one-color Low Input Quick Amp Labeling Kit, Agilent Technologies). Hybridized microarrays were scanned with a G2505C Sure Scan Microarray Scanner (Agilent Technologies) and raw data were extracted with the Feature Extraction 10.7 software (Agilent Technologies). Data quality assessment, preprocessing, normalization, and differential expression analyses were conducted with the R Bioconductor packages limma (Ritchie et al. 2015) and Agi4x44PreProcess, whereas Benjamini-Hochberg adjusted *p*-values (FDR) (Benjamini and Hochberg 1995) smaller than 0.1 were considered statistically significant. Gene ontology (GO) terms of the resulting gene lists were extracted deploying the Ensembl BioMart database.

4.2.15 Immunohistochemistry

The used liver tissues were provided by the DZIF Gewebebank Heidelberg and handled according to the guidelines of the tissue bank and the vote of the ethics commission of the University of Heidelberg. Paraffin-embedded liver tissue sections came from patients with acute or chronic hepatitis B, chronic hepatitis B with HDV superinfection, chronic hepatitis B with HCV co-infection or acute hepatitis C. As control, tissues after metastasis resection but from otherwise healthy patients were considered. Immunohistochemistry data was obtained by Felix Lasitschka (Institute of Pathology/DZIF tissue bank, University of Heidelberg, Heidelberg, Germany): For each clinical entity, liver tissue samples from three different patients were stained with an antibody against ISG20 as described (Lu et al. 2013). ISG20 positive area was measured by Marc Ringelhan using image analysis software Tissue IA (Slidepath, Leica, Wetzlar, Germany) with optimized colour detection and quantification algorithms at 40 x magnification. Data are presented as DAB positive area in % of total recognizable tissue area (each sample 3 – 20 mm^2 tissue area analysed).

4.2.16 Adenoviral transduction

Adenoviral vectors were generated by Jessica Schneider for her master thesis, the detailed description therein is summarized here: For shRNA-mediated knockdown of ISG20, synthetic oligonucleotides (sequences adapted from The RNAi Consortium

Collection, Mission shRNA, Sigma-Aldrich, Steinheim, Germany; shISG20_1 fw: AGCTGCAACGATGGAGCTCTATCAAGGATCCTTGATAGAGCTCCATCGTTGCTTTTT, shISG20_1 rev: TCGAAAAAAGCAACGATGGAGCTCTATCAAGGATCCTTGATAGAGCTCCATCGTTGC) were annealed and ligated into a HindIII- and SalI-digested pEntry-backbone with H1-promoter. For overexpression of ISG20, cDNA from IFN-α-treated dHepaRG cells was PCR-amplified (ISG20 HIII fw: tatcaagctTAGAAACTGAAACAGGGTCGGGATG, ISG20 BHI rev: ataggatccTCAGTCTGACACAGCCAGGCG) and cloned into a HindIII- and BamHI-digested pEntry-backbone behind a CMV-promoter. The empty pEntry-CMV vector was used as control. Plasmids for adenovirus production were generated following the Gateway approach (pAd/PL-DEST Gateway Vectors and Virapower Adenoviral Expression Systems, Invitrogen, Carlsbad, USA) using Gateway LR Clonase II Enzyme Mix (Invitrogen, Carlsbad, USA) and the pAd/PL-DEST plasmid. Resulting constructs were transfected in HEK293 cells for production of adenoviral vectors. Adenoviral vectors for ISG20 knockdown (AdV-shISG20) and overexpression (AdV-ISG20) or control vectors (AdV) were amplified in HEK293 cells to high titres (Schneider 2016). The GFP-expressing adenoviral vector AdV-GHL- was provided by Antje Malo and has been described as AdHBV-L- before (Sprinzl et al. 2001).

The titre of the applied adenoviral stocks was determined by infection of confluent HEK293 cells in 12-well plates. Volumes between 0.03 µl and 100 µl of the adenoviral stock were added per well for infection and cell layers were checked after 48 hours. The minimal volume leading still to detachment of all HEK293 cells was considered to equal an MOI of five and $5x10^6$ infectious units (IU). Following titres were determined by this approach: AdV-shISG20: $5x10^8$ IU/ml, AdV-ISG20: $1.1x10^9$ IU/ml, AdV: $1.7x10^9$ IU/ml, AdV-GHL-: $1.7x10^{10}$ IU/ml.

For transduction of dHepaRG or dHepG2H1.3-A3A cells, adenoviral stocks were diluted in DMEM medium without supplements to achieve indicated MOIs and cells were incubated with the infection medium for two hours in the cell culture incubator. After incubation, the infection medium was replaced by the respective differentiation medium. For ISG20 knockdown or overexpression, dHepaRG or dHepG2H1.3-A3A cells were transduced with an MOI of three of the respective adenoviral vector assuming $1x10^6$ cells per well of a 12-well plate or $0.5x10^6$ cells per well of a 24-well plate.

4.2.17 Statistical analysis

Numeric values are presented as means with standard deviation; *p*-values were calculated with Student's unpaired two-tailed *t*-test with Welch's correction or one-way ANOVA using Prism 5.01 software.

5 Figures

6 References

Addison, W. R., Walters, K.-A., Wong, W. W. S., Wilson, J. S., Madej, D., Jewell, L. D. and Tyrrell, D. L. J. (2002) Half-Life of the Duck Hepatitis B Virus Covalently Closed Circular DNA Pool In Vivo following Inhibition of Viral Replication. *J Virol, 76*(12), pp. 6356-6363.

Aynaud, M. M., Suspene, R., Vidalain, P. O., Mussil, B., Guetard, D., Tangy, F., Wain-Hobson, S. and Vartanian, J. P. (2012) Human Tribbles 3 protects nuclear DNA from cytidine deamination by APOBEC3A. *J Biol Chem, 287*(46), pp. 39182-92.

Baumert, T. F., Rösler, C., Malim, M. H. and von Weizsäcker, F. (2007) Hepatitis B virus DNA is subject to extensive editing by the human deaminase APOBEC3C. *Hepatology, 46*(3), pp. 682-689.

Belloni, L., Allweiss, L., Guerrieri, F., Pediconi, N., Volz, T., Pollicino, T., Petersen, J., Raimondo, G., Dandri, M. and Levrero, M. (2012) IFN-α inhibits HBV transcription and replication in cell culture and in humanized mice by targeting the epigenetic regulation of the nuclear cccDNA minichromosome. *J Clin Invest, 122*(2), pp. 529-537.

Ben-Ari, Z., Mor, E., Papo, O., Kfir, B., Sulkes, J., Tambur, A. R., Tur-Kaspa, R. and Klein, T. (2003) Cytokine gene polymorphisms in patients infected with hepatitis B virus. *Am J Gastroenterol, 98*(1), pp. 144-50.

Benjamini, Y. and Hochberg, Y. (1995) Controlling the False Discovery Rate: A Practical and Powerful Approach to Multiple Testing. *Journal of the Royal Statistical Society. Series B (Methodological), 57*(1), pp. 289-300.

Bertoletti, A. and Ferrari, C. (2012) Innate and adaptive immune responses in chronic hepatitis B virus infections: towards restoration of immune control of viral infection. *Gut, 61*(12), pp. 1754-64.

Bessho, T. and Sancar, A. (2000) Human DNA Damage Checkpoint Protein hRAD9 Is a 3′ to 5′ Exonuclease. *J Biol Chem, 275*(11), pp. 7451-7454.

Biermer, M., Puro, R. and Schneider, R. J. (2003) Tumor Necrosis Factor Alpha Inhibition of Hepatitis B Virus Replication Involves Disruption of Capsid Integrity through Activation of NF-κB. *J Virol, 77*(7), pp. 4033-4042.

Bock, C. T., Schwinn, S., Locarnini, S., Fyfe, J., Manns, M. P., Trautwein, C. and Zentgraf, H. (2001) Structural organization of the hepatitis B virus minichromosome. *J Mol Biol, 307*(1), pp. 183-96.

Boettler, T., Panther, E., Bengsch, B., Nazarova, N., Spangenberg, H. C., Blum, H. E. and Thimme, R. (2006) Expression of the Interleukin-7 Receptor Alpha Chain (CD127) on Virus-Specific CD8+ T Cells Identifies Functionally and Phenotypically Defined Memory T Cells during Acute Resolving Hepatitis B Virus Infection. *J Virol, 80*(7), pp. 3532-3540.

Bohne, F., Chmielewski, M., Ebert, G., Wiegmann, K., Kürschner, T., Schulze, A., Urban, S., Krönke, M., Abken, H. and Protzer, U. (2008) T Cells Redirected Against Hepatitis B Virus Surface Proteins Eliminate Infected Hepatocytes. *Gastroenterology, 134*(1), pp. 239-247.

Bonvin, M., Achermann, F., Greeve, I., Stroka, D., Keogh, A., Inderbitzin, D., Candinas, D., Sommer, P., Wain-Hobson, S., Vartanian, J. P. and Greeve, J. (2006) Interferon-inducible expression of APOBEC3 editing enzymes in human hepatocytes and inhibition of hepatitis B virus replication. *Hepatology, 43*(6), pp. 1364-74.

Burnicka-Turek, O., Kata, A., Buyandelger, B., Ebermann, L., Kramann, N., Burfeind, P., Hoyer-Fender, S., Engel, W. and Adham, I. M. (2010) Pelota interacts with HAX1, EIF3G and SRPX and the resulting protein complexes are associated with the actin cytoskeleton. *BMC Cell Biol, 11*, pp. 28.

Burns, M. B., Lackey, L., Carpenter, M. A., Rathore, A., Land, A. M., Leonard, B., Refsland, E. W., Kotandeniya, D., Tretyakova, N., Nikas, J. B., Yee, D., Temiz, N. A., Donohue, D. E., McDougle, R. M., Brown, W. L., Law, E. K. and Harris, R. S. (2013) APOBEC3B is an enzymatic source of mutation in breast cancer. *Nature, 494*(7437), pp. 366-370.

Chen, H.-W., Koehler, C. M. and Teitell, M. A. (2007) Human polynucleotide phosphorylase: location matters. *Trends Cell Biol, 17*(12), pp. 600-608.

Chen, M., Sallberg, M., Hughes, J., Jones, J., Guidotti, L. G., Chisari, F. V., Billaud, J. N. and Milich, D. R. (2005) Immune tolerance split between hepatitis B virus precore and core proteins. *J Virol, 79*(5), pp. 3016-27.

Chowdhury, S., Kitamura, K., Simadu, M., Koura, M. and Muramatsu, M. (2013) Concerted action of activation-induced cytidine deaminase and uracil-DNA glycosylase reduces covalently closed circular DNA of duck hepatitis B virus. *FEBS Lett, 587*(18), pp. 3148-52.

Crowther, R. A., Kiselev, N. A., Böttcher, B., Berriman, J. A., Borisova, G. P., Ose, V. and Pumpens, P. (1994) Three-dimensional structure of hepatitis B virus core particles determined by electron cryomicroscopy. *Cell, 77*(6), pp. 943-950.

Dane, D. S., Cameron, C. H. and Briggs, M. (1970) Virus-like particles in serum of patients with Australia-antigen-associated hepatitis. *Lancet, 1*(7649), pp. 695-8.

Degols, G., Eldin, P. and Mechti, N. (2007) ISG20, an actor of the innate immune response. *Biochimie, 89*(6–7), pp. 831-835.

Dimitropoulou, D., Karakantza, M., Theodorou, G. L., Leonidou, L., Assimakopoulos, S. F., Mouzaki, A. and Gogos, C. A. (2013) Serum cytokine profile in patients with hepatitis B e antigen-negative chronic active hepatitis B and inactive hepatitis B virus carriers. *World J Gastrointest Pathophysiol, 4*(1), pp. 24-7.

Edgar, R. C. (2004) MUSCLE: multiple sequence alignment with high accuracy and high throughput. *Nucleic Acids Res, 32*(5), pp. 1792-7.

Espert, L., Degols, G., Gongora, C., Blondel, D., Williams, B. R., Silverman, R. H. and Mechti, N. (2003) ISG20, a New Interferon-induced RNase Specific for Single-stranded RNA, Defines an Alternative Antiviral Pathway against RNA Genomic Viruses. *J Biol Chem, 278*(18), pp. 16151-16158.

Espert, L., Degols, G., Lin, Y.-L., Vincent, T., Benkirane, M. and Mechti, N. (2005) Interferon-induced exonuclease ISG20 exhibits an antiviral activity against human immunodeficiency virus type 1. *J Gen Virol, 86*(8), pp. 2221-2229.

Faustman, D. and Davis, M. (2010) TNF receptor 2 pathway: drug target for autoimmune diseases. *Nat Rev Drug Discov, 9*(6), pp. 482-493.

Gerlich, W. H. and Robinson, W. S. (1980) Hepatitis B virus contains protein attached to the 5' terminus of its complete DNA strand. *Cell, 21*(3), pp. 801-9.

Giersch, K., Allweiss, L., Volz, T., Helbig, M., Bierwolf, J., Lohse, A. W., Pollok, J. M., Petersen, J., Dandri, M. and Lutgehetmann, M. (2015) Hepatitis Delta co-infection in humanized mice leads to pronounced induction of innate immune responses in comparison to HBV mono-infection. *J Hepatol, 63*(2), pp. 346-53.

Gongora, C., David, G., Pintard, L., Tissot, C., Hua, T. D., Dejean, A. and Mechti, N. (1997) Molecular Cloning of a New Interferon-induced PML Nuclear Body-associated Protein. *J Biol Chem, 272*(31), pp. 19457-19463.

Gordien, E., Rosmorduc, O., Peltekian, C., Garreau, F., Brechot, C. and Kremsdorf, D. (2001) Inhibition of hepatitis B virus replication by the interferon-inducible MxA protein. *J Virol, 75*(6), pp. 2684-91.

Graham, F. L., Smiley, J., Russell, W. C. and Nairn, R. (1977) Characteristics of a Human Cell Line Transformed by DNA from Human Adenovirus Type 5. *J Gen Virol, 36*(1), pp. 59-72.

Green, A. M., Landry, S., Budagyan, K., Avgousti, D., Shalhout, S., Bhagwat, A. S. and Weitzman, M. D. (2016) APOBEC3A damages the cellular genome during DNA replication. *Cell Cycle*, pp. 0.

Gripon, P., Rumin, S., Urban, S., Le Seyec, J., Glaise, D., Cannie, I., Guyomard, C., Lucas, J., Trepo, C. and Guguen-Guillouzo, C. (2002) Infection of a human hepatoma cell line by hepatitis B virus. *Proc Natl Acad Sci, 99*(24), pp. 15655-15660.

Guidotti, L. G., Ando, K., Hobbs, M. V., Ishikawa, T., Runkel, L., Schreiber, R. D. and Chisari, F. V. (1994) Cytotoxic T lymphocytes inhibit hepatitis B virus gene expression by a noncytolytic mechanism in transgenic mice. *Proc Natl Acad Sci, 91*(9), pp. 3764-3768.

Guidotti, L. G. and Chisari, F. V. (2001) Noncytolytic control of viral infections by the innate and adaptive immune response. *Annu Rev Immunol, 19*, pp. 65-91.

Guidotti, L. G., Ishikawa, T., Hobbs, M. V., Matzke, B., Schreiber, R. and Chisari, F. V. (1996) Intracellular Inactivation of the Hepatitis B Virus by Cytotoxic T Lymphocytes. *Immunity, 4*(1), pp. 25-36.

Guidotti, L. G., Rochford, R., Chung, J., Shapiro, M., Purcell, R. and Chisari, F. V. (1999) Viral clearance without destruction of infected cells during acute HBV infection. *Science, 284*(5415), pp. 825-9.

Guo, Y.-H., Li, Y.-N., Zhao, J.-R., Zhang, J. and Yan, Z. (2011) HBc binds to the CpG islands of HBV cccDNA and promotes an epigenetic permissive state. *Epigenetics, 6*(6), pp. 720-726.

Guo, Y., Kang, W., Lei, X., Li, Y., Xiang, A., Liu, Y., Zhao, J., Zhang, J. and Yan, Z. (2012) Hepatitis B viral core protein disrupts human host gene expression by binding to promoter regions. *BMC Genomics, 13*, pp. 563.

Guo, Y., Li, Y., Mu, S., Zhang, J. and Yan, Z. (2009) Evidence that methylation of hepatitis B virus covalently closed circular DNA in liver tissues of patients with chronic hepatitis B modulates HBV replication. *J Med Virol, 81*(7), pp. 1177-83.

Hantz, O., Parent, R., Durantel, D., Gripon, P., Guguen-Guillouzo, C. and Zoulim, F. (2009) Persistence of the hepatitis B virus covalently closed circular DNA in HepaRG human hepatocyte-like cells. *J Gen Virol, 90*(Pt 1), pp. 127-35.

Haybaeck, J., Zeller, N., Wolf, M. J., Weber, A., Wagner, U., do Kurrer, M. O., Bremer, J., Iezzi, G., Graf, R., Clavien, P.-A., Thimme, R., Blum, H., Nedospasov, S. A., Zatloukal, K., Ramzan, M., Ciesek, S., Pietschmann, T., Marche, P. N., Karin, M., Kopf, M., Browning, J. L., Aguzzi, A. and Heikenwalder, M. (2009) A lymphotoxin-driven pathway to hepatocellular carcinoma. *Cancer cell, 16*(4), pp. 295-308.

Heim, M. H. and Thimme, R. (2014) Innate and adaptive immune responses in HCV infections. *J Hepatol, 61*(1 Suppl), pp. S14-25.

Heise, T., Guidotti, L. G., Cavanaugh, V. J. and Chisari, F. V. (1999) Hepatitis B virus RNA-binding proteins associated with cytokine-induced clearance of viral RNA from the liver of transgenic mice. *J Virol, 73*(1), pp. 474-81.

Hoopes, J. I., Cortez, L. M., Mertz, T. M., Malc, E. P., Mieczkowski, P. A. and Roberts, S. A. (2016) APOBEC3A and APOBEC3B Preferentially Deaminate the Lagging Strand Template during DNA Replication. *Cell Rep*, *14(6),* pp. 1273–1282.

Hu, J. and Liu, K. (2017) Complete and Incomplete Hepatitis B Virus Particles: Formation, Function, and Application. *Viruses, 9*(3).

Hu, X., Zimmerman, M. A., Bardhan, K., Yang, D., Waller, J. L., Liles, G. B., Lee, J. R., Pollock, R., Lev, D., Ware, C. F., Garber, E., Bailly, V., Browning, J. L. and Liu, K. (2013) Lymphotoxin beta receptor mediates caspase-dependent tumor cell apoptosis in vitro and tumor suppression in vivo despite induction of NF-kappaB activation. *Carcinogenesis, 34*(5), pp. 1105-14.

Huang, H. C., Chen, C. C., Chang, W. C., Tao, M. H. and Huang, C. (2012) Entry of hepatitis B virus into immortalized human primary hepatocytes by clathrin-dependent endocytosis. *J Virol, 86*(17), pp. 9443-53.

Iwai, Y., Terawaki, S., Ikegawa, M., Okazaki, T. and Honjo, T. (2003) PD-1 inhibits antiviral immunity at the effector phase in the liver. *J Exp Med, 198*(1), pp. 39-50.

Janahi, E. M. and McGarvey, M. J. (2013) The inhibition of hepatitis B virus by APOBEC cytidine deaminases. *J Viral Hepat, 20*(12), pp. 821-828.

Janssen, H. L. A., van Zonneveld, M., Senturk, H., Zeuzem, S., Akarca, U. S., Cakaloglu, Y., Simon, C., So, T. M. K., Gerken, G., de Man, R. A., Niesters, H. G. M., Zondervan, P., Hansen, B. and Schalm, S. W. (2005) Pegylated interferon alfa-2b alone or in combination with lamivudine for HBeAg-positive chronic hepatitis B: a randomised trial. *The Lancet, 365*(9454), pp. 123-129.

Jarmuz, A., Chester, A., Bayliss, J., Gisbourne, J., Dunham, I., Scott, J. and Navaratnam, N. (2002) An anthropoid-specific locus of orphan C to U RNA-editing enzymes on chromosome 22. *Genomics, 79*(3), pp. 285-96.

Jiang, B., Himmelsbach, K., Ren, H., Boller, K. and Hildt, E. (2016) Subviral Hepatitis B Virus Filaments, like Infectious Viral Particles, Are Released via Multivesicular Bodies. *J Virol, 90*(7), pp. 3330-41.

Jost, S., Turelli, P., Mangeat, B., Protzer, U. and Trono, D. (2007) Induction of antiviral cytidine deaminases does not explain the inhibition of hepatitis B virus replication by interferons. *J Virol, 81*(19), pp. 10588-96.

Kaluza, W., Reuss, E., Grossmann, S., Hug, R., Schopf, R. E., Galle, P. R., Maerker-Hermann, E. and Hoehler, T. (2000) Different transcriptional activity and in vitro TNF-alpha production in psoriasis patients carrying the TNF-alpha 238A promoter polymorphism. *J Invest Dermatol, 114*(6), pp. 1180-3.

Kitamura, K., Wang, Z., Chowdhury, S., Simadu, M., Koura, M. and Muramatsu, M. (2013) Uracil DNA glycosylase counteracts APOBEC3G-induced hypermutation of hepatitis B viral genomes: excision repair of covalently closed circular DNA. *PLoS Pathog, 9*(5), pp. e1003361.

Ko, C., Michler, T. and Protzer, U. (2017) Novel viral and host targets to cure hepatitis B. *Curr Opin Virol, 24*, pp. 38-45.

Köck, J., Rösler, C., Zhang, J.-J., Blum, H. E., Nassal, M. and Thoma, C. (2010) Generation of Covalently Closed Circular DNA of Hepatitis B Viruses via Intracellular Recycling Is Regulated in a Virus Specific Manner. *PLoS Pathog, 6*(9), pp. e1001082.

Königer, C., Wingert, I., Marsmann, M., Rosler, C., Beck, J. and Nassal, M. (2014) Involvement of the host DNA-repair enzyme TDP2 in formation of the covalently closed circular DNA persistence reservoir of hepatitis B viruses. *Proc Natl Acad Sci U S A, 111*(40), pp. E4244-53.

Kramvis, A. (2014) Genotypes and genetic variability of hepatitis B virus. *Intervirology, 57*(3-4), pp. 141-50.

Krokan, H. E., Saetrom, P., Aas, P. A., Pettersen, H. S., Kavli, B. and Slupphaug, G. (2014) Error-free versus mutagenic processing of genomic uracil--relevance to cancer. *DNA Repair (Amst), 19*, pp. 38-47.

Leong, C. R., Funami, K., Oshiumi, H., Mengao, D., Takaki, H., Matsumoto, M., Aly, H. H., Watashi, K., Chayama, K. and Seya, T. (2016) Interferon-stimulated gene of 20 kDa protein (ISG20) degrades RNA of Hepatitis B virus to impede the replication of HBV in vitro and in vivo. *Oncotarget*, *7(42)*, pp. 68179-68193.

Levrero, M., Pollicino, T., Petersen, J., Belloni, L., Raimondo, G. and Dandri, M. (2009) Control of cccDNA function in hepatitis B virus infection. *J Hepatol, 51*(3), pp. 581-92.

Liu, Y., Nie, H., Mao, R., Mitra, B., Cai, D., Yan, R., Guo, J. T., Block, T. M., Mechti, N. and Guo, H. (2017) Interferon-inducible ribonuclease ISG20 inhibits hepatitis B virus replication through directly binding to the epsilon stem-loop structure of viral RNA. *PLoS Pathog, 13*(4), pp. e1006296.

Lopes, A. R., Kellam, P., Das, A., Dunn, C., Kwan, A., Turner, J., Peppa, D., Gilson, R. J., Gehring, A., Bertoletti, A. and Maini, M. K. (2008) Bim-mediated deletion of antigen-specific CD8 T cells in patients unable to control HBV infection. *J Clin Invest, 118*(5), pp. 1835-45.

Lu, X., Qin, B., Ma, Q., Yang, C., Gong, X. Y. and Chen, L. M. (2013) Differential expression of ISG20 in chronic hepatitis B patients and relation to interferon-alpha therapy response. *J Med Virol, 85*(9), pp. 1506-12.

Lucifora, J., Arzberger, S., Durantel, D., Belloni, L., Strubin, M., Levrero, M., Zoulim, F., Hantz, O. and Protzer, U. (2011) Hepatitis B virus X protein is essential to initiate and maintain virus replication after infection. *J Hepatol, 55*(5), pp. 996-1003.

Lucifora, J. and Protzer, U. (2016) Attacking hepatitis B virus cccDNA – The holy grail to hepatitis B cure. *J Hepatol, 64*(1, Supplement), pp. S41-S48.

Lucifora, J., Xia, Y., Reisinger, F., Zhang, K., Stadler, D., Cheng, X., Sprinzl, M. F., Koppensteiner, H., Makowska, Z., Volz, T., Remouchamps, C., Chou, W.-M., Thasler, W. E., Hüser, N., Durantel, D., Liang, T. J., Münk, C., Heim, M. H., Browning, J. L., Dejardin, E., Dandri, M., Schindler, M., Heikenwalder, M. and Protzer, U. (2014) Specific and Nonhepatotoxic Degradation of Nuclear Hepatitis B Virus cccDNA. *Science, 343*(6176), pp. 1221-1228.

Lutgehetmann, M., Volz, T., Kopke, A., Broja, T., Tigges, E., Lohse, A. W., Fuchs, E., Murray, J. M., Petersen, J. and Dandri, M. (2010) In vivo proliferation of hepadnavirus-infected hepatocytes induces loss of covalently closed circular DNA in mice. *Hepatology, 52*(1), pp. 16-24.

Ma, Q., Qin, B., Lu, X. and Kong, L. (2016) Interferon stimulated exonuclease gene 20 kDa promotes the activity of interferon-alpha on the inhibition of hepatitis B virus replication via its exonuclease activity. *Int J Clin Exp Med, 9*(9), pp. 17940-17945.

Mao, R., Zhang, J., Jiang, D., Cai, D., Levy, J. M., Cuconati, A., Block, T. M., Guo, J. T. and Guo, H. (2011) Indoleamine 2,3-dioxygenase mediates the antiviral effect of gamma interferon against hepatitis B virus in human hepatocyte-derived cells. *J Virol, 85*(2), pp. 1048-57.

Mason, W. S., Seal, G. and Summers, J. (1980) Virus of Pekin ducks with structural and biological relatedness to human hepatitis B virus. *J Virol, 36*(3), pp. 829-836.

Modrow, S., Falke, D., Truyen, U. and Schätzl, H. (2010) *Molekulare Virologie,* 3rd ed.*,* Heidelberg: Spektrum Akademischer Verlag, pp.461-483.

Moser, M. J., Holley, W. R., Chatterjee, A. and Mian, I. S. (1997) The proofreading domain of Escherichia coli DNA polymerase I and other DNA and/or RNA exonuclease domains. *Nucleic Acids Res, 25*(24), pp. 5110-5118.

Murphy, K. M. and Weaver, C. (2016) *Janeway's Immunobiology,* 9th ed.*,* New York, NY: Garland Science/Taylor & Francis Group.

Nagarajan, V. K., Jones, C. I., Newbury, S. F. and Green, P. J. (2013) XRN 5′ → 3′ exoribonucleases: Structure, mechanisms and functions. *Biochimica et Biophysica Acta (BBA) - Gene Regulatory Mechanisms, 1829*(6–7), pp. 590-603.

Naghavi, M., Wang, H., Lozano, R., Davis, A., Liang, X., Zhou, M., Vollset, S. E., ..., Vos, T., Lopez, A. D. and Murray, C. J. L. (2015) Global, regional, and national age-sex specific all-cause and cause-specific mortality for 240 causes of death, 1990-2013: a systematic analysis for the Global Burden of Disease Study 2013. *Lancet, 385*(9963), pp. 117-71.

Nakabayashi, H., Taketa, K., Miyano, K., Yamane, T. and Sato, J. (1982) Growth of human hepatoma cells lines with differentiated functions in chemically defined medium. *Cancer Res, 42*(9), pp. 3858-63.

Nassal, M. (2015) HBV cccDNA: viral persistence reservoir and key obstacle for a cure of chronic hepatitis B. *Gut*, *64(12),* pp. 1972-84.

Nguyen, L. H., Espert, L., Mechti, N. and Wilson, D. M., 3rd (2001) The human interferon- and estrogen-regulated ISG20/HEM45 gene product degrades single-stranded RNA and DNA in vitro. *Biochemistry, 40*(24), pp. 7174-9.

Ooms, M., Krikoni, A., Kress, A. K., Simon, V. and Munk, C. (2012) APOBEC3A, APOBEC3B, and APOBEC3H haplotype 2 restrict human T-lymphotropic virus type 1. *J Virol, 86*(11), pp. 6097-108.

Patient, R., Hourioux, C., Sizaret, P.-Y., Trassard, S., Sureau, C. and Roingeard, P. (2007) Hepatitis B Virus Subviral Envelope Particle Morphogenesis and Intracellular Trafficking. *J Virol, 81*(8), pp. 3842-3851.

Pentecost, B. T. (1998) Expression and estrogen regulation of the HEM45 MRNA in human tumor lines and in the rat uterus. *J Steroid Biochem Mol Biol, 64*(1-2), pp. 25-33.

Phillips, S., Chokshi, S., Riva, A., Evans, A., Williams, R. and Naoumov, N. V. (2010) CD8(+) T cell control of hepatitis B virus replication: direct comparison between cytolytic and noncytolytic functions. *J Immunol, 184*(1), pp. 287-95.

Piechaczek, C., Fetzer, C., Baiker, A., Bode, J. and Lipps, H. J. (1999) A vector based on the SV40 origin of replication and chromosomal S/MARs replicates episomally in CHO cells. *Nucleic Acids Res, 27*(2), pp. 426-428.

Pollicino, T., Belloni, L., Raffa, G., Pediconi, N., Squadrito, G., Raimondo, G. and Levrero, M. (2006) Hepatitis B Virus Replication Is Regulated by the Acetylation Status of Hepatitis B Virus cccDNA-Bound H3 and H4 Histones. *Gastroenterology, 130*(3), pp. 823-837.

Protzer, U., Maini, M. K. and Knolle, P. A. (2012) Living in the liver: hepatic infections. *Nat Rev Immunol, 12*(3), pp. 201-13.

Protzer, U., Seyfried, S., Quasdorff, M., Sass, G., Svorcova, M., Webb, D., Bohne, F., Hosel, M., Schirmacher, P. and Tiegs, G. (2007) Antiviral activity and hepatoprotection by heme oxygenase-1 in hepatitis B virus infection. *Gastroenterology, 133*(4), pp. 1156-65.

Qi, Y., Gao, Z., Xu, G., Peng, B., Liu, C., Yan, H., Yao, Q., Sun, G., Liu, Y., Tang, D., Song, Z., He, W., Sun, Y., Guo, J.-T. and Li, W. (2016) DNA Polymerase κ Is a Key Cellular Factor for the Formation of Covalently Closed Circular DNA of Hepatitis B Virus. *PLoS Pathog, 12*(10), pp. e1005893.

Qiao, Y., Han, X., Guan, G., Wu, N., Sun, J., Pak, V. and Liang, G. (2016) TGF-beta triggers HBV cccDNA degradation through AID-dependent deamination. *FEBS Lett, 590*(3), pp. 419-27.

Revill, P., Testoni, B., Locarnini, S. and Zoulim, F. (2016) Global strategies are required to cure and eliminate HBV infection. *Nat Rev Gastroenterol Hepatol, 13*(4), pp. 239-248.

Ritchie, M. E., Phipson, B., Wu, D., Hu, Y., Law, C. W., Shi, W. and Smyth, G. K. (2015) limma powers differential expression analyses for RNA-sequencing and microarray studies. *Nucleic Acids Res, 43*(7), pp. e47.

Rivière, L., Gerossier, L., Ducroux, A., Dion, S., Deng, Q., Michel, M.-L., Buendia, M.-A., Hantz, O. and Neuveut, C. (2015) HBx relieves chromatin-mediated transcriptional repression of hepatitis B viral cccDNA involving SETDB1 histone methyltransferase. *Journal of Hepatology, 63*(5), pp. 1093-1102.

RKI (2015) Virushepatitis B und D im Jahr 2014. *Epidemiologisches Bulletin, Aktuelle Daten und Informationen zu Infektionskrankheiten und Public Health, Robert Koch-Institut (Hrsg.)*, 20.07.2015.

Said, Z. N. A. and Abdelwahab, K. S. (2015) Induced immunity against hepatitis B virus. *World J Hepatol, 7*(12), pp. 1660-1670.

Schaefer, S. (2007) Hepatitis B virus taxonomy and hepatitis B virus genotypes. *World J Gastroenterol : WJG, 13*(1), pp. 14-21.

Schmitz, A., Schwarz, A., Foss, M., Zhou, L., Rabe, B., Hoellenriegel, J., Stoeber, M., Pante, N. and Kann, M. (2010) Nucleoporin 153 arrests the nuclear import of hepatitis B virus capsids in the nuclear basket. *PLoS Pathog, 6*(1), pp. e1000741.

Schneider, J. (2016) *The antiviral effect of the interferon-induced nuclease ISG20 on the hepatitis B virus (HBV)*. Unpublished master thesis, Technische Universität München, München (cited with permission).

Schneider, W. M., Chevillotte, M. D. and Rice, C. M. (2014) Interferon-stimulated genes: a complex web of host defenses. *Annu Rev Immunol, 32*, pp. 513-45.

Schulze, A., Gripon, P. and Urban, S. (2007) Hepatitis B virus infection initiates with a large surface protein-dependent binding to heparan sulfate proteoglycans. *Hepatology, 46*(6), pp. 1759-68.

Schweitzer, A., Horn, J., Mikolajczyk, R. T., Krause, G. and Ott, J. J. (2015) Estimations of worldwide prevalence of chronic hepatitis B virus infection: a systematic review of data published between 1965 and 2013. *Lancet*, *386,* pp. 1546–55.

Seeger, C. and Mason, W. S. (2015) Molecular biology of hepatitis B virus infection. *Virology, 479–480*(0), pp. 672-686.

Sells, M. A., Chen, M. L. and Acs, G. (1987) Production of hepatitis B virus particles in Hep G2 cells transfected with cloned hepatitis B virus DNA. *Proc Natl Acad Sci U S A, 84*(4), pp. 1005-1009.

Shamsadin, R., Adham, I. M., von Beust, G. and Engel, W. (2000) Molecular cloning, expression and chromosome location of the human pelota gene PELO. *Cytogenet Genome Res, 90*(1-2), pp. 75-78.

Sprinzl, M. F., Oberwinkler, H., Schaller, H. and Protzer, U. (2001) Transfer of hepatitis B virus genome by adenovirus vectors into cultured cells and mice: crossing the species barrier. *J Virol, 75*(11), pp. 5108-18.

Stadler, D. (2013) *Mechanism of the Elimination of Hepatitis B Viral (HBV) DNA through Interferons (IFN)*. Unpublished master thesis, Technische Universität München, München.

Stavrou, S. and Ross, S. R. (2015) APOBEC3 Proteins in Viral Immunity. *J Immunol, 195*(10), pp. 4565-70.

Stenglein, M. D., Burns, M. B., Li, M., Lengyel, J. and Harris, R. S. (2010) APOBEC3 proteins mediate the clearance of foreign DNA from human cells. *Nat Struct Mol Biol, 17*(2), pp. 222-229.

Su, A. I., Pezacki, J. P., Wodicka, L., Brideau, A. D., Supekova, L., Thimme, R., Wieland, S., Bukh, J., Purcell, R. H., Schultz, P. G. and Chisari, F. V. (2002) Genomic analysis of the host response to hepatitis C virus infection. *Proc Natl Acad Sci, 99*(24), pp. 15669-15674.

Summers, J., Smolec, J. M. and Snyder, R. (1978) A virus similar to human hepatitis B virus associated with hepatitis and hepatoma in woodchucks. *Proc Natl Acad Sci, 75*(9), pp. 4533-4537.

Suspene, R., Henry, M., Guillot, S., Wain-Hobson, S. and Vartanian, J. P. (2005) Recovery of APOBEC3-edited human immunodeficiency virus G->A hypermutants by differential DNA denaturation PCR. *J Gen Virol, 86*(Pt 1), pp. 125-9.

Tamura, K., Peterson, D., Peterson, N., Stecher, G., Nei, M. and Kumar, S. (2011) MEGA5: molecular evolutionary genetics analysis using maximum likelihood, evolutionary distance, and maximum parsimony methods. *Mol Biol Evol, 28*(10), pp. 2731-9.

Tatematsu, K., Tanaka, Y., Kurbanov, F., Sugauchi, F., Mano, S., Maeshiro, T., Nakayoshi, T., Wakuta, M., Miyakawa, Y. and Mizokami, M. (2009) A genetic variant of hepatitis B virus divergent from known human and ape genotypes isolated from a Japanese patient and provisionally assigned to new genotype J. *J Virol, 83*(20), pp. 10538-47.

Thome, M. and Tschopp, J. (2001) Regulation of lymphocyte proliferation and death by flip. *Nat Rev Immunol, 1*(1), pp. 50-58.

Trépo, C., Chan, H. L. Y. and Lok, A. (2014) Hepatitis B virus infection. *The Lancet, 384*(9959), pp. 2053-2063.

Tropberger, P., Mercier, A., Robinson, M., Zhong, W., Ganem, D. E. and Holdorf, M. (2015) Mapping of histone modifications in episomal HBV cccDNA uncovers an unusual chromatin organization amenable to epigenetic manipulation. *Proc Natl Acad Sci U S A, 112*(42), pp. E5715-24.

Turelli, P., Mangeat, B., Jost, S., Vianin, S. and Trono, D. (2004) Inhibition of hepatitis B virus replication by APOBEC3G. *Science, 303*(5665), pp. 1829.

Valaydon, Z., Pellegrini, M., Thompson, A., Desmond, P., Revill, P. and Ebert, G. (2016) The role of tumour necrosis factor in hepatitis B infection: Jekyll and Hyde. *Clin Transl Immunology, 5*(12), pp. e115.

Watanabe, T., Sorensen, E. M., Naito, A., Schott, M., Kim, S. and Ahlquist, P. (2007) Involvement of host cellular multivesicular body functions in hepatitis B virus budding. *Proc Natl Acad Sci U S A, 104*(24), pp. 10205-10.

Wherry, E. J. (2011) T cell exhaustion. *Nat Immunol, 12*(6), pp. 492-499.

WHO (2017) *Hepatitis B, Fact sheet, Updated April 2017*, Available: http://www.who.int/mediacentre/factsheets/fs204/en/ [Accessed 14.05.2017].

Wieland, S., Spangenberg, H. C., Thimme, R., Purcell, R. H. and Chisari, F. V. (2004) Expansion and contraction of the hepatitis B virus transcriptional template in infected chimpanzees. *Proc Natl Acad Sci, 101*(7), pp. 2129-2134.

Wieland, S., Thimme, R., Purcell, R. H. and Chisari, F. V. (2004) Genomic analysis of the host response to hepatitis B virus infection. *Proc Natl Acad Sci U S A, 101*(17), pp. 6669-6674.

Wolf, M. J., Seleznik, G. M., Zeller, N. and Heikenwalder, M. (2010) The unexpected role of lymphotoxin [beta] receptor signaling in carcinogenesis: from lymphoid tissue formation to liver and prostate cancer development. *Oncogene, 29*(36), pp. 5006-5018.

Xia, Y., Cheng, X., Blossey, C. K., Wisskirchen, K., Esser, K. and Protzer, U. (2017a) Secreted Interferon-Inducible Factors Restrict Hepatitis B and C Virus Entry In Vitro. *J Immunol Res, 2017*, pp. 4828936.

Xia, Y. and Protzer, U. (2017) Control of Hepatitis B Virus by Cytokines. *Viruses, 9*(1), E18.

Xia, Y., Stadler, D., Ko, C. and Protzer, U. (2017b) Analyses of HBV cccDNA Quantification and Modification. In Guo, H. and Cuconati, A. (eds.) *Hepatitis B Virus: Methods and Protocols*, New York, NY: Springer New York, pp. 59-72.

Xia, Y., Stadler, D., Lucifora, J., Reisinger, F., Webb, D., Hosel, M., Michler, T., Wisskirchen, K., Cheng, X., Zhang, K., Chou, W. M., Wettengel, J. M., Malo, A., Bohne, F., Hoffmann, D., Eyer, F., Thimme, R., Falk, C. S., Thasler, W. E., Heikenwalder, M. and Protzer, U. (2016) Interferon-gamma and Tumor Necrosis Factor-alpha Produced by T Cells Reduce the HBV Persistence Form, cccDNA, Without Cytolysis. *Gastroenterology, 150*(1), pp. 194-205.

Xiao, C., Qin, B., Chen, L., Liu, H., Zhu, Y. and Lu, X. (2012) Preactivation of the interferon signalling in liver is correlated with nonresponse to interferon alpha therapy in patients chronically infected with hepatitis B virus. *J Viral Hepat, 19*(2), pp. e1-10.

Xu, C., Guo, H., Pan, X.-B., Mao, R., Yu, W., Xu, X., Wei, L., Chang, J., Block, T. M. and Guo, J.-T. (2010) Interferons Accelerate Decay of Replication-Competent Nucleocapsids of Hepatitis B Virus. *J Virol, 84*(18), pp. 9332-9340.

Yan, H., Zhong, G., Xu, G., He, W., Jing, Z., Gao, Z., Huang, Y., Qi, Y., Peng, B., Wang, H., Fu, L., Song, M., Chen, P., Gao, W., Ren, B., Sun, Y., Cai, T., Feng, X., Sui, J. and Li, W. (2012) Sodium taurocholate cotransporting polypeptide is a functional receptor for human hepatitis B and D virus. *eLife, 1*, pp. e00049.

Ye, H., Zhang, X. W., Mu, R., Fang, L. K., Gu, J. R., Lin, J., Du, J. F., Chen, J. W., Chen, Y. J., Wu, L. J., Pang, X. F. and Li, Z. G. (2014) Anti-TNF therapy in patients with HBV infection--analysis of 87 patients with inflammatory arthritis. *Clin Rheumatol, 33*(1), pp. 119-23.

Yoshida, K., Wang, H. G., Miki, Y. and Kufe, D. (2003) Protein kinase Cdelta is responsible for constitutive and DNA damage-induced phosphorylation of Rad9. *Embo J, 22*(6), pp. 1431-41.

Zhang, Y. Y., Zhang, B. H., Theele, D., Litwin, S., Toll, E. and Summers, J. (2003) Single-cell analysis of covalently closed circular DNA copy numbers in a hepadnavirus-infected liver. *Proc Natl Acad Sci U S A, 100*(21), pp. 12372-7.

Zheng, M. H., Xiao, D. D., Lin, X. F., Wu, S. J., Peng, M. M., Yu, X. Y., Liu, W. Y., Li, L. F., Shi, K. Q., Fan, Y. C. and Chen, Y. P. (2012) The tumour necrosis factor-α-238A allele increases the risk of chronic HBV infection in European populations. *J Viral Hepat, 19*(2), pp. e11-e17.

Zheng, Z., Wang, L. and Pan, J. (2017) Interferon-stimulated gene 20-kDa protein (ISG20) in infection and disease: Review and outlook. *Intractable Rare Dis Res, 6*(1), pp. 35-40.

Zlotnick, A., Venkatakrishnan, B., Tan, Z., Lewellyn, E., Turner, W. and Francis, S. (2015) Core protein: A pleiotropic keystone in the HBV lifecycle. *Antiviral Res, 121*, pp. 82-93.

Acknowledgement

First of all, I thank my supervisor Prof. Dr. Ulrike Protzer for giving me the opportunity to do my PhD thesis in her research group and that I could work on such a fascinating and prosperous project. I am especially thankful for her support and advises in scientific but also organisational questions and that she had always an open door for urgent concerns.

I am grateful to Prof. Dr. Bernhard Küster for his disposability as second supervisor and his valuable input during the thesis committee meetings. Furthermore, I thank PD Dr. Sabrina Schreiner and Dr. Yuchen Xia as members of my thesis committee for offering precious help on the project and beyond.

In particular, I am thankful to Dr. Yuchen Xia who taught me so many methods and techniques in the beginning and for the good collaboration later on.

Special thanks go to all my colleagues at the Institute of Virology for support in the lab and the great working atmosphere. I am especially grateful to Romina Bester, Theresa Asen, Dr. Julie Lucifora, Dr. Florian Reisinger, Dr. Chunkyu Ko, Antje Malo and Dr. Martin Mück-Häusl for appreciated help with experiments and fruitful discussions. Thank you so much for making the past years so pleasant, Wen-Min Chou, Dr. Julia Graf, Oliver Quitt, Julia Hasreiter, Marvin Festag, Dr. Knud Esser, Dr. Xiaoming Cheng, Lisa Wolff, Sophia Schreiber, Jochen Wettengel, Dr. Nina Böttinger, Dr. Karin Wisskirchen, Dr. Katrin Singethan, Christoph Blossey, Sebastian Altstetter, Dr. Clemens Jäger, Dr. Thomas Michler and Dr. Stefanie Graf!

I am deeply thankful to Dr. Karin Wisskirchen, Dr. Chunkyu Ko and Dr. Britta Möhl for proofreading of the thesis and many helpful comments.

Furthermore, I thank Jessica Schneider and Cornelia Götz for their contributions during master theses and research internship as well as stimulating questions.

Ein besonderer Dank gilt meiner Familie und meinen Freunden in Villnöß und München. Meinen Eltern danke ich für die bedingungslose Unterstützung und den Rückhalt, den sie mir geben. Ganz speziell bedanke ich mich herzlich bei Benedikt für die Unterstützung und im Besonderen für den morgendlichen Kaffee!

Publications and meetings

a) Articles in peer-reviewed journals

Lucifora, J.*, Xia, Y.*, Reisinger, F., Zhang, K., **Stadler, D.**, Cheng, X., Sprinzl, M. F., Koppensteiner, H., Makowska, Z., Volz, T., Remouchamps, C., Chou, W.-M., Thasler, W. E., Hüser, N., Durantel, D., Liang, T. J., Münk, C., Heim, M. H., Browning, J. L., Dejardin, E., Dandri, M., Schindler, M., Heikenwalder, M.‡ and Protzer, U.‡ (2014) Specific and Nonhepatotoxic Degradation of Nuclear Hepatitis B Virus cccDNA. *Science, 343*(6176), pp. 1221-1228.

Lucifora, J.*, Xia, Y.*, Reisinger, F., **Stadler, D.**, Heikenwalder, M.‡ and Protzer, U.‡ (2014) [Specific degradation of nuclear hepatitis B virus covalently closed circular DNA]. *Med Sci (Paris), 30*(8-9), pp. 724-6.

Xia, Y.*, **Stadler, D.***, Lucifora, J., Reisinger, F., Webb, D., Hosel, M., Michler, T., Wisskirchen, K., Cheng, X., Zhang, K., Chou, W. M., Wettengel, J. M., Malo, A., Bohne, F., Hoffmann, D., Eyer, F., Thimme, R., Falk, C. S., Thasler, W. E., Heikenwalder, M. and Protzer, U. (2016) Interferon-gamma and Tumor Necrosis Factor-alpha Produced by T Cells Reduce the HBV Persistence Form, cccDNA, Without Cytolysis. *Gastroenterology, 150*(1), pp. 194-205.

Thomsen, M. K., Nandakumar, R., **Stadler, D.**, Malo, A., Valls, R. M., Wang, F., Reinert, L. S., Dagnaes-Hansen, F., Hollensen, A. K., Mikkelsen, J. G., Protzer, U. and Paludan, S. R. (2016) Lack of immunological DNA sensing in hepatocytes facilitates hepatitis B virus infection. *Hepatology, 64*(3), pp. 746-59.

Stadler, D. et al. Identification of ISG20 as the nuclease involved in interferon-induced decline of hepatitis B virus cccDNA. *Prepared manuscript*.

* shared first-authorship
‡ equal contribution

b) Book chapter

Xia, Y., **Stadler, D.**, Ko, C. and Protzer, U. (2017) Analyses of HBV cccDNA Quantification and Modification. In Guo, H. and Cuconati, A. (eds.) *Hepatitis B Virus: Methods and Protocols*, New York, NY: Springer New York, pp. 59-72.

c) International conferences

2015 International HBV Meeting – The Molecular Biology of Hepatitis B Viruses
October 4 – 8, 2015, Bad Nauheim, Germany
Oral presentation: T-cell derived cytokines IFN-γ and TNF-α can reduce HBV cccDNA without cytolysis

2016 International HBV Meeting – The Molecular Biology of Hepatitis B Viruses
September 21 – 24, 2016, Seoul, South Korea
Oral presentation: Identification of the nuclease involved in interferon-induced purging of HBV cccDNA
Travel grant award

6th European Congress of Virology
October 19 – 22, 2016, Hamburg, Germany
Poster: Identification of the nuclease involved in interferon-induced purging of HBV cccDNA
Awarded with a presentation in the Best-of-Posters session